

Electronic Thesis and Dissertation Repository

9-27-2016 12:00 AM

Controlled Guidance of Light in Large Area Flexible Optical Waveguide Sheets

Chloë O. Nicholson-Smith, *The University of Western Ontario*

Supervisor: Dr. George Knopf, *The University of Western Ontario*

Joint Supervisor: Dr. Evgueni Bordatchev, *The University of Western Ontario*

A thesis submitted in partial fulfillment of the requirements for the Master of Engineering Science degree in Mechanical and Materials Engineering

© Chloë O. Nicholson-Smith 2016

Follow this and additional works at: <https://ir.lib.uwo.ca/etd>



Part of the [Computer-Aided Engineering and Design Commons](#)

Recommended Citation

Nicholson-Smith, Chloë O., "Controlled Guidance of Light in Large Area Flexible Optical Waveguide Sheets" (2016). *Electronic Thesis and Dissertation Repository*. 4161.
<https://ir.lib.uwo.ca/etd/4161>

This Dissertation/Thesis is brought to you for free and open access by Scholarship@Western. It has been accepted for inclusion in Electronic Thesis and Dissertation Repository by an authorized administrator of Scholarship@Western. For more information, please contact wlsadmin@uwo.ca.

Abstract

Large surface area, thin, polymer optical waveguides are an emerging technology that enable a wide variety of light collection and illumination systems to be created for passive indoor lighting, mechanically flexible solar energy concentrators, and enhanced safety lighting for motorized vehicles. This research builds on design of rigid concentrator and diffuser waveguides, proposing and evaluating modifications for the design of a flexible waveguide combining both concentrating and diffusing functionalities. The waveguides are thin, mechanically flexible sheets with thicknesses in the range of mm, and active surfaces that can range from a few cm² to several m². Regions of the functional surface are designed to act as light concentrators, light diffusers, light transmission conduits or some combination thereof. This research examines how the geometry and spatial distribution of micro-optical features patterned on a bi-layered thin polydimethylsiloxane (PDMS) waveguides can be used to guide captured light rays through flat and flexible configurations. Zemax OpticStudio software simulation tool is used to investigate the design parameters and the impact of these parameters on concentrator and diffuser performance. A multi-functional concentrator-diffuser waveguide is modelled and analysed in a study which shows the flat waveguide has an overall efficiency of over 94%, however when it is modelled as a flexible waveguide, less than 1% of the incident light is successfully guided. Various design modifications to both the concentrating and diffusing regions of the waveguide are, therefore, considered to mitigate these losses, and the efficiency of the flexible waveguide is improved to nearly 60%. Based on the parametric optimization of the microfeatures, the suitable waveguide design is identified for variations in the waveguide's flexibility, geometry, material and application. Future work will focus on analyzing and optimizing the concentrator-diffuser waveguide design for enhanced performance, thinner profile, and an evaluation of its empirical results.

Keywords

Flexible waveguide sheets, polydimethylsiloxane, large area concentrators, light diffusers, micro-features, Zemax OpticStudio

Acknowledgments

This research is the result of collaboration between the University of Western Ontario (London, Ontario) and National Research Council (London, Ontario). Partial financial support was also provided by Natural Sciences and Engineering Research Council (NSERC) of Canada and AUTO21 Network of Centers of Excellence. I would also like to acknowledge the support of CMC Microsystems (Kingston, Ontario) in providing access to the Zemax OpticStudio software through their Designer subscription programs.

Table of Contents

Abstract	i
Acknowledgments.....	ii
Table of Contents	iii
List of Tables	vii
List of Figures	viii
List of Appendices	xiv
List of Abbreviations and Symbols.....	xv
Chapter 1 Introduction	1
1.1 The Problem.....	2
1.2 Applications of Rigid and Flexible Light Guides	6
1.3 Research Motivation and Objectives	8
1.4 Design Issues.....	9
1.5 Overview of the Thesis	10
Chapter 2 Literature Review of Optical Waveguide Sheets	13
2.1 Properties of Light	13
2.1.1 Light and Electromagnetic Spectrum.....	13
2.1.2 Wave-Particle Duality of Light.....	15
2.1.3 Transmission, Absorption and Reflection.....	17
2.1.4 Geometric Optics	19
2.1.5 Limitations of Geometric Optics	20
2.2 Operating Principles of Flexible Optical Waveguides.....	23
2.2.1 Total Internal Reflection (TIR) in Waveguide Sheets	23
2.2.2 Structure of an Optical Waveguide Sheet.....	25
2.2.3 Optical Losses	26

2.3	Concentrators and Diffusers	33
2.3.1	Edge and Face Lit Waveguides.....	33
2.3.2	Uniform and Non-Uniform Illumination	35
2.3.3	Selection of Core and Cladding Material.....	37
2.3.4	Importance of Optical Microstructures	38
2.4	Key Material Properties of Optically Transparent Polymers.....	41
2.5	Concluding Remarks.....	42
Chapter 3	Design Methodology	43
3.1	Evaluating Optical Waveguide Performance	43
3.1.1	Estimating Light Loss	43
3.1.2	Performance Measures	45
3.2	Role of Simulations in Optical Design	46
3.3	Functionality of Zemax OpticStudio Software	47
3.4	Limitations of Design Methodology.....	53
3.5	Concluding Remarks.....	54
Chapter 4	Establishing Design Parameters for Large Area Waveguides.....	55
4.1	Conceptual Design of Concentrator – Diffuser Waveguide	55
4.2	Waveguide Structure.....	57
4.2.1	Waveguide Layering and Material Selection.....	57
4.2.2	Waveguide Area and Thickness.....	58
4.2.3	Microstructure Functionality.....	59
4.3	Surface Area and Thickness.....	61
4.4	Optical Microstructure Geometry	62
4.4.1	Various Shapes and Sizes	62
4.4.2	Microstructure Density and Distribution	66

4.4.3	Microstructures for Efficient Light Concentrators and Diffuser	67
4.5	Equations for the Design of a Flat Waveguide	68
4.6	Performance of Functionally Designed Flat Waveguide	74
4.6.1	Single Microstructure.....	74
4.6.2	Linear Array of Microstructures	76
4.6.3	Area Array of Microstructures	79
4.7	Discussion – Light Transmission Efficiency of Optimized Planar Waveguide ...	82
4.8	Concluding Remarks.....	83
Chapter 5	Performance of Non-Rigid Waveguide Sheets.....	85
5.1	Key Parameters and Waveguide Performance.....	85
5.1.1	Waveguide Parameters.....	85
5.1.2	Concentrator Parameters	88
5.1.3	Diffuser Parameters.....	93
5.2	Impact on Performance of Waveguide Bending.....	97
5.2.1	Waveguide Bending.....	98
5.2.2	Concentrator Bending	99
5.2.3	Diffuser Bending.....	100
5.3	Microstructure Geometry for Non-Rigid Waveguide.....	102
5.3.1	Concentrator Geometry.....	102
5.3.2	Diffuser Geometry	107
5.4	Evaluating Performance of a Non-Rigid Waveguide	111
5.4.1	Performance of the Concentrator as a Non-Rigid Waveguide.....	111
5.4.2	Performance of the Diffuser as a Non-Rigid Waveguide	114
5.4.3	Combined Controlled Light Guidance and Distribution through Flexible Optical Waveguide Sheet.....	115
5.5	Guidelines for the Design of a Non-Rigid Waveguide Sheet	117

5.6 Discussion – Limitations of Controlled Light Guidance	122
5.7 Concluding Remarks.....	123
Chapter 6 Conclusions	125
6.1 Thesis Summary.....	125
6.2 Concluding Comments.....	126
6.3 Recommendations and Future Work	127
References	129
Appendices.....	133
Appendix A: Derivations and Calculations.....	133
Appendix B: CAD Drawings of Waveguide Geometry.....	151
Appendix C: Sample Zemax Program	154
Curriculum Vitae.....	155

List of Tables

Table 5.1 Data from Zemax simulations representing the uniformity and efficiency of the diffusing region with respect to the diffusing wedge angle (θ_d).....	93
Table 5.2 Summary of concentrator performance for variations in coupling features geometry for both planar, and flexible waveguide orientations.	107
Table 5.3 Summary of diffuser performance of the diffuser, with respect to its efficiency, in consideration of the various feature configurations.....	109
Table 5.4 Summary of the performance of the diffuser, with respect to its uniformity, in consideration of the various feature configurations.	110
Table 5.5 Design guidelines for varying waveguide geometry according to the requirements and limitations of a particular waveguide application.	121

List of Figures

Figure 1.1 Illustrations of large-area thin mechanically flexible waveguides for light harvesting and uniform illumination applications. Note that the thicknesses of the waveguide regions are exaggerated for display.	4
Figure 1.2 Cross-sectional view of a two layer PDMS concentrator-diffuser waveguide. The incident light is focused onto the coupling prisms by the micro-lens array, and directed to the illuminating region, where the light is diffused by micro-wedge features.	11
Figure 2.1 The electromagnetic spectrum encompasses various types of radiation which exhibits both electric and magnetic properties. Visible light occupies the mid-range of the electromagnetic spectrum representing wavelengths from 400 to 700 nm.....	13
Figure 2.2 Depiction of an electron which falls from the outermost (highest energy) electron shell to a lower energy shell; it releases a packet of energy known as a photon. This photon of energy is perceived as light.	14
Figure 2.3 Young’s double slit experiment separated a light source into two wave fronts whose interference pattern was projected onto a subsequent screen. The interference pattern observed confirmed the wave properties of light.....	16
Figure 2.4 Light strikes the interface between two materials, with different refractive indices, it may traverse into the second medium by refraction, or be reflected back into the first medium.	18
Figure 2.5 Wave optics represents light as a wave which propagates outwards from a source, whereas geometric optics simplifies the source into rays travelling perpendicular to the wave fronts.	19
Figure 2.6 Geometric optics does not represent the behaviour of waves well at the micron scale. Interference and diffraction are not accounted for using geometric optics, as the rays do not interact as such.	21

Figure 2.7 Total internal reflection in a waveguide sheet occurs if the core has a refractive index sufficiently larger than that of the cladding, as this will ensure the ray is reflected off the boundary between the media.24

Figure 2.8 The critical radius of curvature of a waveguide represents the minimum radius to which a waveguide may be bent without the propagating light failing to reflect back into the core, and being refracted out.25

Figure 2.9 The acceptance angle of a waveguide is defined by the maximum angle which can be contained in the waveguide by total internal reflection. Angles of incidence greater than θ_a will not be contained in the waveguide core.29

Figure 2.10 The proportion of light lost due to bending relates to the degree to which the waveguide is bent past the critical radius. A smaller radius of curvature results in greater light leakage.31

Figure 2.11 The edge-lit waveguide is illuminated from one side and diffuses incident light to illuminate the waveguide. The face-lit waveguide collects the light incident on the face and directs it to one, or more, waveguide edges.34

Figure 2.12 A typical diffuser light source will illuminate a cone of light from the centre axis to the maximum angle. The concentrator illuminates the diffuser in a unique pattern with light rays only propagating between a minimum and maximum angle.35

Figure 2.13 Uniform illumination of a diffuser waveguide is achieved by increasing the diffuser's efficiency with distance from the source, as the light remaining in the waveguide decreases [18].36

Figure 2.14 Commonly used diffuser micro-features include round tipped, triangular, cone shaped and inverse cone shaped features.39

Figure 3.1 This image depicts the Zemax user interface as well as the key parameters used to import CAD components, and define their properties.47

Figure 3.2 The Non-Sequential Component editor permits the definition of a rectangular source, its total power, size and location.	49
Figure 3.3 Zemax facilitates the definition of detectors and the relevant properties.	51
Figure 3.4 Zemax represents the ray trace data in the 3D layout, providing a visual representation of the results. The detector data gives a more detailed view of the illumination patterns and extensive numerical data.	52
Figure 4.1 Combined concentrator-diffuser waveguide with lens micro-features focusing incident light onto the coupling prisms, which direct light into the transmission layer of the waveguide. The light propagates to the diffusing wedges, which cause refraction.	56
Figure 4.2 Illustration of the concentrator’s functionality; the concentrating lenses focus the light onto the coupling prisms, which reflect the concentrated rays into the waveguide at such an angle that they are confined to the bottom layer of the waveguide.	60
Figure 4.3 The size and distribution of the wedge features must be optimized to enhance the uniformity of the diffuser’s illumination, and the length of the diffuser region must be optimized for both its efficiency and uniformity.	61
Figure 4.4 Illustration of concentrator and diffuser waveguide denoting important features; lenses, pyramids, and wedges, and their relevant parameters.	68
Figure 4.5 Ray diagram for focused light incident on the coupling prisms, illustrating the minimum and maximum angles of incidence and propagation.	70
Figure 4.6 Ray diagram which illustrates the minimum and maximum angles of propagation required to ensure the rays are properly diffused out the face of the illuminating region.	72
Figure 4.7 A single concentrating feature successfully collects over 99% of incident illumination based on the Zemax analysis and results.	75

Figure 4.8 Ray trace of a single diffusing wedge; over 98% of the illumination which strikes the wedge is successfully diffused, while the remaining incident light continues to propagate through the diffuser.	76
Figure 4.9 Detector data from the Zemax simulation of the row of concentrating features, showing light intensity patterns around the edges, and some illumination escaping the bottom face of the concentrator.	77
Figure 4.10 The Zemax simulation of the linear array of diffuser wedges demonstrates high efficiency, high intensity illumination of the waveguide’s face.	78
Figure 4.11 Zemax results from the area array of concentrator micro-features demonstrated high efficiency collection of incident illumination with greater uniformity over the collection region than previous results.	80
Figure 4.12 Zemax simulation results displaying the illumination pattern and cross-sectional profile of the combined concentrator-diffuser waveguide.	81
Figure 5.1 Relationship between the efficiency of the concentrating region (E_C) and the width of the concentrating region (W_C) based on the results of Zemax simulations.	86
Figure 5.2 Relationship between the ratio of the refractive indices of the waveguide layers and the efficiency of the waveguide, demonstrating a large drop in efficiency for insufficient differences in refractive index.	87
Figure 5.3 Relationship between the concentrator region’s efficiency and the Pitch (P) of the concentrator micro-features based on the Zemax results.	88
Figure 5.4 Relationship between the concentrating region’s efficiency and the Radius (R) of the micro-lens features demonstrates a peak efficiency for the Radius as determined by the parametric modelling of the lens dimensions.	90
Figure 5.5 Relationship between the efficiency of the concentrating region, and the base angle (α) of the coupling features, denoting a high efficiency region of acceptable angles. ...	91

Figure 5.6 Relationship between the concentrator efficiency and base width (b) of the coupling prisms.	92
Figure 5.7 Results of Zemax simulations representing the relationship between the performance of the diffuser and the width (w) of the diffuser micro- features.....	94
Figure 5.8 Results of Zemax simulations representing the relationship between the performance of the diffuser and the total length (l) of the diffusing region.	96
Figure 5.9 Relationship between the refractive index of the diffuser region and its efficiency and uniformity of illumination.	97
Figure 5.10 Relationship between radius of curvature (C) of the waveguide and the efficiency, demonstrating a steep drop in efficiency for small radii of curvature.	98
Figure 5.11 Relationship between the efficiency of the concentrator and its radius of curvature (C) comparing the use of a planar light source and a source which conforms to the curvature of the waveguide.	99
Figure 5.12 Relationship between the radius of curvature (C) and the performance of the waveguide, illustrating a large drop in both efficiency and uniformity of the diffuser for small radii.	100
Figure 5.13 Relationship between the radius of curvature (C) and the performance of the waveguide, illustrating the largest drop in efficiency for bending in the concentrator area.	101
Figure 5.14 Deformation of features due to bending of the waveguide results in misalignment between the focal point of the micro-lenses and location of the coupling features.	103
Figure 5.15 Various coupling features shapes, sizes and orientations are considered to evaluate their impact on efficiency of a flexible concentrator waveguide.	104

Figure 5.16 Numerous variations to the geometry of the diffuser micro-features and the diffusing region as a whole are considered in order to optimize the waveguides performance for each flexible and rigid configurations.....	108
Figure 5.17 The concentrator efficiency (E_c) of the simulated waveguide for various bending radii (R) as determined by the Zemax OpticStudio ray-tracing software.	112
Figure 5.18 Impact of waveguide bending changing the angle of incidence (θ_i) of light rays entering the waveguide on concentrator efficiency. Note the rapid reduction in efficiency as the angle of incidence is greater than 1°	113
Figure 5.19 The diffuser efficiency (E_d) of the simulated waveguide for various bending radii (C) as determined by the Zemax OpticStudio ray-tracing software.	115
Figure 5.20 The optimized geometry for the flexible concentrator-diffuser waveguide is modelled in SolidWorks and analyzed in Zemax in order to validate design.	116
Figure A.1 Relationship between the lens feature pitch and the ray angle of incidence.	141
Figure A.2 Relocation of focal point due to reorientation of lens micro-features with respect to the light source.....	144
Figure A.3 Reduction of the scale of the waveguide over the same range of curvature reduces the proportional deformation of the individual micro-features.	149
Figure B.1 SolidWorks drawing of layered concentrator-diffuser waveguide, illustrating geometry used in Chapter 4 simulations.	151
Figure B.2 SolidWorks drawing of concentrator micro-features illustrating radius, pitch, coupling feature and layer dimensions.....	152
Figure B.3 SolidWorks drawing of diffuser micro-features illustrating size and angle of the diffusing wedges, and diffuser region thickness.	153
Figure C.1 Zemax NSC editor for a dual functioning concentrator-diffuser waveguide, including CAD geometry and Zemax defined source and detectors.	154

List of Appendices

Appendix A: Derivations and Calculations	133
A.1: Derivation of Efficiency Equation	
A.2: Relationship between Angle and Pitch	
A.3: Calculation of Layer Thickness	
A.4: Feature Stretching and Deformation	
Appendix B: CAD Drawings of Waveguide Geometry	151
Appendix C: Sample Zemax Program.....	154

List of Abbreviations and Symbols

Abbreviations

MOS	Micro-Optical Structure
PDMS	Polydimethylsiloxane
BLU	Backlight Unit
TIR	Total Internal Reflection
LED	Light Emitting Diode
NA	Numerical Aperture
PV	Photovoltaic
LGP	Light Guide Plate
CAD	Computer Aided Drafting
NSC	Non-Sequential Component

Terminology

Collector

A collector is an optical device which increases the intensity of light, *concentrating* incident light onto an area smaller than the region of incidence

Illuminator

An illuminator is an optical device which *diffuses* incident light evenly, over a region larger than the area of incidence

Symbols

n	Index of refraction
n_1	Index of refraction of upper waveguide layer
n_2	Index of refraction of lower waveguide layer
t_1	Thickness of upper waveguide layer (mm)
t_2	Thickness of lower waveguide layer (mm)
E	Photonic energy (J)
h	Planck's constant (J·s)
ν	Frequency of light (s^{-1})

c	Velocity of light ($\text{m}\cdot\text{s}^{-1}$)
λ	Wavelength of light (nm)
θ_C	Critical angle ($^\circ$)
R_C	Critical radius of curvature (mm)
θ_a	Acceptance angle ($^\circ$)
D	Lens diameter (mm)
f	Lens focal length (mm)
E_C	Concentrator efficiency (%)
N	Number of times a propagating ray strikes the waveguide's bottom face
b	Width of coupling prism base (mm)
P	Pitch of concentrator micro-features (mm)
E_{C-D}	Efficiency of combined concentrator-diffuser waveguide (%)
L_D	Light diffused by illuminator region (W)
L_C	Light incident on concentrator region (W)
U_D	Uniformity of diffuser illumination (%)
I_{avg}	Average detector irradiance (W/cm^2)
I_{peak}	Peak detector irradiance (W/cm^2)
α	Base angle of coupling features ($^\circ$)
h_c	Height of coupling features (mm)
θ_d	Diffuser wedge angle ($^\circ$)
w	Diffuser wedge width (mm)
θ_i	Angle of incidence of focused ray ($^\circ$)
θ_P	Ray angle of propagation ($^\circ$)
CF	Geometric factor of concentration
SA	Waveguide surface area (mm^2)
W_C	Concentrator width (mm)
E_D	Diffuser efficiency (%)
C	Waveguide radius of curvature (mm)
θ_S	Source angle of incidence ($^\circ$)
D_P	Density of coupling features
E_T	Material transmission efficiency

θ_1	Angle of incident ray on micro-lens ($^\circ$)
θ_2	Angle of focused ray in upper layer of waveguide ($^\circ$)
θ_3	Angle of focused ray in lower layer of waveguide ($^\circ$)
x_0	Position of incidence of ray on lens (mm)
m	Slope of focused ray
x_f	X-position of micro-lens focal point (mm)
y_f	Y-position of micro-lens focal point (mm)
ρ	Slope of ray based on angled source

Chapter 1 Introduction

Current research on micro-patterned, large area optical waveguides has made significant advances in the design of both concentrating and diffusing waveguides. Micro-patterned concentrator waveguides are typically composed of two waveguide sheets; the upper layer patterned with micro-lenses and the lower patterned with coupling prisms [1-5]. The micro-lens features focus the light incident on the upper layer onto the coupling features in the lower layer. The coupling features reflect the light back into the waveguide, by either *total internal reflection* (TIR) or reflection off a mirrored surface, at such an angle that it propagates through the lower layer to the concentrator edge, where it typically strikes a *photovoltaic* (PV) cell for solar collection.

Research in the design and development of micro-patterned diffuser waveguides is significantly more extensive. Rigid diffuser waveguides have been examined with various micro-feature patterns including: wedges [6], domes [7], grooves [8] and dot features [9]. These waveguide configurations are often applied to *backlight units* (BLUs) for electronic displays which are typically rigid structures, however there is some research on flexible diffuser waveguides as well. Yeon et al. [10] look at the design of a flexible diffuser waveguide patterned with inverse cone features. In all cases the diffusing micro-features disrupt the path of the propagating illumination, such that it decouples from the waveguide core and illuminates the diffuser face. This research on both rigid and flexible micro-patterned waveguides provides the basis for the research which follows.

The research presented in this thesis has two primary distinctions from the existing work; it permits the design of mechanically flexible waveguides, and it accommodates targeted illumination. There has been significant research in the field of flexible diffusers, or light guide plates, and the designs and findings from this work are built upon in this thesis. The design principles which may be extracted from existing research are the general configuration of diffusing features and the geometry of the features themselves. Essential to the uniformity of the diffuser's illumination is the density of features with respect to distance from the source. As well, previous research presents multiple potential diffuser features geometries, all of which will be considered in the design of the diffuser

micro-features. While substantial research exists in the design of micro-patterned diffusers, the diffuser region in the proposed waveguide is distinct in that it is illuminated not by an external source, but by the concentrating region of the waveguide, and the diffuser itself is mechanically flexible.

For the concentrating region, however, there is minimal research on the design of a flexible micro-patterned waveguides, thus various adaptations on the design of a rigid solar collector waveguides are considered, evaluated and optimized for the design of a flexible concentrator. Although they only address the design of rigid, micro patterned, concentrating waveguides the work of Karp et al. [5] and Thibault et al. [1] provide the fundamental principles of functionality for the flexible waveguide too. The same concentrating lens and coupling prism configuration will be applied, but altered and optimized for the design of a flexible concentrator waveguide. The flexibility of the waveguide enhances the versatility of the waveguide's potential applications, while reducing the invasiveness of the waveguide itself. A thin, flexible, large-area waveguide could conform unobtrusively to the geometry of any underlying surface, and act as a collector, illuminator, electronic display, optical sensor or any number of other applications.

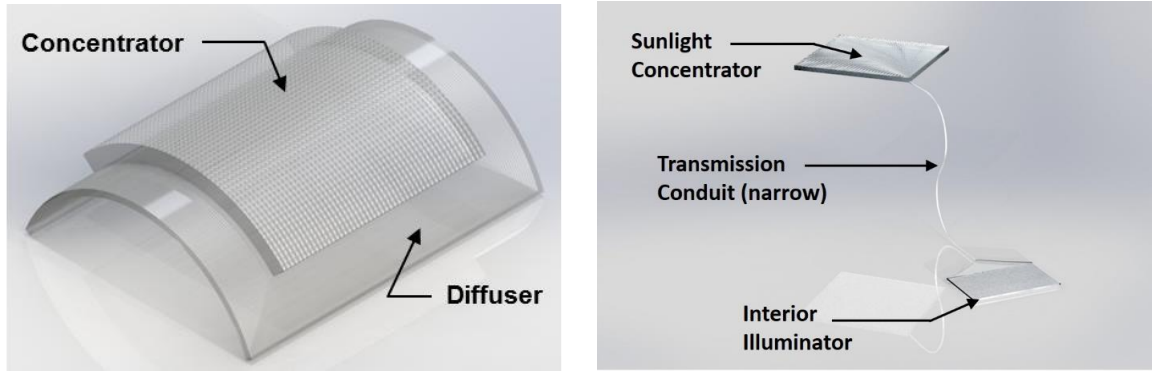
The other element of this research which differentiates it from similar work, is its combination of light collection and diffusion, permitting the use of the concentrator's illumination as the source for the diffuser region of the hybrid waveguide. This configuration permits the controlled guidance of light for targeted illumination by accommodating the collection of light in the area of greatest ambient illumination, transmission to the diffusing region, and illumination of the diffusing region at the target location. This is essential for applications such as light harvesting, but is also ideal for any application for which illumination is required in a low-light area.

1.1 The Problem

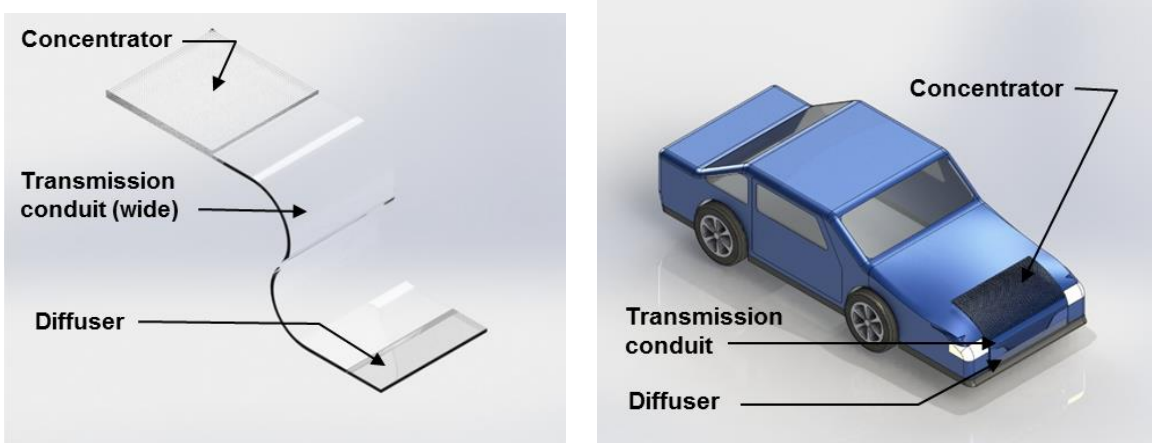
Large-area optical waveguides are a new technology that may significantly impact the future of: wearable devices for light harvesting [11], optically based biosensors in healthcare [12,13], flexible displays on clothing [14], sunlight capture systems for passive

indoor lighting, signature and safety lighting on motorized vehicles [15], and non-planar solar concentrators. These devices are constructed from one or more optically transparent polymer sheets with thicknesses in the range of mm and surface areas that range of from a few cm^2 to several m^2 . Regions of the functionalized waveguide surface can be designed to act as either light concentrator – collectors, light diffuser – illuminators, and/or high efficiency light transmission conduits that perform like a fiber optic strand. These thin polymer layers are constructed from materials that can be bent or even modestly stretched without fracturing or losing their optical properties. The optical performance of the large area waveguide is a function of the location and geometry of the *micro-optical structures* (MOSSs), thickness and shape of the flexible waveguide, refractive indices of the constituent layers, and the characteristics of the incident light source [5].

The non-rigid nature of the large area waveguide means that it can rest upon surfaces with arbitrary geometry. Figure 1.1 illustrates a number of simple and more complex thin large area optical waveguides including a simple curved (Figure 1.1a) light harvesting waveguide with a square concentrator region surrounded by a diffuser that acts as an illuminator [16]. More sophisticated designs where light is directed through a transmission conduit to a distant illumination panel (diffuser) is shown in Figures 1.1b and 1.1c. This basic design is used in solar capture systems that redirect sunlight into buildings for natural illumination. The flexible waveguide sheet can also be made to conform to an underlying three-dimensional geometry (Figure 1.1d). By careful selection of the waveguide materials and design of micro-optical features on the active surfaces it is possible to control the direction of light rays entering, propagating through, and exiting the functionalized large area waveguide.



(a) Small concentrator-diffuser waveguide. (b) Light harvesting indoor waveguide.



(c) Minimal loss light collecting waveguide. (d) Light harvesting automotive waveguide.

Figure 1.1 Illustrations of large-area thin mechanically flexible waveguides for light harvesting and uniform illumination applications. Note that the thicknesses of the waveguide regions are exaggerated for display.

Although a variety of optically transparent materials can be used to create a large area waveguide, the goal of the research reported in this thesis is on developing mechanically flexible waveguides from *polydimethylsiloxane* (PDMS) [17]. These large area waveguide sheets can be fabricated from PDMS using soft-lithography techniques. PDMS has high optical transmittance properties ($> 95\%$) over the visible and near-infrared regions of the electromagnetic spectrum. Furthermore, the viscoelastic properties of the thermosetting PDMS make it an ideal material for accurately producing the inverse

pattern of the micro-features imprinted on the casting mould. This elastomeric material also makes it possible to create multi-layered waveguide structures because the index of refraction of the optically transparent PDMS can be controlled during fabrication by either modifying the ratio of base to curing agent, adjusting the curing temperature or time, applying deep ultra-violet irradiation, or adding high refractive index nanoparticles such as titanium dioxide. In this manner the core and cladding layers can be moulded separately and then bonded together using oxygen plasma or corona discharge bonding to obtain total internal reflection over the prescribed working area of the waveguide. Alternatively, it is possible to fabricate multiple PDMS layers through a multi-stage curing process [17]. The fabrication process, however, is beyond the scope of this research.

Current research on micro-patterned optical devices focuses on the design of rigid planar waveguides. Some important conclusions can be drawn from the design of rigid, large area micro-patterned concentrators and applied to the design of flexible concentrators. Principally, the use of an array of micro-patterned lenses in one layer, aligned with an array of coupling prisms in another layer, beneath the lens array, proves to be the optimal configuration for a large area micro-patterned concentrator with a high concentration ratio [4]. Another important conclusion which follows from the design of rigid micro-patterned concentrators is the importance of minimization of the coupling prism features to prevent losses of propagating rays. This presents an additional challenge in the design of a flexible concentrator, as it significantly limits the acceptance angle of the waveguide.

The research on flexible diffuser waveguides, while also limited, is significantly more robust than that on flexible concentrators. The design of a micro-patterned diffuser has two primary targets: illumination uniformity and light extraction efficiency. The efficiency can be maximized by lengthening the diffuser, however this is detrimental to the uniformity of the diffuser, and thus the light extraction efficiency must increase with distance from the light source to maximize uniformity [18]. While previous research on the design of flexible diffuser waveguides helps guide the design of the diffuser region of the waveguide, there are some aspects of the hybrid collector-illuminator waveguide which make the design unique.

The differences in the design of a rigid waveguide as compared to a mechanically flexible waveguide are discussed in greater detail Chapters 4 and 5, but the primary differences relate to the size, shape and distribution of the coupling prisms. By varying the geometry and spatial distribution of the coupling prisms, the range of acceptance angles of the concentrator, and thus the performance of concentrator undergoing bending, is improved [19]. Another challenge which must be addressed in the design of mechanically flexible concentrators and diffusers is the stretching and deformation of micro-features due to waveguide bending. This challenge has not been significantly investigated in relation to the design of a flexible waveguide however, it has been demonstrated that for mechanically flexible features, the deformation can be limited by reducing feature size.

The impact of design parameters on the performance of these non-rigid light guiding structures is discussed and the parametric optimization of the size, shape, orientation and position of the micro-optical features for maximum efficiency is investigated using Zemax OpticStudio software. The appropriate geometry and spatial distribution of the micro-optical features are, however, application dependent. To illustrate the concept of controlled light guidance and distribution, a non-rigid PDMS waveguide (Figure 1.1a) that performs both controlled light collection (concentrator) and targeted illumination (diffuser) is introduced. For this study the concentrator region utilized an array of focusing micro-lenses and reflecting micro-prisms. The radius, size and spatial distribution of the lens features, and the size, location and shape of the reflecting features will dictate the performance of the concentrator. In contrast, the diffuser is comprised of reflecting wedge-shaped micro-features. Photo-sensors, photovoltaic cells or illumination windows may be located at the light diffusing regions [5]. This design is analyzed and optimized according to a theoretical application, and guidelines are presented for how the design would best be modified for variations in geometry, material properties and applications.

1.2 Applications of Rigid and Flexible Light Guides

Rigid concentrator and diffuser waveguides are predominantly used as solar collectors, and backlight units for electronic displays, respectively. The use of micro-patterned

collectors as a means of collecting solar radiation, permits the focusing of sunlight onto a smaller area of photovoltaic cell, minimizing the cost of the harvested energy [5]. Micro-patterned diffuser waveguides are commonly used as BLUs for electronic displays. The implementation of a diffuser waveguide permits the use of a single light source at one end of the display, which transmits illumination across the entire screen, via the diffuser. This minimizes the size and cost of the displays, allowing for thinner, more compact, electronic devices.

While there are many potential applications for rigid waveguides, by adding the flexibility of the waveguides their applications become much more numerous. Flexible waveguides would be able to conform to the geometry of their underlying surface, and could unobtrusively form a waveguiding membrane on nearly any surface. Potential applications include; wearable devices for light harvesting [11], optically based biosensors in healthcare [12,13], flexible displays on clothing [14], sunlight capture systems for passive indoor lighting [11], signature and safety lighting on motorized vehicles [15], and non-planar solar concentrators. The flexibility of the waveguide is of utmost importance in the consideration of wearable devices, as the waveguide must bend and flex with the users' movements if it is to be a viable, wearable, technology. In this case, the waveguide may harvest incident light over the collecting region of the waveguide, and transmit to the diffusing region for low light photo-therapy, displays on clothing, or other wearable technology.

Light harvesting applications necessitate the combination of both the concentrating and diffusing regions of the waveguide, and perhaps the addition of a transmission fiber. This configuration allows the concentrator to act as the light source for the diffuser region of the waveguide, permitting the illumination of the diffuser without the requirement for any additional source or energy. This is ideal for solar applications, such as: indoor lighting, automotive safety lighting or wearable displays. While these describe some of the applications envisioned for the waveguide, its mechanical flexibility, combined with the diversity of the concentrator-diffuser hybrid design, and the scalability of the product, result in a highly adaptable waveguide which could be used for many other applications.

1.3 Research Motivation and Objectives

Although there is significant literature on the design, optimization, and application of various micro-patterned concentrator and diffuser waveguides, there is little research on the design of flexible waveguides. Flexible waveguides are very common in the field of optical communication, particularly the use of fiber optic cables, however there is minimal research on the design of flexible waveguides for light collection or illumination. Fiber optic cables, while flexible, use typically rigid materials, commonly silica glass, with a small enough fiber diameter that the waveguide is able to bend. This technique could not be applied to the field of micro-patterned optical waveguides at the materials used for fibers in this context, would be too brittle and render the waveguide rigid. For this reason, among other challenges, there is very little research on the design and fabrication of large area flexible waveguides, and this thesis will address some of the shortcomings in this field, and how they can be overcome.

This research endeavors to design and optimize large area waveguides, incorporating a large concentrating region of the waveguide, which collects and directs light to a small, high intensity diffusing region, for targeted illumination. The objective of this research is to identify appropriate geometry for the micro-optical structures patterning both the concentrator and diffuser regions of the waveguide. These parameters are to be parametrically optimized in order to identify the geometric and material properties for which the waveguide is able to perform at maximum capacity.

One of the challenges, and benefits, of the proposed waveguide is its high degree of adaptability. This ensures that the design may be applied for waveguides with various shapes, sizes and applications, however the optimal geometrical parameters will vary in each of these conditions. Where Chapter 4 will investigate and identify the optimal waveguide for maximum performance, Chapter 5 will lay out how this design may be adapted for various applications. The two parallel objectives of this research are: to identify the geometric and material properties for maximum performance of a large area waveguide for targeted illumination, and to establish design guidelines for modifying the waveguide's geometry according to the material and geometric constraints of a given application.

1.4 Design Issues

Although there exist many feasible designs for the development of large area flexible waveguides, each design presents some challenges which must be addressed in the optimization of a large area flexible waveguide. In the design of a typical diffusing waveguide, or in this case a hybrid concentrator-diffuser waveguide, there are two performance targets; efficiency and uniformity of output illumination. For the concentrating region this means that the collection efficiency and transmission efficiency must both be maximized, and for the diffusing region the light extraction efficiency and uniformity must be maximized. Both the large area, and flexibility of the waveguide present challenges in regards to optimization.

Creating a large area waveguide compromises the transmission efficiency, as the longer a ray has to travel, the greater the likelihood that it is decoupled by a subsequent feature, or absorbed by the material. To combat these losses, the coupling features should be made as small as possible to prevent the decoupling losses, and the transmission efficiency of the waveguide material must be optimized. Additionally, to ensure the rays are confined to the propagation region of the waveguide, the waveguide layers must have a sufficient difference in refractive indices, with the core having a significantly higher index than the cladding. It is thus essential that the core is composed of an optically transparent polymer with a high refractive index.

The flexibility of the waveguide presents numerous additional design issues which must be considered. A flexible waveguide will undergo variations in geometry which will affect the orientation of the light source with respect to the features, the orientation of the lens features with respect to the coupling features, and the geometry of the micro-optical features themselves. If the orientation of the concentrating features is unknown, with respect to either the source or to each other, the acceptance angle of the coupling features must be increased to accept the orientation of maximum deformation. This will correspond with larger coupling features, and will in fact be a limiting factor in defining the maximum flexibility of the waveguide. The deformation of the features themselves must also be considered, stretching of the features on the outer surface of the bend, and compression of the features on the inside of the bend will occur. If the waveguide is

designed for applications with a great deal of bending, it must account for these changes in geometry and positioning of the micro optical structures.

It is also important to note that some the solutions to the issues arising from waveguide flexibility, contradict the design guidelines for a creating a large area waveguide. For this reason, it is important to design a waveguide with the constraints of a particular application in mind so that it can be optimized for the given conditions. The design guidelines for creating the optimal waveguide for various conditions, are presented in Chapter 5 of this thesis.

1.5 Overview of the Thesis

This thesis seeks to identify the ideal waveguide geometry for the controlled guidance of light in both rigid and flexible waveguide sheets. The final design is composed of two regions; the region of the waveguide sheet that acts as the light collector, or concentrator, consists of two superimposed PDMS layers with slightly different indices of refraction. The top layer is patterned with micro-lenses that focus the incident light rays onto the pyramid features embedded in the second layer (Figure 1.2). The pyramid shaped feature imprinted on the bottom surface of the second layer act as couplers which reflect the rays and direct the light to the edge of the concentrator region. The difference in index of refraction between the first (n_1) and second layer (n_2) ensures that the light rays striking the pyramid micro-structures propagate laterally toward the concentrator edges by total internal reflection [21]. The boundary region around the concentrator area of the waveguide acts as a light diffuser, or illuminator. The bottom face of the PDMS layer for the diffusing region is patterned with triangular-wedge shaped features that run the full width of the waveguide. These optical wedges are angled such that when the propagating rays strike the micro-feature surface they are reflected at an angle that causes the rays to be refracted out of the layer surface.

Although there are specific design parameters for both the concentrator and the diffuser, these regions of the waveguide must function in unison and therefore the parameters must be optimized simultaneously to achieve the desired light ray transmission through the structure. For example, the thickness of the two bonded layers

$(t_1 + t_2)$ is determined by the focal length of the micro-lenses and the height of the bottom layer (t_2) is selected to ensure that all light rays can be efficiently transmitted from the concentrator to the diffuser. In addition, the refractive indices for the two layers (n_1 and n_2) must be selected so that the rays that enter the bottom layer and reflect off the coupling micro-features are forced to travel along the waveguide to the diffuser region.

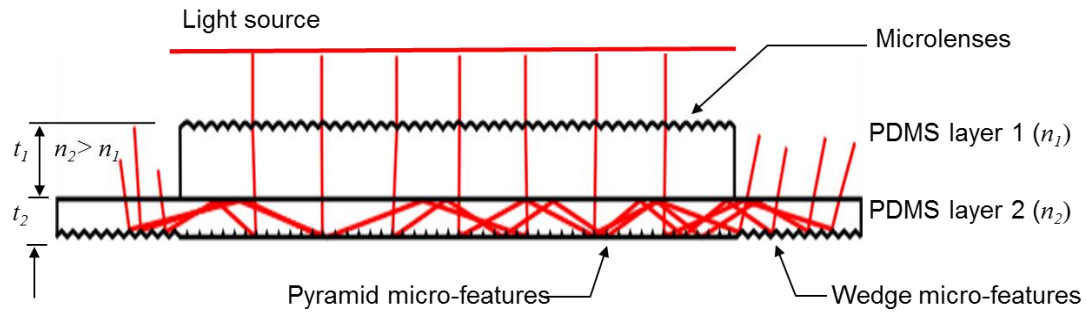


Figure 1.2 Cross-sectional view of a two layer PDMS concentrator-diffuser waveguide. The incident light is focused onto the coupling prisms by the micro-lens array, and directed to the illuminating region, where the light is diffused by micro-wedge features.

This thesis is composed of six chapters, which address the design and parametric optimization of a flexible large area optical waveguide. Chapter 2 explains the fundamental concepts relating to the functionality of a flexible waveguide, and presents an overview of the state of the art in the field of optical concentrators and diffusers. Chapter 3 describes the design methodology used for the subsequent design and analyses. It provides a description of the software used, how it was applied and its limitations, as well as a summary of the metrics used to evaluate waveguide performance.

Chapters 4 and 5 describe the design, analysis and optimization of various waveguides. Chapter 4 focuses on the design of an ideal, optimized waveguide, attaining maximum efficiency for a rigid waveguide in a planar orientation. Chapter 5 looks at how the ideal waveguide may be modified for enhanced performance in various conditions and applications, particularly improving the performance of the flexible waveguide. Additionally, Chapter 5 proposes design guidelines addressing which parameters must be

varied for optimal performance for any variations in constraints of the application. The waveguide presented in Chapter 4 is optimized for high efficiency in ideal conditions and attains efficiencies up to 95%. In Chapter 5, however the waveguide modelled is somewhat more realistic, and much more adaptable, and thus the overall efficiency of the waveguide falls closer to 60%. Finally, Chapter 6 offers conclusions based on the work presented in this thesis, as well as recommendations for future work which could build on this research.

Chapter 2 Literature Review of Optical Waveguide Sheets

2.1 Properties of Light

In order to effectively understand the functionality, and design a novel optical waveguide sheet it is necessary to understand the fundamental properties of light, and how it interacts with the media through which it travels. This section presents an overview of the properties of the light as they relate to optical waveguides.

2.1.1 Light and Electromagnetic Spectrum

Light is a form of electromagnetic radiation, typically referring to the ultraviolet, visible and infrared regions of the electromagnetic spectrum, represented in Figure 2.1, with wavelengths from 10-400 nm, 400-700 nm and 750 nm-1 mm respectively [21]. Visible light is the range of wavelengths which can be detected by the human eye, ranging in colour from violet to red. Blues and violets lie at the lower end of the visible range with shorter wavelengths, and higher energy, and reds and oranges at the upper end of the visible spectrum, with longer wavelengths and less energy.

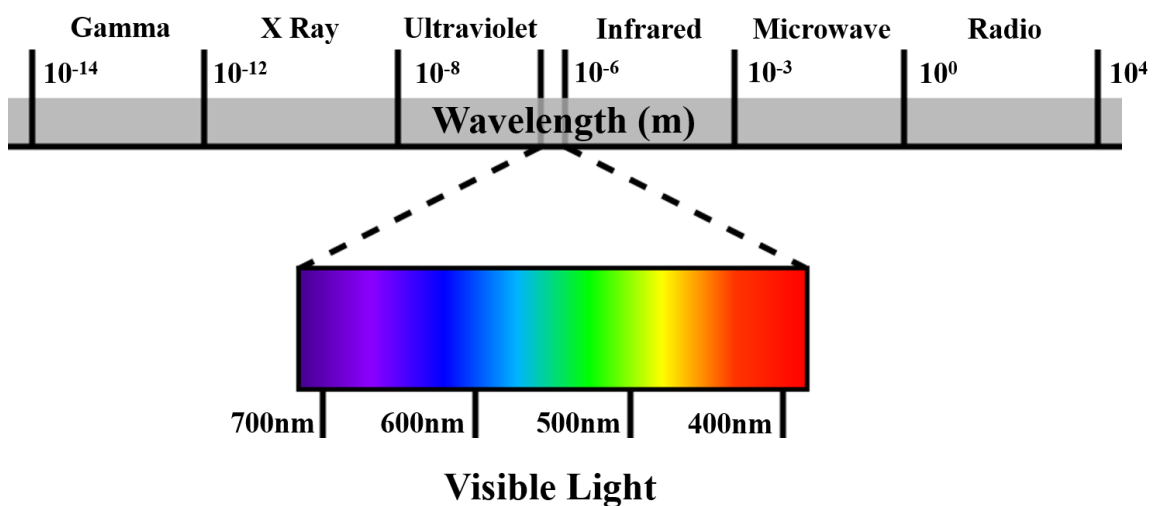


Figure 2.1 The electromagnetic spectrum encompasses various types of radiation which exhibits both electric and magnetic properties. Visible light occupies the mid-range of the electromagnetic spectrum representing wavelengths from 400 to 700 nm.

Typically, the light detected by the human eye is the actually being reflected off objects, and perceived by our eyes, few objects are actually light sources. When object do act as light sources, they emit light in the form of energy. This packet of energy, emitted as light, is known as a photon, as seen in Figure 2.2. On an atomic level, when an electron gains energy, or becomes excited, it jumps up to a higher orbital ring. This is a temporary state of excitement, however, and when the electron falls back to a lower-level shell, the excess energy is emitted as a photon.

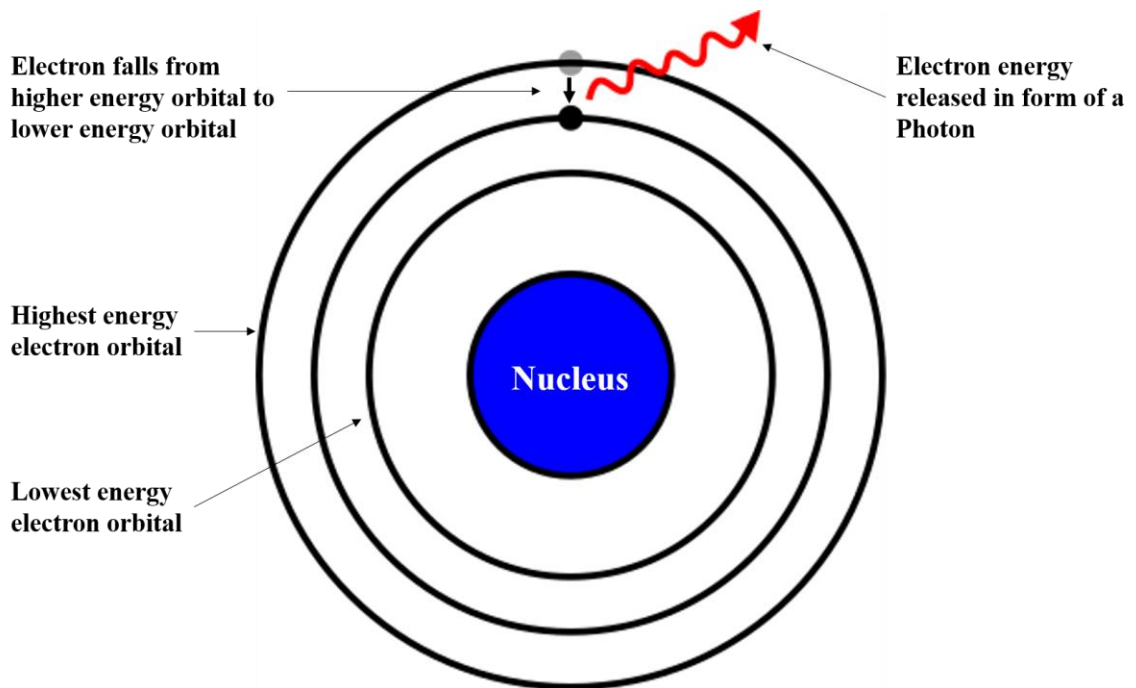


Figure 2.2 Depiction of an electron which falls from the outermost (highest energy) electron shell to a lower energy shell; it releases a packet of energy known as a photon. This photon of energy is perceived as light.

This fallen electron will have a particular photonic energy (E) which is related to the distance which it falls [23]. The photonic energy is related to the wavelength of the radiation by:

$$E = \frac{hc}{\lambda} = h\nu \quad , \quad (2.1)$$

where the energy E is a quantum of electromagnetic radiation, h is Planck's constant of 6.63×10^{-34} J-s and ν is the frequency of radiation. The frequency is $\nu = \frac{c}{\lambda}$ where c is the velocity of light (2.99×10^8 ms⁻¹) and λ is the wavelength of light in meters. As h and c are both constants, the photonic energy is inversely proportional to the wavelength of the radiation. The natural frequency of the material acting as the light source will dictate the photonic energy released by the atom. For materials which emit radiation in the visible range, the photonic energy released will be between 1.65 and 3.26 eV, corresponding to wavelengths between 400 and 700 nm.

2.1.2 Wave-Particle Duality of Light

For centuries physicists have questioned the fundamental nature of light, settling over time on two seemingly contradictory theories; light as a wave, and light as a particle. One of the earliest descriptions of the wave properties of light appears in Christiaan Huygens' 1690 explanation of his undulatory theory, in which he speculated the vibrational nature of light. Less than 15 years later, however, Isaac Newton contradicted Huygens' undulatory theory, with a particle theory of light. Unlike the wave-theory, Newton's description could account for the ray-like properties of light, including propagation and reflection [22].

While both theories had their merits and believers, neither could be proven nor disproven, until Thomas Young conducted his famous double-slit experiment in 1801. Young shone light through a small hole at a card with two slits cut in it side by side, and observed the light patterns projected on a screen beyond the card. If the particle theory of light were to hold up, it would be expected that the light would project directly out the slits, forming an image mimicking the slit pattern. This is not what Young observed. He saw, instead, that the light created bands of brightness and darkness on the screen, which could only be explained by wave-theories of light. The waves emanating from the two slits had created interference patterns, illuminating the screen where the waves exhibited constructive interference and creating dark bands where the interference was destructive, as illustrated in Figure 2.3.

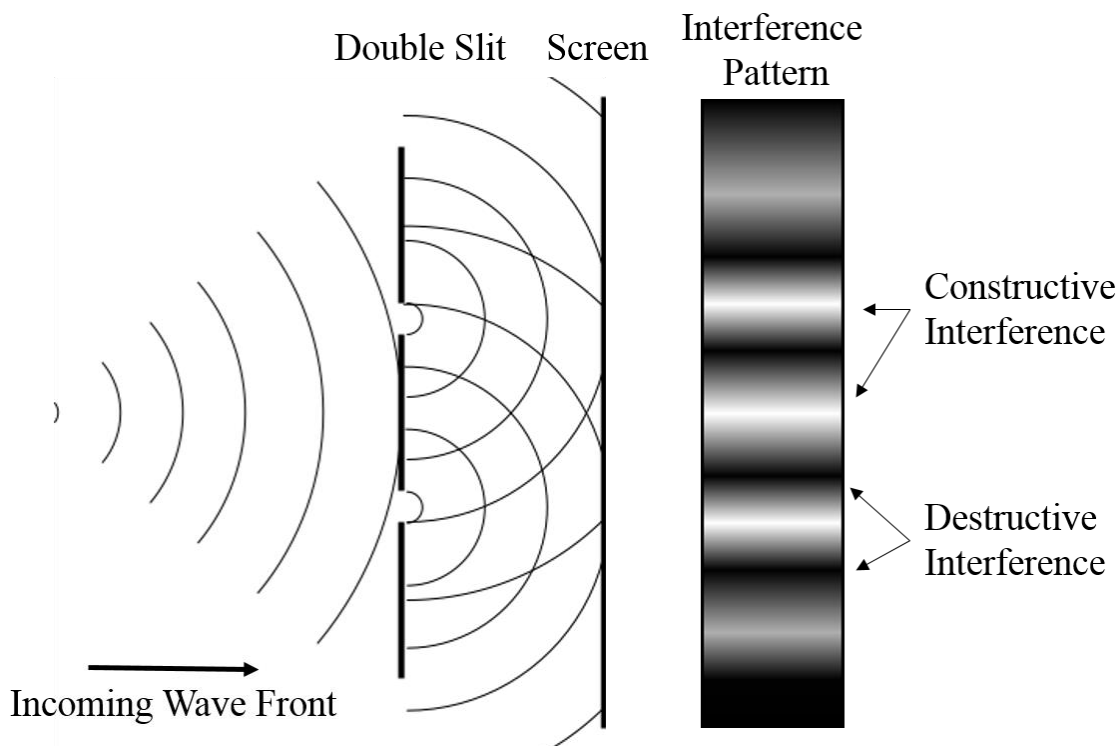


Figure 2.3 Young's double slit experiment separated a light source into two wave fronts whose interference pattern was projected onto a subsequent screen. The interference pattern observed confirmed the wave properties of light.

Thanks to Young's double slit experiment, it was widely accepted that light was in fact a wave for the majority of physicists through the 19th century. That is, until the early 20th century, when Albert Einstein studied the photoelectric effect. Einstein observed that when shining electromagnetic radiation onto a metal object, he was able to detect electrons emanating from its surface. His proposed explanation was that the light struck the metal's surface in discrete packets of energy, photons. These photons strike the surface, and transfer their energy to the atom, displacing an electron. This energy packet, or photon, can either be absorbed, reemitted, or transferred through the material. Einstein's explanation of the particle theory of light, is still widely upheld, and forms the basis for modern day quantum mechanics.

Neither the particle theory nor the wave theory, however, fully describes and predicts the behavior of light. It is widely accepted by modern scientists that light exhibits

properties of both a particle and a wave. This theory is known as the Wave-Particle duality. It is often best to consider light as a wave for larger scale analyses of its properties, while at an atomic scale, light is best treated as a particle.

2.1.3 Transmission, Absorption and Reflection

Although some objects behave as light sources, emitting light, the majority of media serve to absorb, reflect or transmit light from external sources. Whether the light is absorbed, transmitted, or reflected can also be explained by the behavior of the material at an atomic level. It is best to consider light as a particle to explain its atomic behavior. When a photon strikes a material's surface, it will transfer its energy to the atom which it hits. Depending on the properties of this material, the photon may be absorbed, reflected or transmitted [23].

If the photon's frequency is equivalent to the resonant frequency of the atom it strikes, the atom will begin to vibrate, exciting neighbouring atoms, and eventually the vibration dissipates the photon's energy as heat. This results in the absorption of the incident photon, and also accounts for materials' colours. For example, the resonant frequencies of a red object will be equivalent to the frequencies of orange, yellow, green, blue, indigo and violet photons, such that the only incident light that is not absorbed is red.

If the photon strikes an atom with a frequency other than its resonant frequency, the atom will momentarily absorb the energy, and an electron will jump to a higher orbital, but in doing so will become unstable. To regain its stability, the electron will quickly fall back to its original position, emitting a packet of energy, a photon, equivalent to that which originally struck the atom. This photon may be reflected back towards the source, or transmitted through the material. If the material is optically transparent, the photon is reemitted by the atom, and strikes an adjacent atom, which briefly absorbs and then reemits it. This is repeated throughout the material, transmitting the photon, and therefore the light, through it. If a material is opaque, it is unable to transmit the light through it, but rather the photon is reemitted in the direction it came from, resulting in a reflection off the surface. Nearly all materials do some degree of absorption, transmission and

reflection, but the degree to which they do each dictates the optical properties of the material.

With an understanding of the quantum behavior of light, it is beneficial to consider its wave properties as well, especially when contemplating the laws of reflection and refraction. When a light waves strikes the interface between two materials it will either be reflected off this surface, and travel back through the original medium, or traverse the boundary and travel into the new medium. If it is reflected, it will travel back at an angle (θ_2) equivalent to that at which it struck the interface (θ_1), whereas if it continues into the new medium, it will continue travelling in the same direction, but at a slightly different angle, as seen in Figure 2.4. This change in angle is known as refraction [24].

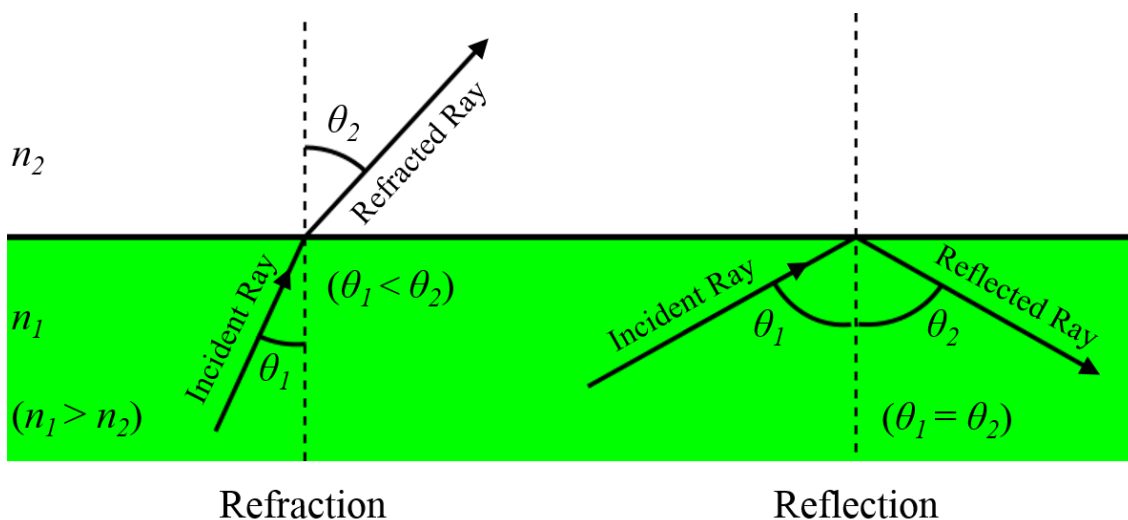


Figure 2.4 Light strikes the interface between two materials, with different refractive indices, it may traverse into the second medium by refraction, or be reflected back into the first medium.

Although particle-theories of light offer an explanation for why light may be reflected or refracted, they do not account for the path taken by the reflected or refracted photon. Wave theory, however, provides a thorough understanding for the propagation of light through various media. This highlights the importance of understanding the duality of light, and having an appreciation for both its wave and particle nature.

2.1.4 Geometric Optics

While the atomic-level properties of light are important in analyzing how it interacts with a material, in the context of understanding and predicting the behavior of light in an optical waveguide, it is primarily the large scale properties of light which are of concern. In this case, the behaviour of light can be represented as a straight line, largely ignoring the wave and particle properties of light, and considering it to be simply a ray. This is known as geometric optics [24].

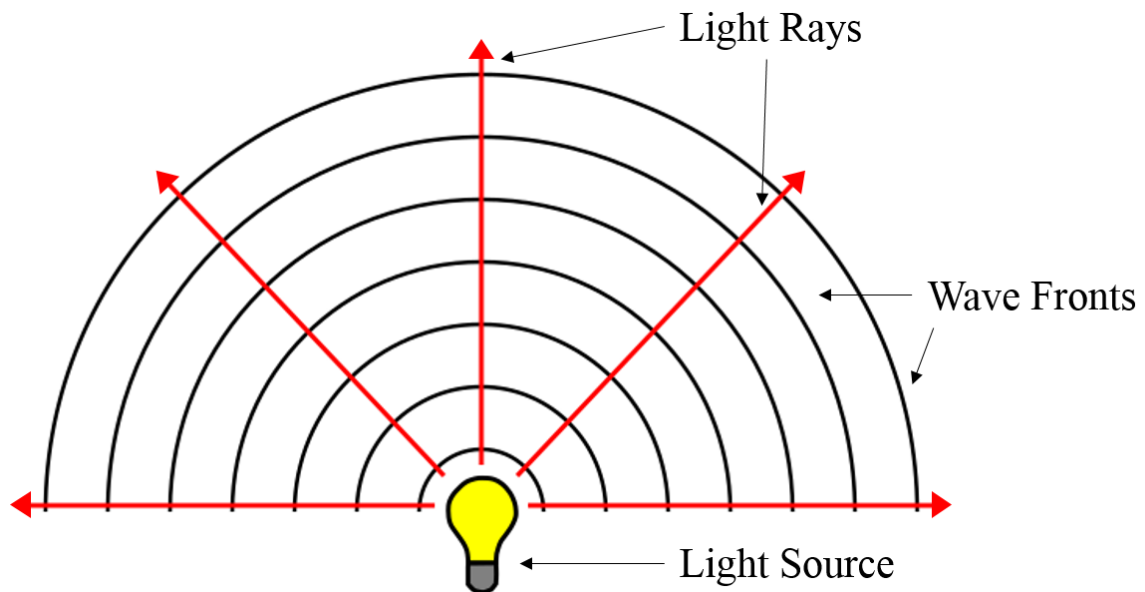


Figure 2.5 Wave optics represents light as a wave which propagates outwards from a source, whereas geometric optics simplifies the source into rays travelling perpendicular to the wave fronts.

Geometric optics represents the propagation of light as a straight line through a media, travelling perpendicular to the wave front, represented by the red rays in the above Figure 2.5. While geometric optics fails to account for some of the micro- and atomic-scale properties of light, it accounts for all of its macroscopic behaviour. Geometric optics assumes that in any medium light will travel along its same path, until it reaches an interface between two media. Upon striking the interface between the media, the ray will

either be reflected back into the media from which it originated, or transmitted into the new medium, according to the laws of total internal reflection.

Geometric optics provides a simple approach by which the path of a ray of light may be predicted, according to its expected interaction with optical devices, such as mirrors and lenses. This permits the analysis of an optical system without having to construct it, as the path of a ray can easily be calculated according to the laws of reflection and refraction, if the geometric and material properties of the system are known. This theory is implemented in the Zemax OpticStudio software, which traces the ray path according to geometric optics and can be used to analyze the functionality and performance of various optical systems.

2.1.5 Limitations of Geometric Optics

Although geometric optics provides a simple and effective method of analyzing the performance of optical systems, it is also important to appreciate the limitations of this method. Because geometric optics neglects the consideration of the wave and particle behaviour of light, some optical effects cannot be analyzed using geometric optics. Notably, since the wave nature of light is not considered, the effects of interference and diffraction cannot be assessed by ray optics [24].

As discussed above, interference occurs when two wave-fronts of light cross path with each other. Where the crests or troughs of the wave meet the interference is constructive, increasing the amplitude of the wave. Where a crest of one wave meets the trough of another the interference is destructive, flattening the wave [25]. Diffraction occurs when light interacts with an object with geometry close to, or smaller than, the wavelength of light in consideration. The light wave interacts with the feature, such that it causes some bending of the wave around the feature, typically emphasizing the emanation of waves from this location [26]. Diffraction was prominently visible in Young's double-slit experiment. The experiment relied on the diffraction of the wave through each slit, creating the two separate wave fronts, emanating from each slit, and ultimately producing the interference pattern which made the experiment famous.

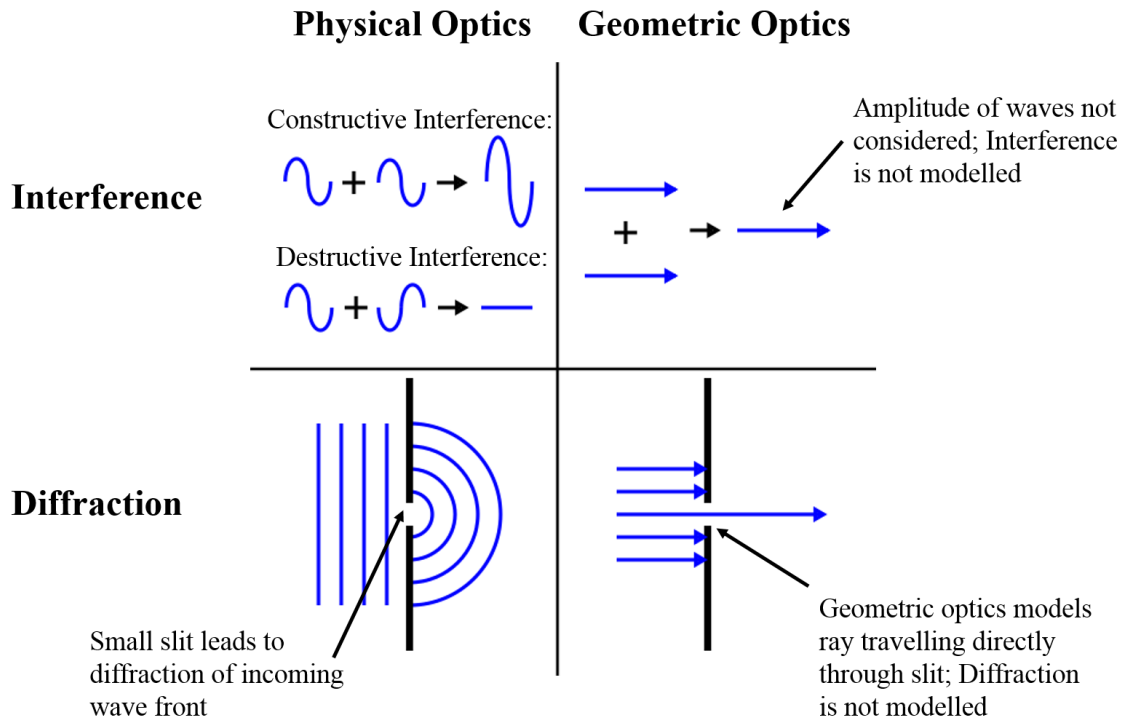


Figure 2.6 Geometric optics does not represent the behaviour of waves well at the micron scale. Interference and diffraction are not accounted for using geometric optics, as the rays do not interact as such.

While these are both important optical effects, which must be understood, they can be neglected in the geometric optics analysis of a waveguide under certain circumstances. Because the effects of wave interference, and diffraction are most prominent for features of the scale of the wavelength of light, if the geometry in consideration is substantially larger than the wavelength of light, the effects are essentially negligible. These limitations of the geometric optics analysis are illustrated in Figure 2.6. In order to apply geometric optics analysis, the feature size of the relevant geometry should be no less than 10 times the wavelength of light, to mitigate the effects of interference and diffraction. In the case of visible light, the wavelength is between 400 and 700 nm, therefore the smallest dimensions should be no less than $7\mu\text{m}$. When considering the possibility of interference, the limiting dimension is the thickness of the waveguide layers, since if they become too thin the light will begin to interfere with itself as it propagates through the

waveguide. To mitigate the impact of diffraction, it is necessary that no optical features are smaller than the minimum size, as the lens and prism features approach the wavelength of light, the waves will diffract around them [24]. Thus, no waveguide layer, or optical feature, should be less than $7\mu\text{m}$ if geometric optics theory is to be applied.

Additionally, when considering reflection and refraction, there are some specific optical effects which are not accounted for with geometric optics. Particularly when considering reflection of light off a surface, geometric optics fails to differentiate between specular and diffuse reflections. A specular reflection is similar to that off of a mirror, in which incident light is reflected at the same angle which it strikes the surface, whereas a diffuse reflection scatters the reflected illumination. In order to be able to predict the orientation of rays as they reflect off surfaces, by means of geometric optics, it is assumed that the reflection is specular. To ensure that the geometric optics model accurately represents the physical optics, all waveguide surfaces should be made as smooth as possible to increase the specularity of reflections. The geometric optics model also, assumes that light crossing an interface will be either completely reflected, or completely refracted. While this is largely true, for every ray interaction there will be small amounts of reflection and refraction both. This can be limited by ensuring consistent geometric and material properties.

Material properties of the waveguide, must too, be considered, when addressing the limitations of the waveguide analysis. The geometric optics analysis done, assumes transparency of the material in consideration, however even transparent materials absorb some of the transmitted illumination, this is known as attenuation. The attenuation of the illumination occurs as the light propagates through the material, and can be predicted according to the material's attenuation coefficient, and the length over which the light travels. Another fundamentally important material property, is its *refractive index*. The refractive index of the material is the dimensionless ratio of the speed of light in that material, compared to the speed of light in a vacuum, and it dictates whether the light will reflect or refract at an interface between transparent materials. It is important that both the attenuation coefficient and the refractive index are constant through the material. This will ensure that the geometric optics calculations and simulations apply to the whole body, and prevent aberrations to the predicted ray path.

Although there are numerous limitations to the application of geometric optics theory, if all the necessary conditions are met, it provides a simple, thorough and accurate analysis of the optical system. Specific requirements for the application of geometric optics to the design and analysis of the optical waveguide are; minimum dimensions of waveguide layers and features, clearly defined and constant materials properties, smooth surfaces and interfaces between media, and consistency between the simulated and manufactured geometries. If these conditions are met the geometric optics model will provide a highly accurate prediction of performance. However, it is likely that a real-life waveguide will differ slightly from the idealized geometric optics model, whether it be in variations to the waveguide geometry or material properties. If these variations are predictable, they may be incorporated into the model and simulations, but it is still expected that unpredicted deviations from the simulations will occur. In this case, the model may slightly over-predict the waveguide's efficiency, as it would fail to account for some of the losses, but it will still serve to sufficiently predict its performance.

2.2 Operating Principles of Flexible Optical Waveguides

2.2.1 Total Internal Reflection (TIR) in Waveguide Sheets

Total internal reflection is the principal by which the light propagating in the waveguide sheet is confined to the desired region. Total internal reflection occurs when light travelling through a medium of a particular refractive index (n_2), strikes another material with a lower refractive index (n_1), at an angle greater than the critical angle [23], causing the ray to be reflected back into the medium it is travelling through (Figure 2.7). The critical angle, θ_c between any two media is wholly dependent on their refractive indices:

$$\theta_c = \sin^{-1}\left(\frac{n_1}{n_2}\right) \quad (2.2)$$

In the case of a waveguide sheet, or an optical fiber, the light is confined to a particular region by surrounding the medium through which the light is travelling (the core), by a material of a lower refractive index (the cladding). This method ensures that no matter where the rays strike the core surface they will be contained by total internal reflection as

they strike the cladding, so long as they are propagating at an angle greater than the critical angle.

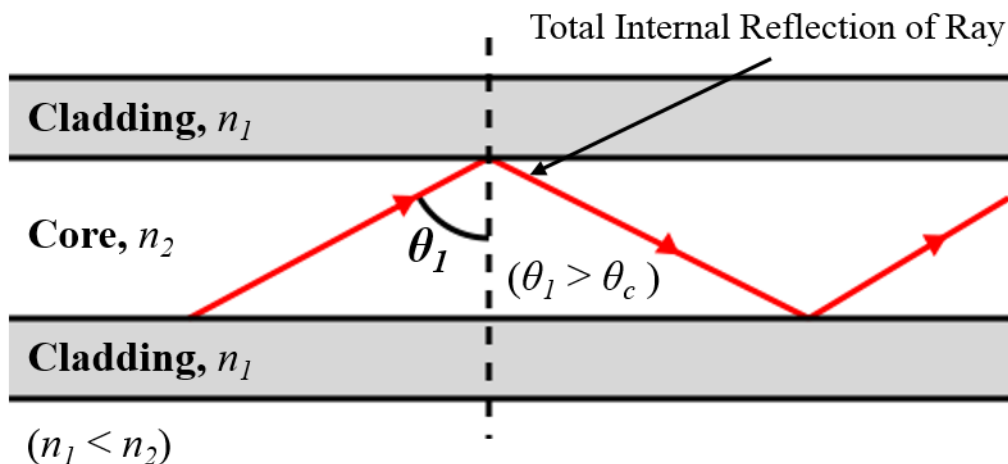


Figure 2.7 Total internal reflection in a waveguide sheet occurs if the core has a refractive index sufficiently larger than that of the cladding, as this will ensure the ray is reflected off the boundary between the media.

In some cases, this cladding material is simply air. Air is an excellent cladding in that it has a refractive index close to 1, therefore permitting lower critical angles, but it is also a relatively unreliable cladding material. Because the cladding must surround the core, the waveguide would have to be suspended in air, in a controlled environment to inhibit other materials, such as dust and dirt, coming into contact with the core. Although there are some obvious challenges in using air as a cladding, it can often be found as a cladding material in electronics displays and similar waveguide applications.

When considering bending of an optical waveguide, the critical angle will correspond to a minimum allowable radius of curvature; the critical bend radius (R_c). Since the rays must strike the cladding at an angle greater than θ_c , if there is a bend in the waveguide which exceeds the critical bend radius, it will cause the rays to strike the cladding at an angle lower than θ_c and they will refract out of the waveguide. Figure 2.8 illustrates the difference between a curve with a radius (R_1) that does not exceed the critical radius, and a bend (R_2) which is smaller than the critical radius, leading to light leakage.

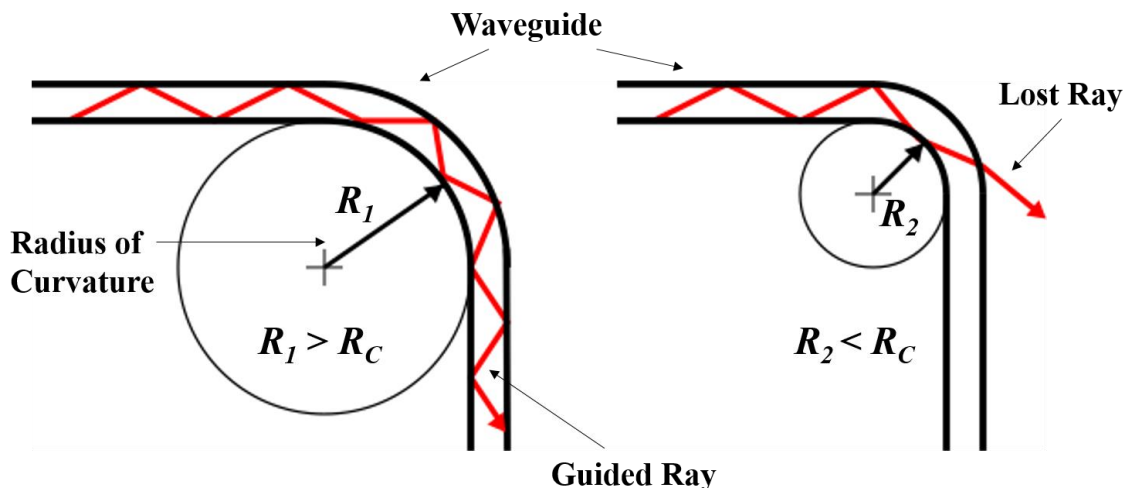


Figure 2.8 The critical radius of curvature of a waveguide represents the minimum radius to which a waveguide may be bent without the propagating light failing to reflect back into the core, and being refracted out.

The critical angle is directly related to the relative refractive indices of the core and cladding layers, and thus the critical bend radius can be made smaller by increasing the ratio of the core to cladding refractive indices. For bends smaller than the critical bend radius, the propagating rays attenuate quickly and significantly, therefore bends greater than the critical radius should always be avoided.

Besides the inherent limitations of waveguiding by total internal reflection, it is an excellent method for transmitting illumination through an optical waveguide. It avoids the use of a potentially expensive, non-uniform, and complicated reflective coating, while still confining all rays propagating at an angle greater than or equal to the critical angle.

2.2.2 Structure of an Optical Waveguide Sheet

A typical optical waveguide sheet confines light by total internal reflection using a cladding-core-cladding layering structure. The cladding layers have a lower refractive index than the core material, and thus when a ray strikes the interface of the layers at angle greater than the critical angle, it will be reflected back into the core [24]. If the rays' angle of propagation, however, is less than the critical angle it may exit the core

into the cladding, and may exit the waveguide altogether, or continue to propagate in and out of the cladding. This often occurs in a waveguide when a bend causes the ray to strike the interface at angle less than the critical angle, and decouple.

Although a ray which exits the core can still be guided by the cladding, this is undesirable for many reasons. Primarily the cladding protects the core, and acts as a boundary for the propagating rays, so that they do not interact with the outer surface of the waveguide. This will ensure that any surface scratches do not impact the efficiency of the waveguide, and that the core does not come into contact with a high refractive index or absorptive material. In some cases, it is ideal to use air as a cladding-like material, as it has a lower refractive index than any other substance. This will induce a much lower critical angle, and allow for more dramatic feature orientations, however this removes the protective capabilities that a traditional cladding provides. This is especially beneficial with the use of micro-optical structures which incorporate varied ray-feature interactions which may depend on substantial differences between core and cladding refractive indices. Depending on the nature and application of a waveguide, the use of a physical cladding may be necessary, or an air “cladding” may be used for optimal waveguide flexibility.

There exist many other waveguide structures which do not conform to the standard core-cladding-core structure, which are often used for signal transmission in optical fibers. Another common fiber structure is the graded-index fiber. As the name suggest, graded index fiber have a varying refractive index throughout the core, with the highest index at the center, decreasing outwards. This allows the rays to take a sinusoidal path through the fiber, which while beneficial in signal processing, is not typically used in illumination applications. Similarly, single mode fibers are a method of limiting the transmitted signal to a single wavelength, and again it is typically not used for illumination optics.

2.2.3 Optical Losses

In order to design a high efficiency waveguide for controlled guidance of light, it is necessary to understand and predict the causes of optical losses in order to mitigate their

effects. The primary sources of loss and their effects on waveguide performance are discussed in this section.

2.2.3.1 Light Entry into the Waveguide

There are typically two ways by which light enters concentrating and diffusing areas, concentrators' faces are illuminated and the lenses serve to collect the illumination, and diffusers' are typically illuminated by LEDs which are coupled with, or embedded in the waveguide core layer [27]. In the case of the concentrator lenses, it is essential that all light is focused onto the coupling prisms in order to efficiently collect the light. There are some potential sources for loss as the light enter the waveguide, particularly caused by the shape and distribution of the lens features.

Light can only be coupled into the concentrator if it is collected by the lenses, thus it is essential that all incident illumination strikes a lens feature. If there is any gap between the lens features, the incident light will travel directly through the concentrating layers without being focused or coupled, and it is therefore lost. Additionally, the shape of the lenses will dictate the size of the focal location. An aspheric lens will have the smallest focal point, however a spheric lens is much easier to reliably and efficiently manufacture so it may be used as well. This will result in a slight dispersion of rays at the focal point which can be offset by making the coupling prisms slightly larger such that all focused rays are coupled. Finally, the focused light can only be coupled into the concentrator's propagation layer if it strikes the coupling prisms at the appropriate angle. The angle must be large enough that the reflected rays propagate at the desired angle, but not so large as to not be reflected off the prism face. If these conditions are met all the focused light can successfully be coupled.

In the case of the diffusing region of the hybrid waveguide, it is unlike a traditional diffuser, as it is not lit by an external, or embedded source, but rather is illuminated by the concentrated light from the collector. Because the proposed fabrication of the waveguide is monolithic, the concentrating region and diffusing region are in fact one continuous piece of a single material, thus 100% of illumination propagating in the

concentrator will be transmitted to the diffuser. This unique aspect of the hybrid waveguide eliminates the losses typically associated with the diffuser's light entry.

In order to ensure that the maximum amount of light is captured into the waveguide, it is essential that the entire active surface is patterned with lenses and the coupling features are sufficient in size, and angle. If this is the case the light entry into the waveguide will result in minimal losses, conducive to a high efficiency waveguide.

2.2.3.2 Numerical Aperture

The numerical aperture (NA) describes the ability of an optical device to collect light, and is expressed in relation to its acceptance angle. The acceptance angle of a particular medium can be defined in relation to its refractive index, thus the numerical aperture may also be expressed in terms of refractive indices. The numerical aperture is calculated as:

$$NA = n_0 \sin \theta_a , \quad (2.3)$$

where n_0 is the refractive index of the medium in which the optical device is located, and θ_a is the maximum angle at which a ray can strike the optical device [27]. For a lens, the acceptance angle is dependent on the diameter of the lens, and the focal length of the lens. The maximum angle can be estimated by:

$$\theta_a = \tan^{-1} \left(\frac{D}{2f} \right) , \quad (2.4)$$

where D is the diameter, and f is the focal length, of the lens in consideration. In the case of a cladding-core-cladding waveguide the maximum angle is defined by the difference in refractive indices of the core (n_1) and cladding (n_2) and may be expressed as:

$$NA = \sqrt{n_1^2 - n_2^2} \quad (2.5)$$

Therefore, the acceptance angle of the waveguide, as seen in Figure 2.9, can be calculated in relation to the refractive indices according to:

$$\theta_a = \sin^{-1} \frac{\sqrt{n_1^2 - n_2^2}}{n_0} \quad (2.6)$$

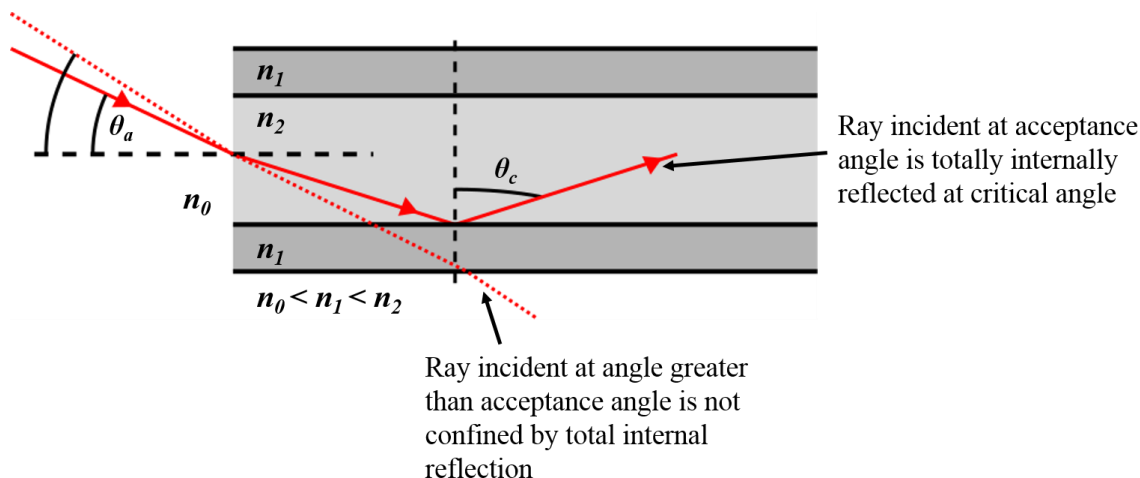


Figure 2.9 The acceptance angle of a waveguide is defined by the maximum angle which can be contained in the waveguide by total internal reflection. Angles of incidence greater than θ_a will not be contained in the waveguide core.

2.2.3.3 Transmission Efficiency

There are two primary sources of loss associated with the transmission efficiency of the waveguide; losses caused by the material's own transmission efficiency, and losses caused by propagating rays' undesired interactions with features. In both cases the longer the length of transmission through the waveguide, the greater the losses will be, thus a smaller waveguide area will minimize the transmission losses, however these losses can be mitigated to create efficient large area waveguides.

Regarding the properties of the material itself, the primary cause of lost illuminations is the material absorbing some of the light [23]. As mentioned in Section 2.1, all materials reflect, transmit and absorb light to some degree, however materials which absorb the majority of light are called opaque, whereas materials which transmit visible light are known as optically transparent. Transparent materials absorb small amounts of light, but they are able to transmit light at very high efficiencies, the degree to which it transmits light is known as its clarity or optical transparency. In order to transmit light through the waveguide with high efficiency, it is necessary that the material selected for the waveguide has a high optical transparency.

The geometry of the waveguide also presents a challenge with respect to the transmission losses in the waveguide. Upon being collected into the concentrator's lower layer by the coupling prisms, all interactions with the prisms should be avoided, as any ray which strikes the prisms as it propagates through the waveguide will be decoupled. While the coupling prisms are necessary for the collection of light, after serving their function they become obstacles in the path of the light rays travelling to the concentrator's edge, and thus their size should be minimized. Their size should not exceed the minimum required size for coupling of rays and application of geometric optics, as any features in excess of this size will reduce transmission efficiency. Although the waveguide's efficiency will decrease with size, due to the transmission losses in the material, as well as the geometry, these losses can be managed by appropriate material selection, and minimization of the coupling features in order to design a large area, high efficiency waveguide.

2.2.3.4 Losses Due to Material Faults in Core and Cladding

Losses arising due to inconsistencies, or imperfections in the material's composition will result in losses directly and indirectly. Some material irregularities which will result in these losses are inconsistent material composition, and localized imperfections in the material. Inconsistencies may be variations in refractive index throughout a particular layer, which will cause undesired redirection of all rays which interact with this layer. Local imperfections may be a foreign object, such as dust between the layers, or an air bubble within the polymer, or a scratch or structural defect on the surface of a layer or feature.

If incident rays strike a material irregularity, their path will likely be irreparably altered such that they do not strike the coupling prism, and cannot enter the propagation layer. If a ray which is successfully coupled subsequently strikes an imperfection, its ray path will be altered. It may be redirected at such an angle that it is immediately decoupled, or it may continue to be transmitted, however its subsequent interactions with the MOSs will be altered to the extent that it is not successfully diffused, further reducing the overall efficiency. Because any imperfections will result in significant losses, all of

which are intensified over a large area waveguide, it is important that the material is consistent in composition, and there are no foreign particles in the material.

2.2.3.5 Bending Losses

Bending losses in optical waveguide are classified into two categories; micro-bends and macro-bends. Macro-bends are large scale flexing of the waveguide which are easily visible, and often intentional. These are the bends which would occur in a flexible waveguide, and the associated losses must, therefore be mitigated. Micro-bends are bends in the waveguide which are less than about 1 mm, and typically result from the manufacturing process. Both macro- and micro-bends will result in propagating rays decoupling, as they strike the interface between the core and cladding at an angle less than the critical angle [28].

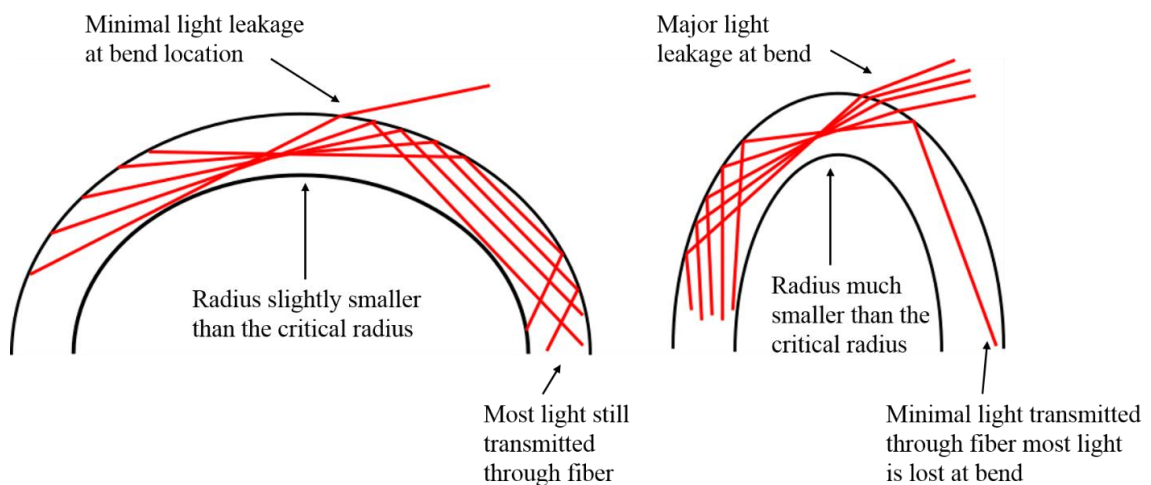


Figure 2.10 The proportion of light lost due to bending relates to the degree to which the waveguide is bent past the critical radius. A smaller radius of curvature results in greater light leakage.

This phenomenon, seen in Figure 2.10, is known as light leakage and happens gradually according to the severity of the bend, and the angle of propagation of the light. If the rays are propagating through the waveguide at an angle much higher than the critical angle, they are much less likely to be lost, and can tolerate large bends. If the rays

are propagating at an angle close to the critical angle, then even small macro-bends, or micro-bends will result in significant losses. Additionally, the difference in refractive indices will correspond to the degree of light leakage, a larger difference in refractive indices will permit larger bends with less losses. Similarly, if the waveguide is in air, then the light which escapes the core may still be confined to the cladding of the waveguide, and transmitted to the ray's destination, albeit at a lower efficiency. To mitigate the effect of micro-bending losses, care must be taken in the manufacturing process to create a smooth finish on the waveguide layer. To control losses arising from macro-bends, the waveguide may be designed to uphold efficiency for the desired degree of bending, and bending outside this range must be avoided.

2.2.3.6 Impact of Surface Scratches on TIR

Similar to the impact of losses due to material faults, surface scratches will cause rays which strike irregularities to decouple. Fortunately, if cladding is used, the impact of surface scratches can be minimized. If surface scratches exist only on the outside of the cladding, they will have a minimal impact on total internal reflection, as the rays should be confined to the core and will not interact with the scratches. A deep scratch however, may reach the core, or cause deformation to the core, leading to substantial losses, thus even scratches to the cladding should be avoided where possible. Although much less likely to occur than a surface scratch, if during the manufacturing stages, the surfaces between the layers are scratched, the impact of the scratch is intensified. In this case if a propagating ray strikes the scratch as it interacts with the interface between the layers, it will either refract or reflect at an angle which causes the ray to decouple. Additionally, if the scratch is of the micron scale in size it may even lead to interactions inducing the light's wave properties and causing additional losses by diffraction and interference. It is thus necessary to minimize the occurrence of scratches between the waveguide layers.

While less significant, the impact of scratches on the outer surfaces of the waveguide must also be considered. If there exist scratches on any of the exposed optical features, such as the lenses, coupling prisms and diffusing wedges, it will lead to undesired interactions between the rays and the features. If there is a surface scratch on the concentrating lens, the incident rays which strike this location on the lens will not be

focused, and therefore will not be coupled into the waveguide. Similarly, rays which strike a scratch on the coupling prism will not be collected in the waveguide, however the impact of a scratch on the coupling features will be much greater as the features are much smaller in scale. Therefore, even a small scratch on the prism could lead to substantial losses. The impact of a scratch on the diffusing wedges is less detrimental, as depending on the orientation of the scratch, it may actually enhance diffusion, thus lessening the negative impact. In general, surface scratches must always be avoided, with particular attention to smaller features and the surfaces joining the waveguide layers.

2.3 Concentrators and Diffusers

Optical waveguides are most commonly used in fiber optic applications, in which they transmit a signal, transmitting rather than collecting or diffusing illumination. Although less common than fiber optic cables, waveguides are also used in concentrating and diffusing applications. Concentrators serve to collect illumination over a large area, and concentrate it to a smaller area, intensifying the illumination. The most common application for light concentrators are solar collectors, which permit the concentration of illumination onto photovoltaic cells, thereby reducing the size and therefore the cost, of the required PV cell. Diffusing waveguides work in the opposite way, by distributing light from a source over a larger area, illuminating the surface of the waveguide. Diffusing waveguides are widely used in electronic displays, acting as the backlight of the device's screen, these waveguides are known as *light guide plates* (LGPs).

Both concentrating and diffusing waveguides operate on the principal of total internal reflection within a layered structure, and interaction with micro-optical structures. The geometry, placement and size of the MOSs determines their interaction with the source illumination and dictates whether the waveguide acts as a concentrator or diffuser.

2.3.1 Edge and Face Lit Waveguides

One primary distinction between whether the waveguide acts as a collector or illuminator, is the lighting configuration. The waveguide may be either edge-lit, a diffuser, or face-lit, a collector, as illustrated in Figure 2.11. When considering the micro-patterned optical diffuser and concentrator waveguides, the distinction between edge-lit

and face-lit waveguides is important. An edge-lit waveguide has the source illuminating an edge of the waveguide, the diffuser is patterned with MOSs which cause the light to exit the waveguide, illuminating the waveguides face. The edge illuminated by the source is smaller than the face through which the illumination exits, resulting in dispersion of the source light.

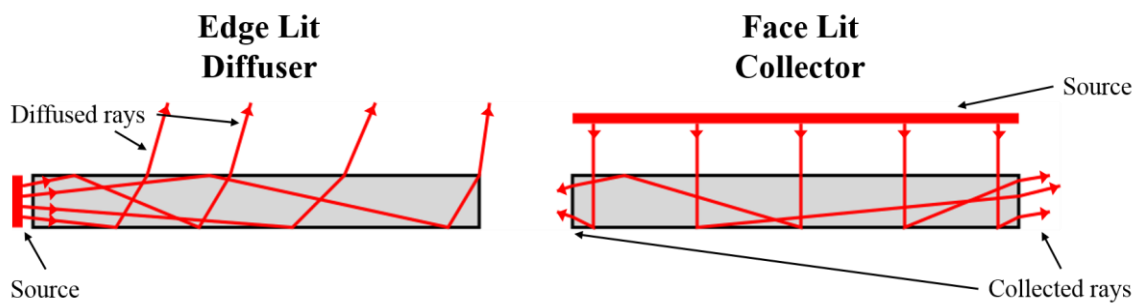


Figure 2.11 The edge-lit waveguide is illuminated from one side and diffuses incident light to illuminate the waveguide. The face-lit waveguide collects the light incident on the face and directs it to one, or more, waveguide edges.

A face-lit waveguide has its face illuminated by the source, and it patterned with MOSs which collect the illumination, and direct it out one or more of the waveguide's edges. This configuration permits collection of illumination over the large, illuminated face, and concentration of the source light to the waveguide's edge(s). The geometric factor of concentration for a concentrating waveguide is dictated by this relationship. If the concentrator has a larger illuminated area, as compared to the concentrated edges, it will have a larger geometric factor of concentration, and vice-versa.

Typically, an illuminator waveguide is lit at one edge, by an external source, resulting in illumination to the waveguide with angle from 0° to the maximum cone angle (θ_{max}) of the source, as in Figure 2.12. Often this results in significant losses at the source if the sources cone angle exceeds the acceptance angle of the waveguides core. In the dual functioning concentrator-diffuser waveguide, this challenge is eliminated, since the light transmitted from the concentrating region illuminates the diffusing region of the waveguide. This configuration is unique in that it guarantees that all illumination which

can propagate through the concentrator will be accepted by the diffuser, as they share the same medium. Additionally, the rays propagate between a minimum and maximum angle (θ_{min}), rather than from 0° to a maximum angle. This allows for a greater specificity to the diffuser features, since the particular angles at which the rays strike the features will be known. The concentrator illuminating the diffuser, thus enhances both the efficiency and uniformity of the final illumination pattern.

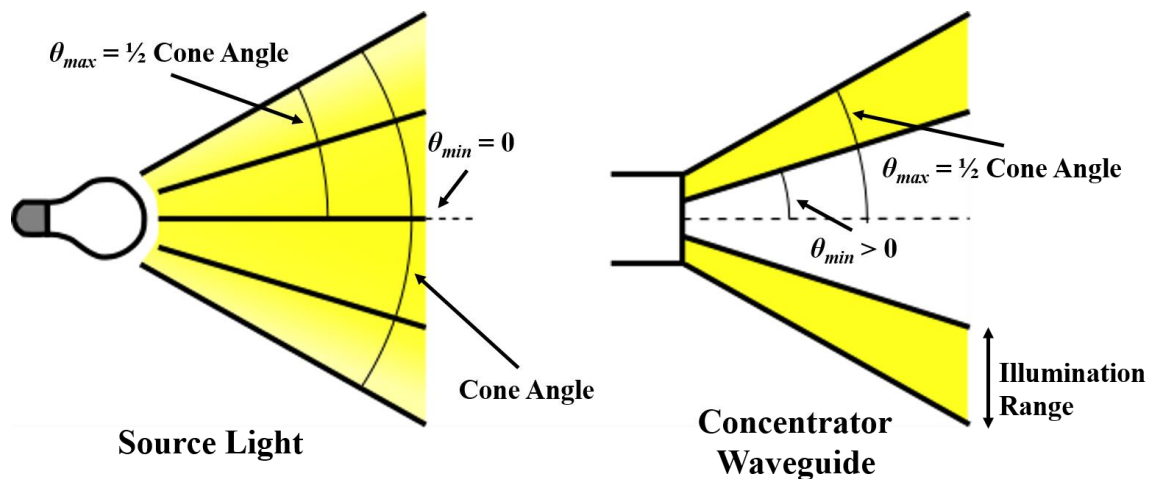


Figure 2.12 A typical diffuser light source will illuminate a cone of light from the centre axis to the maximum angle. The concentrator illuminates the diffuser in a unique pattern with light rays only propagating between a minimum and maximum angle.

2.3.2 Uniform and Non-Uniform Illumination

In the analysis of the waveguide's performance it is important to evaluate the uniformity of the illumination. This is of most importance when considering the illumination from the face of the diffuser. This is essentially the final destination of the guided light, and it is important that the final output has high efficiency and high uniformity. It is also important to give regard to the uniformity of the concentrator's illumination. Although the concentrating region's uniformity is an intermediate stage of the guided light's path, the concentrated light illuminates the diffuser, thus it will have some bearing on the diffuser's ultimate illumination pattern.

In order to evaluate the uniformity of the diffuser, the point of most intense illumination is compared to the average illumination intensity across the diffuser's face.

This method can be used both theoretically, through the Zemax simulations, and empirically in waveguide evaluation. In the case of the Zemax simulations, the detector data is examined to determine the peak and average intensity. The user defined detector dictates the size and placement of the detector with respect to the waveguide surface, and Zemax returns the peak incoherent irradiance in Watts/cm², and total irradiance in Watts across the detector surface. The average irradiance is calculated by dividing the total irradiance over the total area, and then the average irradiance is divided by the maximum irradiance, giving an estimate of the percent uniformity of the illumination from the diffuser's active face.

The primary challenge in achieving uniform illumination from a diffuser waveguide is that, as the distance from the light source increases, the light remaining in the waveguide decreases. This results in a lowering of the intensity of illumination with distance from the source. Figure 2.13, below, illustrates the decrease in light remaining in the waveguide (green) as distance from the source increases. By increasing the diffuser's efficiency (red), with distance from the source, uniform illumination of the diffuser can be achieved.

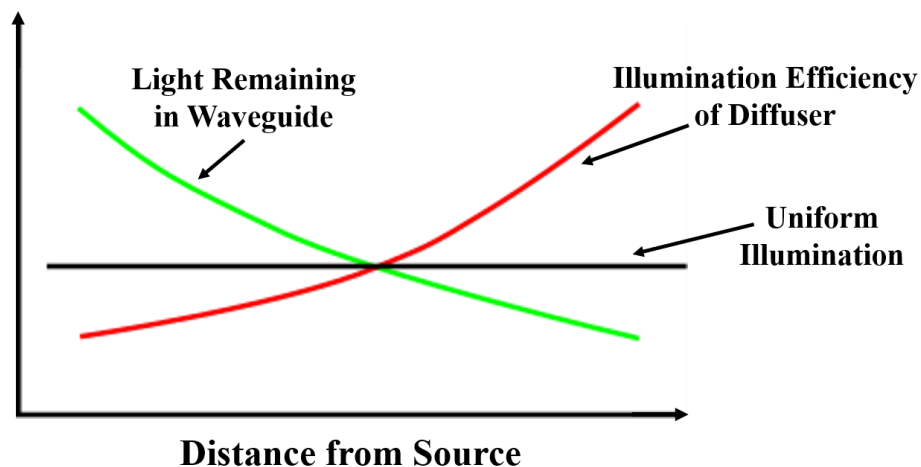


Figure 2.13 Uniform illumination of a diffuser waveguide is achieved by increasing the diffuser's efficiency with distance from the source, as the light remaining in the waveguide decreases [18].

The losses seen with increasing distance from the source, can be rectified by increasing the efficiency with which light is diffused as distance increases from the light source, offsetting the loss of light through the waveguide. This is done by either increasing the size, depth, or density of features as distance from the source increases. By increasing the efficiency with distance from the waveguide, however, you must settle for less than optimal efficiency for features closest to the source. While, near 100% efficiency can still be attained by this method, it requires an increased diffuser length which, depending on the application, may be undesirable. Alternatively, the edge farthest from the source could be coated with a reflective coating, such that the light travels through the diffuser twice. In this case, the light travelling back off the reflective face will be at a higher concentration further from the source, thus serving to reverse the previous effect, and enhance uniformity.

2.3.3 Selection of Core and Cladding Material

The selection of core and cladding materials is multi-faceted. For the purpose of a highly efficient design the refractive indices, and optical transparencies of the materials are the relevant parameters. When considering the physical properties of the waveguide, the strength, flexibility and durability of the materials become more important. At least two materials are required for the design of a multilayer concentrator-diffuser waveguide, so it is essential that the materials selected are compatible in terms of both optical and mechanical properties.

In order to allow the rays to be confined to one layer, the two materials selected must have different refractive indices. The minimum difference in refractive indices is quite small if it is only necessary for the rays to be confined to a planar waveguide, however if a flexible design is desired a much larger difference in refractive indices is necessary. The larger the difference of indices, the more versatile the waveguide becomes, thus a large difference in refractive indices is ideal. However, the materials must share their mechanical properties so that when bending occurs, the layers remain bonded and properly aligned. Another important characteristic of the layers is their ability to bond with one another without the use of an adhesive, as an adhesive will interrupt the optical properties of the interface between the layers. Therefore, the ideal layering configuration

would use the same material for all layers with the refractive index modified through the manufacturing process, or the use of a dopant.

2.3.4 Importance of Optical Microstructures

The fundamental functionality of both the concentrating and diffusing regions of the proposed design, is based on their microstructures. There is significant precedent for the use of optical microstructures for the collection and diffusion of light in both multilayered and monolithic optical waveguides. Whether based on the principles of total internal reflection, the use of reflective coatings, or the refraction of light off optical micro-features, the use of these structures for controlled guidance of light is highly prevalent.

2.3.4.1 Optical Microstructures for Collectors

The concentrating region of the waveguide incorporates two types of MOSs in order to successfully collect incident light into the waveguide; lens features and coupling prisms. The lens features concentrate the incident light onto a coupling prism feature. It is essential that the micro-lens features cover the entire illuminated surface of the concentrator region to ensure all incident light is collected. The size of the lens feature is directly proportional to the thickness of the waveguide, therefore the desired thickness of the concentrator will dictate the size and number of lenses. The density of coupling features will be determined by the concentration of lens features, as it is essential that the coupler is located at the focal point of the micro-lenses. The coupling feature may be pyramid, wedge or cone-shaped depending on the desired directionality of the coupled light, and the manufacturing process being used.

This configuration was successfully presented in the work of Karp et al., [2] as they used the micro-patterned lens-coupler configuration for a solar collector. Although Karp et al. presented a viable design for a large area concentrator waveguide, the design is composed of two separate, rigid bodies, and thus it cannot be directly applied to the design of a flexible hybrid concentrator-diffuser optical system. The same optical features are applied to a monolithic polymer concentrator, for the design of a flexible large area optical waveguide. The coupling features used in this design, must be minimized in size

in order to maximize waveguide efficiency of the waveguide, however even at a very small scale, there will be some decoupling losses as propagating rays strike the features.

Alternative designs are able to avoid interactions with subsequent feature altogether, or to incorporate these interactions into the guidance of the light, however these designs require increased waveguide thickness [29]. Since one of the targets of this design is its large area, this would correspond with an unreasonably thick waveguide if there were to be no decoupling losses of propagating rays. Therefore, the lens-coupler configuration is used, with the understanding that some propagating illumination will be lost, but attention must be given to the coupling feature size and placement to limit the losses.

2.3.4.2 Optical Microstructures for Illuminators

There is greater variability in the literature for which optical micro-structures are best suited for an illuminator waveguide. The most commonly used diffusing features are round-tipped features (Figure 2.14a), triangular features (Figure 2.14b), and cone (Figure 2.14c) or inverse cone features (Figure 2.14d). Round-tipped features are ideal if the angles of propagation through the diffuser waveguide are unknown, or have a very large range [7]. This is because the round tipped features have varying angles at each point on their surface, thus the light will interact with the feature differently depending on where it strikes the features. This makes round tipped features one of the most versatile options, but with a lower efficiency. The shape of the features randomizes the interaction with the propagating rays and the diffusing features, and therefore if the interaction is suboptimal the ray may be lost.

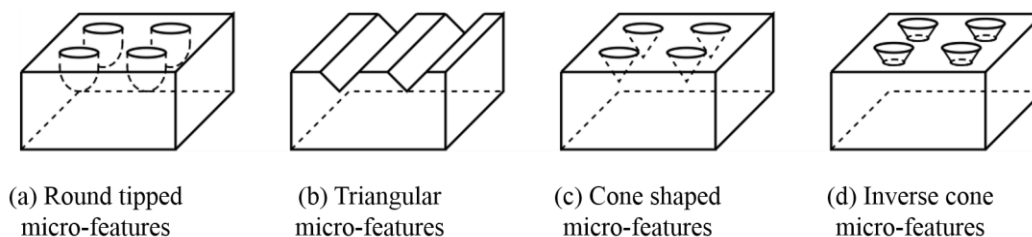


Figure 2.14 Commonly used diffuser micro-features include round tipped, triangular, cone shaped and inverse cone shaped features.

Both triangular-shaped, and cone-shaped features have the advantage of having a constant feature angle across their surface [30, 31]. This makes the interactions with propagating rays much more efficient and predictable for rays within a particular range. Rays outside this range will not be suitably reflected, or refracted, and therefore the cone or triangle features are best used when the propagation range is well defined and relatively small. The triangle-shaped features have the disadvantage of not being able to strike rays that strike from the feature sides, whereas the cone features have a constant angle around the entire feature. The cone features, however, have the disadvantage of having a circular base, and therefore cannot be patterned with as high a density as the triangular features with a square base.

The desired density of features is dependent on the size of the diffuser region. If a minimum diffuser region is desired than a maximum diffuser feature density is essential. In order to maximize the uniformity of the diffuser's illumination, however, there must be some variation in feature density or depth. If a constant feature density is used, the illumination will be brighter closer to the source, where there is more illumination remaining in the waveguide. As the light in the waveguide diminishes, so does the illumination intensity on the diffuser's face, thereby decreasing its uniformity. Closer to the light source diffuser feature must be patterned with lower density, increasing with distance from the source to improve uniformity.

In the case of the concentrator-diffuser hybrid waveguide, the concentrator acts as the source for the diffuser region of the waveguide, therefore the range of angles is well defined and quite small. The triangle-shaped wedge features are thus suitable for the diffuser MOSs, not only because they are appropriate for the particular light source, but because they are the most adaptable in terms of density [16]. If a minimum diffuser region is desired, this can be attained with high density diffuser features, and if a larger region is desired, the feature density can be varied.

2.4 Key Material Properties of Optically Transparent Polymers

As discussed in previous sections, there are a number of material properties essential to the fabrication and performance of the waveguide. These include; the optical transparency, the mechanical flexibility, the consistency and the refractive indices of the material. The optical transparency of the material becomes especially important for large area waveguides, as the impact of transmission losses increases with area. For a large area waveguide, the material selected must have a very high optical transmission efficiency.

In order for the waveguide to be mechanically flexible, the material from which it is made must also be flexible. This corresponds to the material selected exhibiting a low Young's modulus [32], as this will permit flexing of the waveguide as well as modest stretching. Although all materials can be deformed if they are sufficiently thin, selecting a polymer with a low Young's modulus, for the waveguide material, will ensure the scalability of the design. Also important to the waveguides flexibility, is the difference in refractive indices. Typically to have layers of different refractive indices, different materials can simply be used, however in this case the layers must be bonded without the use of an adhesive, so one material with a variable refractive index is ideal. Finally, it is necessary that the material selected is able to replicate the desired micro-structures for light guiding, while otherwise having a consistent composition free of material and geometry imperfections.

The material selected for this waveguide is thus polydimethylsiloxane (PDMS). It fulfills the requirements of mechanical flexibility and maintains an optical transmission efficiency of over 95 percent [33]. Additionally, the material is compatible with soft lithography, permitting the exact replication of the desired geometry with minimal flaws and imperfections. Another significant, unique property of PDMS is that it is a thermosetting polymer, which requires the mixing of a base and agent. The ratios with which the components are mixed and the temperature and time for which they are cured will dictate the optical and mechanical properties of the material permitting variations in the refractive index of the layers while maintaining constant mechanical properties [34-36]. Additionally, if a greater difference of refractive indices is required, this can be

achieved by adding a dopant to increase refractive index. While, PDMS is a suitable material and will be used for the design of this waveguide, the design may be adapted for different materials if so desired.

2.5 Concluding Remarks

This chapter provides an overview of the fundamental concepts relating to the design of a large area flexible waveguide, as well as some of the research recently conducted in this field. The advantages and limitations of existing research are outlined providing the groundwork for the design proposed in the following chapters. The concentrator-diffuser system for controlled guidance of light will incorporate features used in previous literature, adapting their design for a more versatile waveguide. In summary, based on the existing literature the optimal configuration of the lens and coupler micro-features in the concentrating region of the waveguides, and wedge shaped diffuser micro-features were selected. Their geometry, size and orientation are optimized in Chapter 4, and Chapter 5 examines the impact in variations to their geometry, as well as proposed guidelines for the design of various waveguides.

Chapter 3 Design Methodology

3.1 Evaluating Optical Waveguide Performance

In order to evaluate the performance of the optical waveguides, there must be some means of quantifying their performance. In this research Zemax OpticStudio is used to evaluate the waveguides. Zemax OpticStudio is a powerful ray tracing software which can evaluate the light path through complex geometries [36]. The geometry of the waveguide was first designed on SolidWorks and then imported as a STEP file into the Zemax OpticStudio ray-tracing software. The material properties are then defined for each of the imported bodies, there is a large library of materials predefined in Zemax, which can be applied to the bodies. If the material does not exist in the Zemax library, as is the case for the varying refractive index PDMS, it can be added to the library by defining its relevant properties. The illumination conditions are then defined in Zemax, typically using a rectangular light source which allows the user to define the position, orientation and wavelength of the incident illumination. Finally, a set of detectors is defined which are used to quantify the waveguide's output and evaluate its performance. Among other data, the detectors will measure what proportion of the incident illumination hits the detector, and the peak intensity on the detector. These variable are used to evaluate and compare the performance of various waveguide designs.

3.1.1 Estimating Light Loss

In order to predict the light lost through the concentrating region of the waveguide the geometric and material properties of the waveguide features must be considered. The theoretical losses can be computed based on the geometric optics of the waveguide sheet, with respect to the feature geometry, and the number of times a propagating ray strikes the waveguide surface by equation 3.1.

$$E_C = \left(1 - \frac{b^2}{P^2}\right)^N, \quad (3.1)$$

where E_C is the efficiency of the concentrating region of the waveguide, b and P are the width and pitch of the coupling features respectively, and N is the average number of

times a propagating ray strikes the bottom face of the concentrator, based on the angle of propagation, and the surface area and thickness of the waveguide. Details about the efficiency equation, and its derivation are provided in Appendix A1.

This equation relates to a theoretically optimal waveguide functionality, and does not take into account the focal dispersion of the rays at the focal point. The impact of this dispersion on the waveguide's efficiency is two-fold; losses caused by the rays failing to strike the concentrating prisms, and rays which hit the prisms at an undesirable angle. Rays which do not hit the coupling prism at all are immediately lost out the bottom face of the concentrator. Rays which hit the prisms at the wrong angle may be refracted out the bottom of the features, refracted out at the interface between the layers, or they may propagate through the concentrator, but fail to strike the diffusing wedges at the appropriate angle for illumination. Although Equation 3.1 fails to account for these losses, the Zemax simulations do take them into consideration, thus these losses may account for variation between an ideal model, and the Zemax results.

What Zemax fails to take into consideration are the material's absorption coefficient and the wave properties of light. At the micron-scale there may be some losses, whether it be due to diffraction or interference, which are not accounted for with a geometric optics analysis of the waveguide. The absorption of the waveguide material must also be considered when evaluating the performance of a particular waveguide against the predicted Zemax results. In this case, the PDMS has a transmission efficiency of approximately 95%, thus all numerical efficiencies calculated from the Zemax results should be scaled by 0.95 in order to predict the actual waveguide efficiency.

Additionally, the losses due to bending must be considered when examining the performance of a flexible waveguide. If the radius of curvature of the bent waveguide is greater than the critical radius, according to the materials' refractive indices, the bend losses will be minimal, however for smaller radii, these losses will be significant. Zemax takes into account these losses by calculating the theoretical maximum acceptable bend, and refracting out lost rays in the analysis. What also must be considered is the deformation and relocation of the features due to bending. In this respect it is important that the CAD model accurately reflects the deformed geometry, and then the Zemax OpticStudio

software is able to accurately account for the subsequent losses. In order to model such deformations in SolidWorks, the original planar waveguide is altered using the “Deform” feature and flexing the waveguide according to the appropriate parameters.

3.1.2 Performance Measures

To estimate the efficiency of the concentrator-diffuser waveguide, the power from the light source was set to 1 Watt, and the total power detected in the diffusing region was measured. The measured power divided by the input power was calculated by

$$E_{c-d} = \frac{L_d}{L_c}, \quad (3.2)$$

where E_{c-d} is the efficiency, L_d is the light detected from the diffuser faces and L_c is the light incident on the concentrator face. Equation 3.2 is used as the estimate of the percent efficiency of the waveguide.

Similarly, the uniformity of the illumination was estimated based on the illumination of the detectors. The total power across the diffuser region was divided by the total area of the diffuser, to estimate the average irradiance of the waveguide in Watts/cm². The peak irradiance is identified from the detector data and the average irradiance was divided by the peak irradiance to estimate the percent uniformity for the illumination from the diffuser using

$$U_d = \frac{I_{d_{avg}}}{I_{d_{peak}}}, \quad (3.3)$$

where U_d is the uniformity of the diffuser region, $I_{d_{avg}}$ is the average diffuser irradiance, and $I_{d_{peak}}$ is the peak diffuser irradiance.

Based on these performance measures, a parametric optimization of the waveguide micro-feature geometry is conducted in order to identify the design which will maximize both the uniformity and efficiency of the device. The parametric optimization consists of a repeated analysis of the same waveguide, varying only one parameter, in order to identify the value of this parameter for which the performance is maximized; this is

repeated for each of the key geometric parameters of the waveguide. The results of these analyses are summarized in Chapter 5, and the process by which they are analysed follows in this chapter.

3.2 Role of Simulations in Optical Design

While ray tracing techniques can be applied without the use of a ray tracing software, Zemax provides a highly reliable and efficient method of analysis. Based on the simulations, the efficiency of a particular waveguide, and the uniformity of the diffuser may be calculated and are used to quantify performance. This is essential to the process of the optical design, as it permits numeric comparison of various designs, identification of sources of loss, and a benchmark for assessing acceptability of performance.

With every new concentrator or diffuser design, a single feature is modelled according to the parameters of the proposed model. Using the Zemax detector data, the performance of a single feature is evaluated based on its efficiency and uniformity. If the single feature performs according to the desired specifications, an array of features is simulated and evaluated, to determine the performance of the new waveguide. The efficiency and uniformity data for the whole waveguide can then provide a numerical means by which different models can be compared. If the single feature does not produce the desired results, the design may be modified to achieve the desired results, or it may be abandoned. This process of analyzing a model in Zemax OpticStudio is presented in greater detail in Chapter 4.

As well as providing quantitative data by which the performance of the waveguide may be evaluated and compared, Zemax also provides immense qualitative data which assists in the design process. Zemax has very good model “viewers” by which one can see the original geometry, the ray trace through the model, the geometry including the detector data, or the detector data alone. Each of these viewers allows the user to visually interpret the results of the simulations, whether it be identifying a source of loss by looking at the ray trace, or noting the uniformity of the concentrator’s illumination as it passes into the diffuser waveguide. The quantitative analysis also permits the

visualization of the illumination profile across the waveguide, and gives a greater understanding of illumination patterns, as well as validation of design performance.

3.3 Functionality of Zemax OpticStudio Software

Zemax OpticStudio is a ray-tracing software which allows the user to define the geometry and material properties of their optical device, and predicts how it will interact with the light source by ray tracing methods. OpticStudio provides two primary functions; sequential and non-sequential ray tracing [37]. Sequential ray tracing analyzes a series of optical devices and their interactions with light in sequence, whereas non sequential analysis can be used for optical features in any position, sequence and orientation. The non-sequential functionality permits the analysis of complex optical devices, such as the waveguide in consideration, thus the OpticStudio *Non-Sequential Component* (NSC) Editor is used.

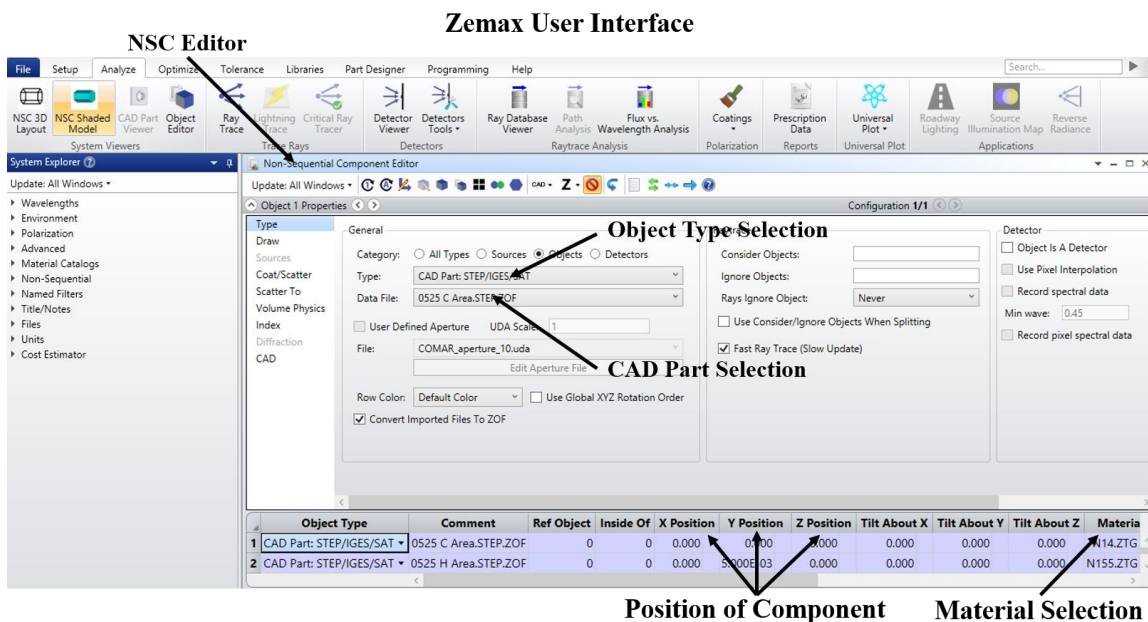


Figure 3.1 This image depicts the Zemax user interface as well as the key parameters used to import CAD components, and define their properties.

Since Zemax permits the import of CAD models to replicate the waveguide geometry, all significant geometrical modelling is done in SolidWorks and imported into OpticStudio in STEP format. This is done by creating a new Zemax object in the NSC editor, seen in Figure 3.1, and defining it as a “CAD Part: STEP/IGES/SAT”, which permits the selection of the appropriate STEP file of the SolidWorks model. For each imported file, the desired material must be assigned to the part, if no material is assigned, the default material is air. It is thus necessary that each layer of the waveguide is imported as a separate part in order to apply different refractive indices to each layer. Using the x -, y -, and z -position parameters the layers may be positioned with respect to one another to ensure proper orientation. Additionally, the position, size and orientation of particular feature geometries can be modified in Zemax. This is especially beneficial when considering the optimization of the waveguide geometry, as multiple variations can quickly be modelled and simulated, in order to investigate their impact on performance.

With the geometry imported from the CAD files, and the material properties applied, a light source must be defined for the simulation. The light source used for the majority of the simulations was a rectangular source, however in some cases a source object or source file is used. A source file is especially beneficial when examining only the diffuser region of the waveguide, as the concentrator’s illumination pattern can be replicated with a source file, rather than modelling the entire concentrating region. In most cases, the source rectangle is appropriate as it provides illumination for the entire collecting region, whether it be as an overhead source, or a discretized, curved source. Once again the component must be positioned and oriented with respect to the existing components, and the source properties must be applied.

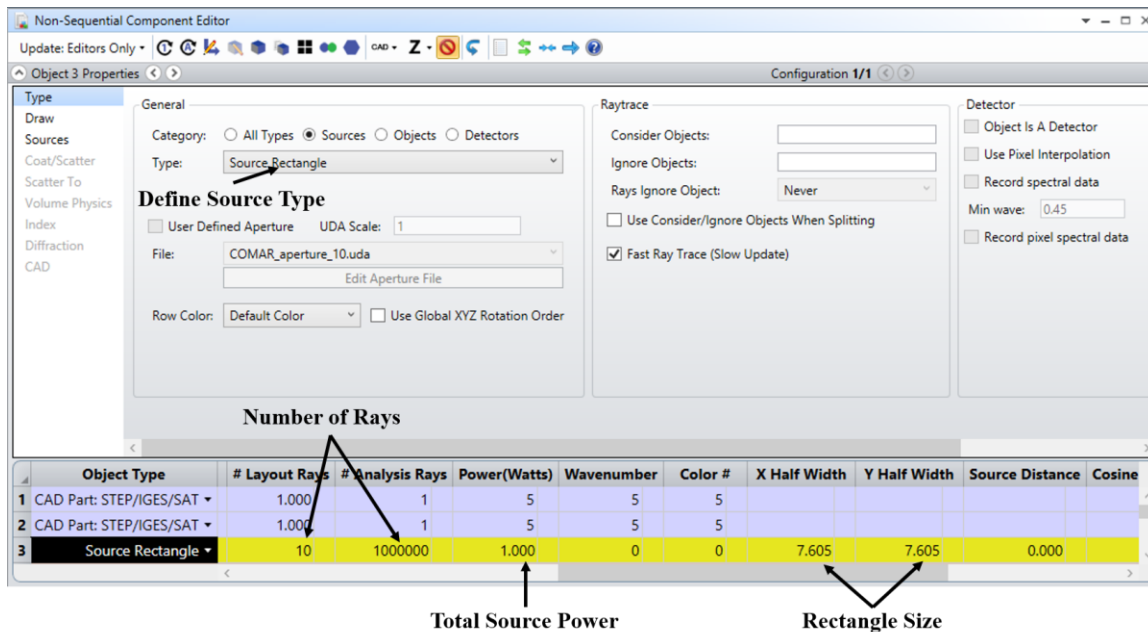


Figure 3.2 The Non-Sequential Component editor permits the definition of a rectangular source, its total power, size and location.

The most important properties in consideration of a source are the number of rays, the total power, and the size of the source rectangle, as identified in the NSC Editor shown in Figure 3.2. There are two ray sets which must be defined; layout rays and analysis rays. Layout rays represent the rays which will be illustrated in a ray-tracing image of the waveguide, while analysis rays are the ray set which are used for the computation of ray paths and the final detector data. Typically, a much lower number of rays is used for the layout set, as this is simply a visual representation, while the analysis should be significantly more thorough; the number of analysis rays used will dictate the of the detector illumination data. In this case 10 layout rays are used, compared to 1,000,000 analysis rays.

Additionally, the total power of the source, and the size of the rectangle must be defined. In this case a total source power of 1 Watt is used in order to simplify calculations, and facilitate comparisons between number of rays and the waveguide's efficiency. The source rectangle's size is equivalent to the size of the collecting region in

order to be able to compute the ability of the waveguide to successfully capture illumination which strikes the concentrating features.

Finally, in order to be able to meaningfully interpret the results, detector components must be defined. Detector data permits the analysis of illumination patterns, illumination intensity, and component efficiency, thus their data is essential to the design process. For this analysis detector rectangles are used, and as before the position, orientation and size may be defined in accordance with the existing components. Also important for the definition of the detector components are the number of pixels-as this defines the resolution of the results-and the colour of the data. In this case the colour “1” is selected as this represents the data in greyscale with the most intense illumination as the brightest, and least intense illumination in black.

In the above example, five detectors are used in order to evaluate the waveguide’s performance; four of which surround the concentrating region, and the last of which covers the entire top face of the waveguide. The four detectors on the boundaries of the concentrating region are able to detect how much incident light is collected by the concentrator, by comparing the total power from these detectors, to the total incident power. The fifth detector permits the analysis of the waveguide as a whole, by determining what proportion of the incident light is successfully diffused out the illuminating region of the waveguide, as well as noting distribution and intensity of illumination. Since the fifth detector is located on the surface of the waveguide, the incident light would illuminate the centre of the waveguide, rendering the data meaningless. To mitigate this effect, Zemax permits the detector to ignore the rays on layout, and this feature is applied to ensure all illumination detected is via the waveguide’s features, as illustrated in Figure 3.3.

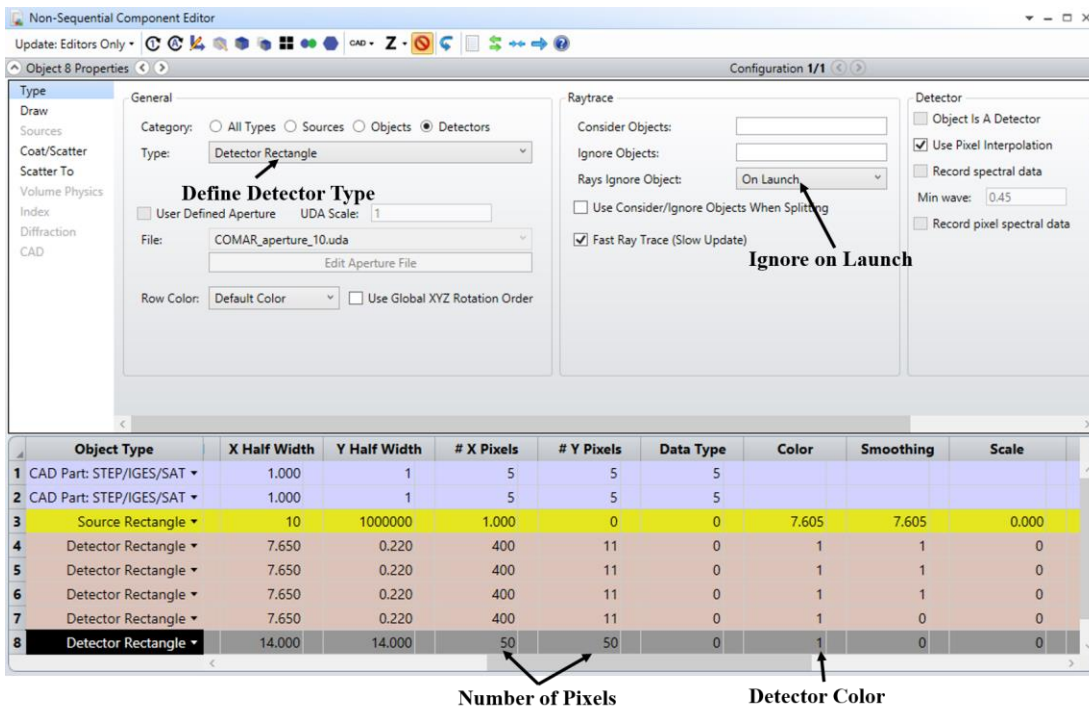
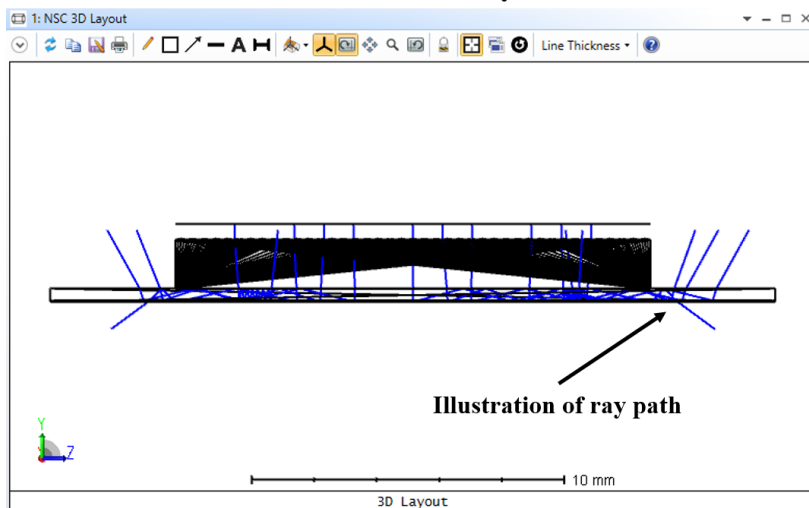


Figure 3.3 Zemax facilitates the definition of detectors and the relevant properties.

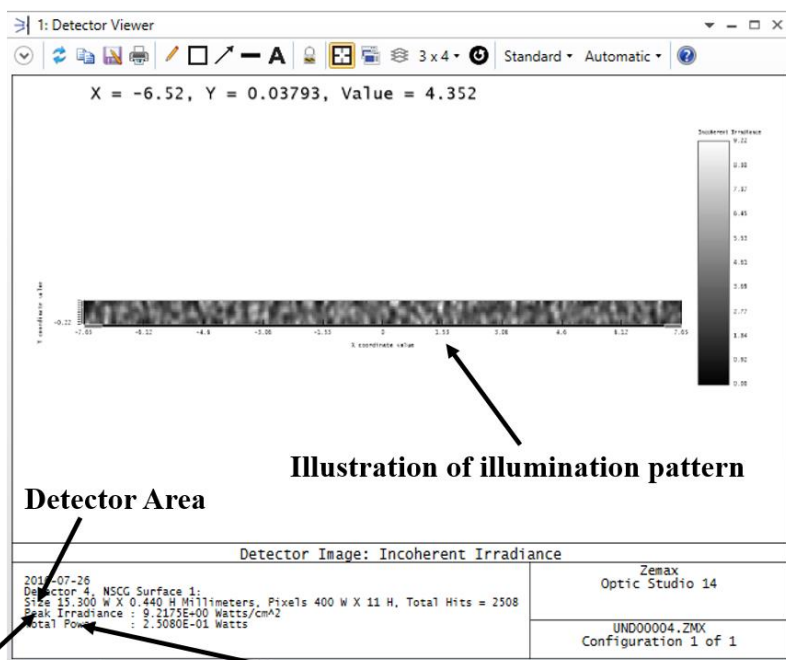
Two Zemax tools were primarily used to evaluate the performance of a particular waveguide design; the NSC 3D layout, and the detector viewer. The 3D layout provides a visual representation of the imported geometry, the layout rays and any other components, as defined. This tool is suitable for quick, visual analyses of a particular design, as they allow the user to determine if the rays follow the desired path. The detector viewer, while not demonstrating the ray path, gives much more detailed data than the 3D layout. The detector data evaluates the location of each ray, and predicts which pixel it will strike on the detector. Each pixel is coloured according to the illumination intensity at this location, based on how many rays struck a particular location. Additionally, the detector data provides numerical data for each pixel, as well as maximums and averages for the illumination intensity. The ray tracing image, and detector data for the above example are shown in Figure 3.4.

Zemax NSC 3D Layout



(a) NSC 3D layout depicts the ray trace through the optical device.

Zemax Detector Viewer



Peak Irradiance

Total Power

(b) Zemax detector viewer depicts illumination pattern, and includes numerical data.

Figure 3.4 Zemax represents the ray trace data in the 3D layout, providing a visual representation of the results. The detector data gives a more detailed view of the illumination patterns and extensive numerical data.

Interpretation of the detector data permits the calculation of the key performance parameters, as discussed above. The efficiency of the entire waveguide, or a portion thereof, can be calculated by dividing the power measured on a particular detector, by the total source power, to determine efficiency according to Equation 3.2. Similarly, the uniformity of a detector region can be calculated according to Equation 3.3 with the peak incoherent irradiance given in the detector data, and the average irradiance calculated by dividing total power by total area. With the method to calculate the efficiency and uniformity of any waveguide defined, Zemax provides the necessary irradiance data to evaluate and compare the illumination results of various designs.

3.4 Limitations of Design Methodology

While the design methodology proposed provides a thorough understanding of the performance of the waveguide, there are some associated limitations. Particularly with the application of geometric optics analysis, there is likely to be additional losses which are not accounted for due to the effects of diffraction and interference. Although an effort is made to keep all feature dimensions and layer thicknesses significantly larger than the wavelength of visible light, in order to be able to treat the light as a ray, there are still some interactions at the wavelength-scale which are not considered. Whether it be the focused rays striking the very top of the pyramid features, or the propagating rays striking the intersection between the coupling pyramid and the waveguide base, there may be some amount of diffraction which is not measured.

While these additional losses are not accounted for in the simulations or optimization of the waveguide, they are important to keep in mind when evaluating the performance of a real waveguide experiment against the theoretical results, as they will account for some of the variation in performance. The refractive indices of the materials too, may cause variation between predicted performance and measured performance of a waveguide, since for the purpose of the simulations, it was assumed that the refractive index of the PDMS could be varied between 1.4 and 1.7 without an impact on its transmission efficiency or composition.

Another major limitation of the design methodology is the limitation of the software itself. While Zemax OpticStudio is a robust tool for analyzing the performance of various waveguides, and other optical devices, there are some inherent limitations in its abilities. Specifically, in the design and simulation of the flexible waveguide, a large degree of discretization was necessary. The flexibility of the waveguide could not directly be modelled in Zemax, but rather varying waveguide geometries, degrees of curvature, and orientations were modelled in SolidWorks and imported to Zemax in STEP format. This still permitted any particular waveguide shape to be analyzed in Zemax, however rather than modelling a continuous, flexible waveguide, it must be modelled in each position for which you wish to evaluate it. Another challenge associated with discretization is the use of curved sources and detectors in Zemax. Although Zemax has the capacity to model curved light sources and detectors, the degree of control over the setup and results is reduced with the curved sources and detectors. For this reason, in order to be able to extract and interpret maximum data from the results, it is necessary in many simulations to use a number of discretized detectors and/or sources. While this discretization can be done with little or no impact on the simulation and its results, it is important to be aware of the need for discretization, and its potential limitations.

3.5 Concluding Remarks

This chapter presents an overview of the methods by which the designs, discussed in subsequent chapters, are to be evaluated. It is necessary to understand the applications and limitations of the tools being used for analysis, as well as to gain as much insight into the design as possible by applying these tools. In summary, there are two metrics by which the performance of the waveguide is assessed; its efficiency and its uniformity. These are both calculated by evaluating the detector data arising from the Zemax simulations, and allow for the comparison of various designs, and prediction of performance for experimental analyses.

Chapter 4 Establishing Design Parameters for Large Area Waveguides

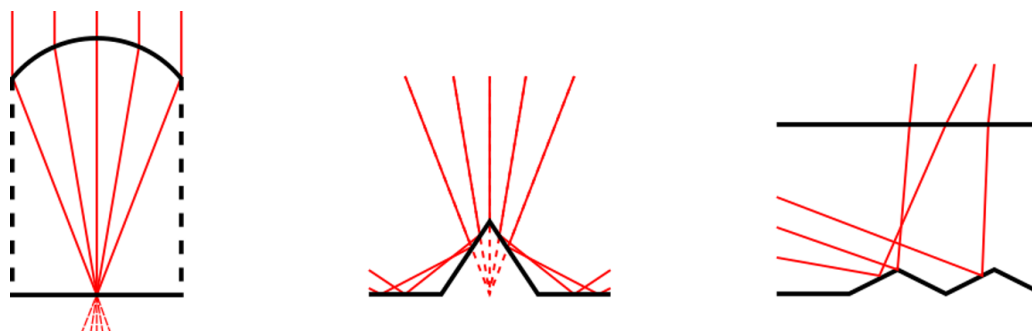
4.1 Conceptual Design of Concentrator – Diffuser Waveguide

The waveguide proposed in this work is unique in its dual-functionality; that is, it combines both light collection and illumination in the same waveguide sheet. In order to successfully perform both functions, the waveguide must be capable of concentrating the light, redirecting it and transmitting it to the illumination area, and diffusing the light. In order to perform each of these functions various micro-features are used.

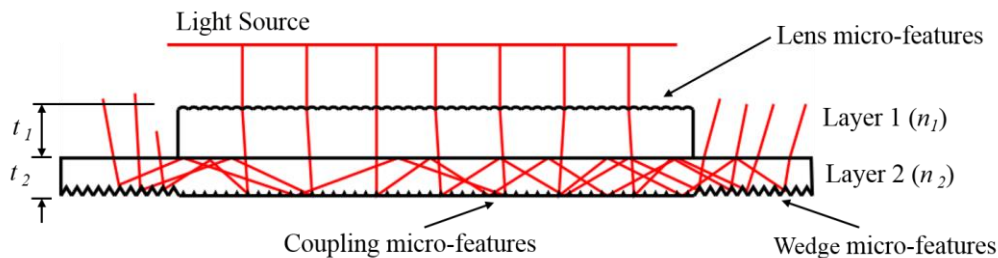
Micro-lens features (Figure 4.1a) are suitable for collection as they serve to focus the incident light, thereby concentrating the light. These lens features focus incident light onto pyramid shaped micro-features which are embedded in the concentrator waveguide. These pyramids act as coupling features (Figure 4.1b) which redirect the focused light, by total internal reflection, towards the diffusing area of the waveguide. The coupling features must be located directly underneath the lens micro-features – at their focal point – in order to maximize the concentrating ability of the waveguide, and minimize the size of the coupling prisms. This set of micro-lenses and coupling prisms, is patterned in an array to compose the collecting area of the waveguide.

In order to successfully illuminate the diffusing area of the waveguide, the concentrated light must first be transmitted to this region. While the coupling micro-features successfully divert the light's path in the direction of the diffusion area, the light must be transmitted from the collector to the diffuser. For this reason, a dual-layered waveguide design is used; the upper layer has a lower refractive index acting as a cladding, and the bottom layer has a higher refractive index and acts as the core, through which the propagating light is transmitted. The dual-layered approach eliminates interactions between the micro-lens features and the propagating rays, improving the waveguide's transmission efficiency, as well as preserving the concentration factor of the light. Finally, the illumination area of the waveguide must be capable of diffusing the propagating rays, thus diffusing micro-wedge features (Figure 4.1c) are embedded on the bottom face of the waveguide. These optical wedges are angled so that when the

propagating rays strike the micro-feature surface they are reflected at such an angle that the rays are refracted out the layer's upper surface.



(a) Micro-lens features focus light onto the bottom face of the concentrator
 (b) Coupling feature, located at the lens' focal point, redirect light towards the diffuser area
 (c) Diffusing wedges reflect propagating light up to waveguide surface, where light is refracted out



(d) Dual – functioning waveguide is composed of arrays of the required micro-features

Figure 4.1 Combined concentrator-diffuser waveguide with lens micro-features focusing incident light onto the coupling prisms, which direct light into the transmission layer of the waveguide. The light propagates to the diffusing wedges, which cause refraction.

Based on the desired waveguide functionality and previous research in the field of micro-patterned optical waveguides, the approach to controlled light guidance was determined. The waveguide is composed of two layers with different refractive indices; the concentrating layer which allows the incident illumination to be focused, and the transmission layer through which the collected light rays are guided. The top layer acts as the collecting face of the waveguide and is patterned with the concentrating micro-lenses,

which focus the incident light onto the pyramid features. In the collection area, the bottom layer of the waveguide is embedded with the coupling pyramid micro-features, which direct the focused light towards the diffuser area. In the illumination area of the waveguide, the bottom face is patterned with diffusing wedges that cause propagating light to refract out the waveguide surface, as illustrated in Figure 4.1d.

4.2 Waveguide Structure

The structure of the waveguide has three essential categories; the geometry of the waveguide in its entirety, including its area and thickness, the geometry of concentrator microstructures, and geometry of the diffuser microstructures. There are numerous configurations for each of these parameters which result in high efficiency controlled guidance of light, and thus this design can be adapted for many applications. The important parameters are discussed in this section, followed by the relevant equations.

4.2.1 Waveguide Layering and Material Selection

Essential to the waveguide's ability to confine light to the transmission layer of the waveguide, is a difference between the refractive indices of the upper layer (n_1) and the lower layer (n_2). In a layered waveguide, it is therefore necessary that the material used for the waveguide's transmission layer has a higher refractive index than the upper layer. The difference between refractive indices n_1 and n_2 , will determine the maximum allowable angle of propagation to ensure confinement of the light to the transmission layer, thus a greater difference will permit a larger range of angles and greater flexibility of the waveguide.

Also important to the material selection is the interface between the layers. It is necessary that the layers are able to bond without the use of an adhesive, which would inhibit the optical performance of the interface. Because PDMS is an optically transparent polymer with an adjustable refractive index, it is an optimal material to use for this flexible, layered design.

4.2.2 Waveguide Area and Thickness

The waveguide's surface area and thickness are also essential to the optimization of its performance. One of the unique aspects of this particular waveguide design is its ability to cover large areas, it can be used to cover areas up to 1m^2 and beyond. Not only can the micro-features be patterned over large areas, but the design is also fully scalable so it may be scaled up to cover large areas without an accompanying decrease in transmission efficiency, or it can be scaled down to reduce the thickness of the waveguide.

Additionally, the waveguide's area and thickness are important as the ratio of the concentrator region's surface area to the thickness of the lower layer (t_2) represents the geometric concentration factor of the collector. The geometric concentration factor is simply the input area divided by the output area, therefore for a higher concentration ratio, the surface area may be increased or the thickness may be decreased. While both these modifications will increase the likelihood that a propagating ray strikes a subsequent coupling pyramid, thereby decreasing the waveguide's transmission efficiency, if a high factor of concentration is necessary, it can easily be obtained with minimal changes to the waveguide geometry.

The thickness of the diffusing waveguide must be equivalent to that of the lower layer, t_2 , to ensure 100% transmission between the concentrating and diffusing regions. A thinner diffuser waveguide will result in both a higher efficiency waveguide, and a shorter diffusion length, therefore a thinner t_2 , is desirable. With regard to the diffuser area, it is presumed that in order to maintain a level of illumination intensity achieved by the collector, the diffuser length, and therefore area, should be minimized. This ensures that the concentration factor of the hybrid waveguide is maintained, while upholding a high diffuser efficiency.

It is important to define the desired factor of concentration and surface area for a given application, as these parameters are used to define the geometry of the optical microstructures and the related waveguide geometry.

4.2.3 Microstructure Functionality

Both the collecting and illuminating regions of the waveguide are patterned with microfeatures which control the ray path in order to guide the ray path as desired. The waveguide's efficiency and uniformity are largely dependent on the microstructures' effectiveness, thus their functionality and design must be analyzed thoroughly.

4.2.3.1 Concentrator Microfeatures

The role of the concentrator (Figure 4.2) is to collect light over a large region and transmit it efficiently to the edges of the two layer structure where it enters the diffuser that creates an illuminating output on the waveguide sheet. An effective and efficient design for the concentrator depends on the geometry and position of the microlenses imprinted on layer 1 and the optical reflective structures (i.e. pyramids) embedded in layer 2 [38]. Both the geometry of the microfeatures and the geometry of the entire concentrator must be considered for the optimization of the waveguide. The waveguide thickness, surface area and concentration ratio must all be considered when designing the concentrator waveguide. The geometric concentration ratio of the waveguide is given by the input area, or surface area, of the concentrator, divided by the output area or the sum of the area of the concentrator faces. Since only the bottom layer of the waveguide consists of the active concentrator faces, the concentration ratio is dependent on the thickness of the bottom layer only. To achieve a high concentration ratio, a large collection area for the concentrator is desirable, with a thin active layer of the waveguide. While these targets will increase the concentration ability of the waveguide, they will also decrease its efficiency by increasing decoupling losses [4].

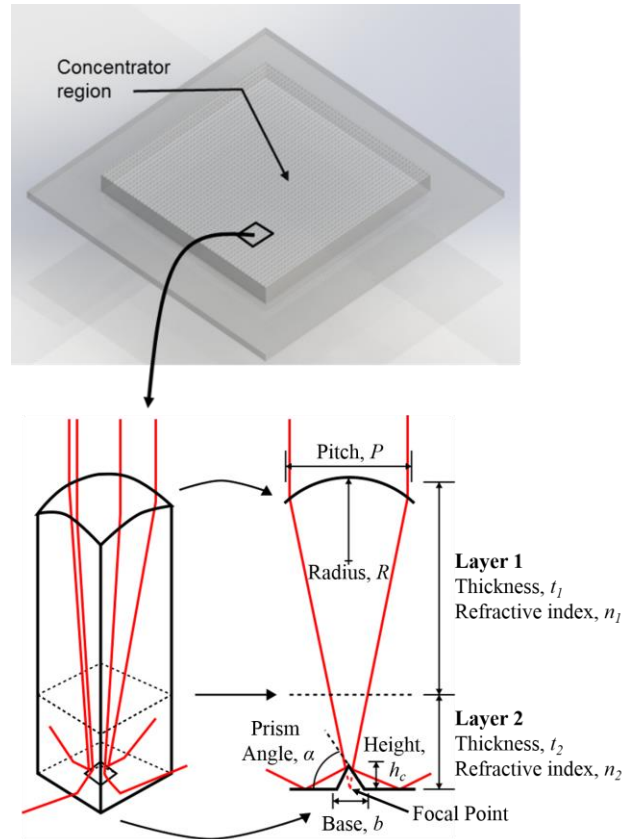


Figure 4.2 Illustration of the concentrator's functionality; the concentrating lenses focus the light onto the coupling prisms, which reflect the concentrated rays into the waveguide at such an angle that they are confined to the bottom layer of the waveguide.

4.2.3.2 Diffuser Microfeatures

The diffuser design (Figure 4.3) incorporates a series of wedge features which reflect the light off their surface, causing the light to refract out of the waveguide. The propagating ray strikes the sloped face of the diffuser feature and is totally internally reflected off this face at such an angle that it refracts out of the waveguide upon striking the illuminating surface. In order to optimize the performance of the diffuser, the efficiency of the waveguide and the uniformity of illumination must be considered. These characteristics are primarily affected by the shape, size and spatial distribution of the wedge features. The shape of the wedges is governed by the condition that the face of the wedge features must be tilted at an angle, θ_d , small enough that the incident light is reflected off the

features, but large enough that the ray is diffused out of the illuminating face upon reflection [39].

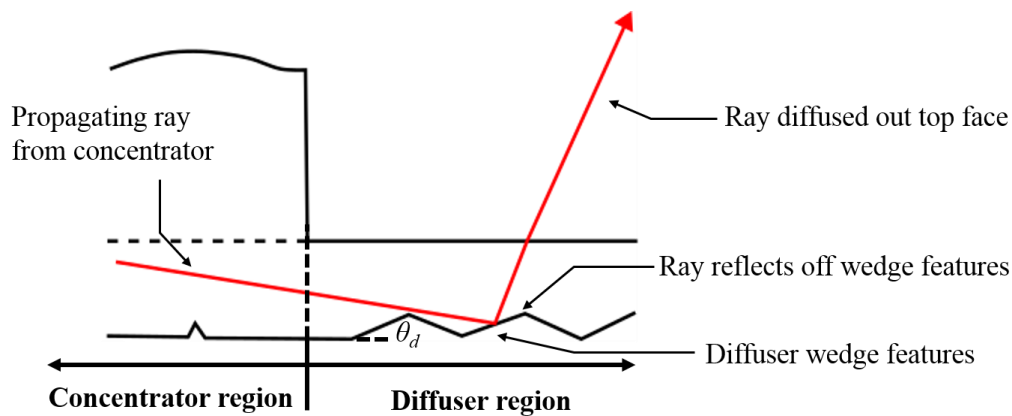


Figure 4.3 The size and distribution of the wedge features must be optimized to enhance the uniformity of the diffuser's illumination, and the length of the diffuser region must be optimized for both its efficiency and uniformity.

4.3 Surface Area and Thickness

As discussed above, the surface area and thickness of the waveguide dictate its geometric factor of concentration. If a higher level of concentration is required for a particular application, the thickness of the bottom layer may be reduced or the overall concentrator area may be increased. For the sake of the models and simulations considered in this chapter, the desired surface area, thickness, and factor of concentration of the waveguide are considered fixed as defined by the needs of a particular application. However, it is still important to understand how variations to these parameters effect waveguide performance.

Increasing the surface area of the waveguide will correspond with an increased factor of concentration, but will also result in a decreased efficiency. The primary source of losses in an optimized waveguide are decoupling losses caused by interactions between propagating rays and coupling features, as the rays travel through the lower layer of the concentrator. Increasing the surface area means that each ray must travel farther to reach the concentrator's edge, increasing the probability that it will decouple [2].

Similarly, if the thickness of the lower layer, t_2 , is reduced, the likelihood of a ray striking a coupling feature will reduce the concentrator's efficiency. However, modifying the thickness of the bottom layer means modifying the thickness of the diffusing region. Reducing the thickness of the diffusing region corresponds with an increase in efficiency, but also results in a decreased uniformity as a greater proportion of rays are diffused closer to the concentrator region, causing reduced illumination intensity moving away from the concentrator. Of course reducing the thickness also results in the increased factor of concentration, therefore if a high geometric factor of concentration is required for a particular application this can be achieved by increasing the surface area, or reducing thickness, t_2 , but this will come with some reduction to overall efficiency.

Variations in the total thickness of the concentrating region (t_1+t_2) must also be considered. The total thickness dictates the required radius of the concentrating lenses, and subsequently dictates the geometry of both the lens and prism features. For this reason, variations to the desired thickness of the waveguide simply result in a scaling of the entire concentrator region with no impact on its performance, however scaling the waveguide will result in an increase, or decrease in surface area. If a constant surface area is required, a reduction in thickness will require more features patterned to cover the desired area, resulting in a reduced efficiency, and conversely an increase in thickness will correspond with an increase in efficiency.

4.4 Optical Microstructure Geometry

4.4.1 Various Shapes and Sizes

The key design parameters for the micro-lens features are the radius (R) of the lenses and the spacing of the features, or pitch (P) as shown in Figure 4.2. For the general case discussed, a grid-pattern with equivalent spacing, P , of lens in both the x and y directions are used. The radius of the lens will dictate the focal length and, thereby, the thickness of the waveguide (t_1+t_2). The lens radius (R) will also affect the lens pitch and the angle of incidence of the focused rays on the pyramid micro-features. The maximum angle of incidence ($\theta_{i_{\max}}$) exists between the outermost rays and the prism features, and can be calculated as a function of pitch and radius.

From the lens radius and pitch the relevant geometry of the coupling features can be determined. Based on the desired angle of propagation of the rays in the waveguide, as well as the constraints imposed by the concentrating lens geometry and the layers' refractive indices, the angle of the prism base (α) and the propagation angle (θ_p) can be calculated. In order for the device to function as a concentrator it is also important that the prism micro-features are appropriately located directly below the micro-lenses, so that all focused rays are coupled into the propagation layer of the waveguide [3]. The shape of the prism features is dependent on the desired functionality of the concentrator. To achieve a maximum proportion of incident light being directed into the diffuser, it is necessary to ensure an even distribution of light to all four faces of the concentrator. This can be achieved by using a square based pyramid feature which reflects the concentrated light off the prisms, evenly to all four concentrator edges. While pyramid features will produce the most uniform, predictable light distribution, they may prove difficult to manufacture, so cone-shaped or wedge-shaped features may be considered as well. In particular, cone features will provide a similar distribution to all four concentrator faces, with high efficiency, so long as the base width (b), and base angle (α) remain constant.

Finally, the size of the prism features must be considered. In order to limit the decoupling losses caused by the prisms, the size of the features should be minimized. The minimum feature size is dictated by the dispersion of the rays at the focal point, and is of the magnitude of 1/100 of the lens radius. For very thin waveguides, the radii of the lenses become quite small, and it would be implausible to manufacture features one one-hundredth of this size, in this case the prisms should be made as small as possible. Additionally, as all calculations and simulations for this analysis are based on geometric optics, all feature dimensions must be much larger than the wavelength of visible light, limiting the minimum reflecting feature size. For a high efficiency concentrator, the prism base should not exceed 1/10 of the lens pitch; if the prism size is minimized, the likelihood of undesired interactions between the propagating rays and the prism features can be reduced, maximizing the overall efficiency of the concentrator [24].

The decoupling losses can also be mitigated by limiting the number of times each ray strikes the patterned face on the bottom of the concentrator. This can be achieved by reducing the surface area of the concentrator, or increasing the thickness of the bottom

layer of the waveguide. For most applications, reducing the surface area of the concentrator is not desirable, as this will reduce the concentration factor, and output power of the waveguide. In addition, the thickness of the bottom layer of the concentrator waveguide dictates the thickness of the diffuser region, so careful consideration must be given to the performance of the diffuser.

If a higher degree of concentration is desired rather than maximum efficiency, different prism shapes and spatial distributions may be used. Rather than illuminating all four edges of the concentrator, a more localized concentration can be obtained by adjusting the micro-optical reflecting features and features distribution. In order to illuminate instead, only one or two faces, a wedge feature, rather than a pyramid, may be used. The position of the wedge with respect to the focal point of the lens may be adjusted to control the distribution of light to one face only, or two opposite faces of the waveguide. These approaches still attain high levels of efficiency, however they are somewhat less efficient than the pyramid design since some illumination is lost out of the edges adjacent to the active faces. A higher degree of concentration can also be achieved, by again using the wedge-shaped features, but rather than a rectangular-grid distribution of the features, a circular pattern may be used. If the lens and prism features are patterned in an arc around the point where illumination is desired, an even higher degree of concentration can be attained. Again, the reduction in active space on the concentrator edge results in some illumination losses on these faces, but allows for much higher factor of concentration [38].

In addition to permitting variations in the illumination pattern of the concentrator, these modifications may also facilitate fabrication. Although the pyramid features provide the optimal distributed illumination for the concentrator, they are also the most difficult to manufacture. Due to the necessity for sharp corners, they cannot easily be machined and would make the manufacturing process more complex, expensive and time consuming. The cone features would be easier to machine since they have a smooth edge, however the pointed tip is still essential and would be difficult to manufacture precisely. For ease of machining, the wedge features are ideal since the pointed tip may be offset from the focal point, meaning that a perfectly pointed tip is not required. The resulting

waveguide may in fact have a higher efficiency than those manufactured with the cone or pyramid features since the losses at the feature tip will be minimized.

There are numerous alternative design configurations which may be used for the concentrator feature type, size, and pattern, which will all result in different manufacturing requirements and performance characteristics. Depending on the manufacturing constraints and the desired concentrator output, the appropriate features must be selected and optimized.

Similarly, the design and optimization of the diffuser features must be considered. The primary parameters for the design of the diffusing region are the angle of the diffusing wedges, θ_d , the width of the features, w , the length of the diffusing region, l , and the thickness of the waveguide. The minimum and maximum allowable wedge angles are dictated by the angle of propagation of the source illumination, and the refractive index of the diffuser, thus the appropriate θ_d for the diffusing features may be calculated.

Since the concentrating region and diffusing region of the waveguide are monolithic, the thickness of the diffusing region is equivalent to the thickness of the concentrator's lower layer, t_2 . In order to minimize the length of the waveguide, the longest ray path must be considered. If the height of the diffuser layer (t_2), and the angle of propagation (θ_p) are known, based on the concentrator design; the maximum distance which a ray travels before striking the patterned face can be predicted. This distance corresponds to the minimum length required for a high efficiency diffuser waveguide.

To achieve a high degree of uniformity for the diffuser region, the waveguide geometry can be modified according to the desired waveguide area. If a small diffusing region is desirable, the density of features must be maximized, and the feature size may be reduced to enhance uniformity. Additionally, if a smaller diffuser region is desired, in order to minimize the diffuser area, a reflective coating may be applied to the face opposite the concentrator edge. This will allow the rays to propagate through the diffusing region twice, thereby halving the minimum length for the diffuser region. Conversely, if a larger diffuser area is desirable, the density of the diffusing features must be varied according to the length of the diffuser, so that only the appropriate proportion of rays is diffused on each interaction with the patterned face [18].

The wedge features' shape, size and spatial distribution, as well as the geometry of the diffusing region, are largely dependent on the optimized concentrator waveguide, and must be designed accordingly. The optimized diffuser design may be modified according to the desired application, in order to maximize both the efficiency and uniformity of the diffusing region of the waveguide.

4.4.2 Microstructure Density and Distribution

The density and distribution of the micro-features in both the concentrating and diffusing regions of the waveguide, are essential to their efficiency and uniformity. In the patterning of the concentrator features, the illumination pattern, and transmission efficiency must be considered. In the general case of an optimized planar waveguide, a rectangular feature pattern is suitable as it directs illumination evenly to all four faces, and permits a maximum distance between coupling features. Different feature densities and distributions may be used for alternate applications. If directional concentration is desired, to a point or region of the concentrator, rather than all four edges, a circular feature pattern may be used, with coupling wedges. The circular pattern of the wedge features will direct all illumination in the direction which they are oriented, permitting a much higher factor of concentration with a modest reduction in efficiency. Thus, if a more focused concentration is required, it can be achieved with a modified feature pattern. Additionally, if the concentrator is to be flexible, and the orientation of the waveguide is unknown, it may be beneficial to increase the density of coupling features without varying the density of micro-lens features, in order to increase the likelihood that the focused rays strike a coupling feature, thereby improving the waveguide's flexibility.

Similarly, the performance of the diffusing region of the waveguide may be controlled with variations in the features' density and distribution. In order to maximize the efficiency of the diffusing region, the density of features must also be maximized, however this approach limits the uniformity of illumination. Since the intensity of illumination decreases with distance from the source, if maximum uniformity is desired over efficiency, the diffuser features should be patterned with density increasing with distance from the source. Additionally, the depth of the diffuser features may be

increased with distance from the waveguide, to improve extraction efficiency with distance without sacrificing feature density closer to the source.

Additionally, if the region targeted for illumination is some distance from the location of collections, an unpatterned region of the waveguide may be used for transmission of illumination. This is essential in light harvesting applications, where solar light is collected and transmitted via optical fiber to the illumination location. In this case only the concentrating and diffusing regions will be patterned with their respective micro-features, and the transmission region will not incorporate any microstructures. The performance, and functionality of the waveguide can therefore be widely adapted to different settings and applications, with appropriate variations to the features' density and distribution.

4.4.3 Microstructures for Efficient Light Concentrators and Diffuser

As outlined above there are many features shapes, sizes and configurations which can be selected depending on the desired parameters of performance. However, the specific micro-structures for high efficiency light guiding in a flat waveguide are as follows. For the concentrating region of the waveguide, the optimal configuration of features will include the micro-lens features positioned directly above a single coupling feature, with a rectangular distribution. The coupling features will be the square-based pyramid features, which direct the focused light evenly and predictably to the four concentrator faces. The pyramids should be minimized in size to reduce decoupling losses of propagation illumination. For the diffusing region of the waveguide, symmetrical wedge features with their angle optimized, should be used to permit diffusion in both the forwards and reverse directions of propagation in the case that a reflective coating is used. As well, the wedge features must be patterned uniformly with maximum density for high efficiency diffusion. The surface area of the waveguide should not be any larger than the minimum required area for the desired application, and the thickness should be no smaller than the required thickness, so as to maintain maximum efficiency.

4.5 Equations for the Design of a Flat Waveguide

The theoretically optimal geometry for the planar waveguide's concentrating and diffusing microfeatures can be determined by the equations below. The equations are based on the assumption that the desired application of the waveguide will dictate some of its geometrical constraints. It is therefore assumed that the materials' refractive indices (n_1 and n_2); the maximum waveguide thickness (t_{max}); the desired surface area (SA); and the minimum factor of concentration (CF) are known. General equations which can be used to determine the optimal geometry for various applications are given, as well as an illustrative example to be used in subsequent models and simulations. For the example the following parameters are used: $n_1=1.4$, $n_2=1.55$, $t_{max}=2$ mm, $SA=50,000$ mm² and $CF=500x$. In order to fully define the waveguide geometry for the collector and illuminator regions, the thicknesses (t_1 and t_2), the radius (R) of the lens micro-features, the pitch (P) of the concentrator features, the angle of incline of the coupling prisms (α), the width of the base of the coupling features (b), the wedge angle (θ_d) of the diffusing wedges, the length of the diffuser (l) and the width (w) of the diffusing wedges, must be calculated based on the known constraints.

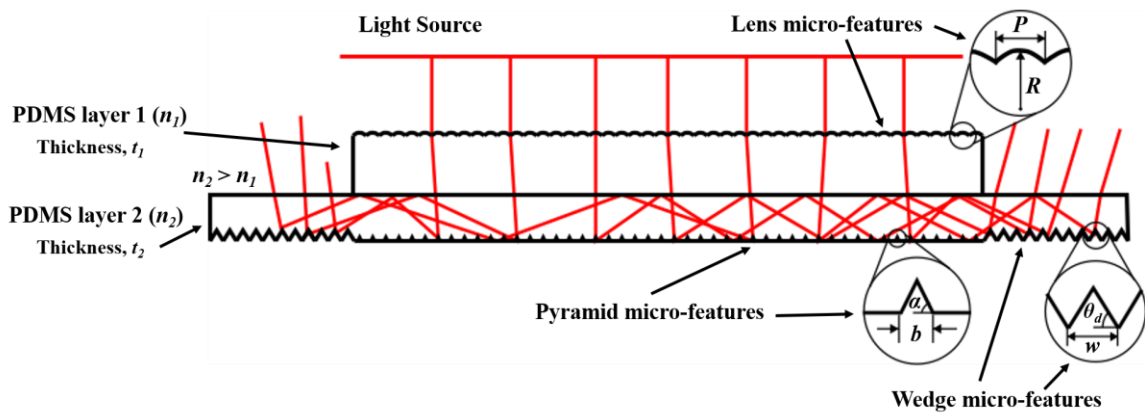


Figure 4.4 Illustration of concentrator and diffuser waveguide denoting important features; lenses, pyramids, and wedges, and their relevant parameters.

- (i) Based on the minimum required concentration factor, the thickness of the lower layer t_2 , can be estimated. This value is later refined based on the lens radius, but

the estimate allows the calculation of dependent variables, including the thickness of the upper layer t_1 .

$$t_2 = \frac{\sqrt{SA}}{CF} = \frac{\sqrt{50000}}{500} = 0.4 \text{ mm} \quad (4.1)$$

$$t_1 = t_{max} - t_2 = 2 - 0.4 = 1.6 \text{ mm} \quad (4.2)$$

- (ii) Based on the materials' refractive indices, and the waveguide thickness the lensmakers' equation [23] can be used to determine the appropriate radius for the concentrating lens microfeatures.

$$R = \frac{(t_1 + t_2) * (n_1 - 1)}{n_1} = \frac{2 * (1.4 - 1)}{1.4} = 0.57 \text{ mm} \quad (4.3)$$

- (iii) The maximum allowable angle of propagation (θ_{Pmax}) of rays in the waveguide is limited by the critical angle between the waveguide layers, dictated by their refractive indices;

$$\theta_{Pmax} = 90 - \sin^{-1} \left(\frac{n_1}{n_2} \right) = 90 - \sin^{-1} \left(\frac{1.4}{1.55} \right) = 25^\circ \quad (4.4)$$

Although the above equation accurately defines the maximum angle of propagation for total internal reflection in the waveguide, it is undesirable to have rays propagating at the maximum angle, as any variation in angle of the rays, or geometry of the waveguide will result in significant losses. If a greater degree of flexibility in the waveguide is desired, the angle of propagation should be much lower than the maximum allowable value, however reducing θ_P will result in a longer diffuser length, thus the angle must be optimized according to the desired application.

- (iv) Based on the ray path and the desired angle of propagation in the waveguide, the maximum allowable angle (α_{max}) of the coupling prisms, is calculated:

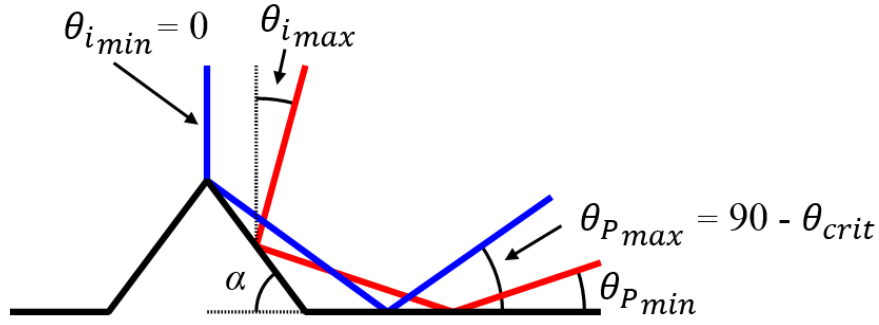


Figure 4.5 Ray diagram for focused light incident on the coupling prisms, illustrating the minimum and maximum angles of incidence and propagation.

$$\alpha_{max} = \frac{\theta_{P_{max}} + 90}{2} = \frac{25 + 90}{2} = 57.5^\circ \quad (4.5)$$

Based on the critical angle between the lower layer of the waveguide and the surrounding medium, and the maximum angle of incidence of concentrated rays on the coupling prism, the minimum angle (α_{min}) is calculated:

$$\alpha_{min} = \sin^{-1} \left(\frac{n_0}{n_2} \right) + \theta_{i_{max}} = \sin^{-1} \left(\frac{1}{1.55} \right) + 5 = 45.2^\circ \quad (4.6)$$

For the example in consideration the maximum angle of incidence (Figure 4.5) was assumed to be 5° , however this must be optimized according the waveguide's application. The angle of incidence dictates the pitch of the concentrator features, a lower angle of incidence corresponds with a smaller feature pitch and therefore a higher density. This results in an increase in decoupling losses for propagating rays, but also results in a more flexible waveguide and higher diffuser efficiency, therefore the application must be known to suitably optimize the angle of incidence.

The base angle for the coupling prisms must therefore lie somewhere between α_{min} and α_{max} . For a more flexible waveguide a value closer to α_{min} should be selected, but for the example waveguide a mid-range angle of $\alpha = 52.5^\circ$ is used to maximize the acceptance ability of the prism, for rays which deviate from the expected angle of incidence.

- (v) Since the pitch of the concentrating micro-features is based on the angle of incidence of the rays on the coupling prisms, and the lens' radius, the pitch, P , can be calculated according to:

$$\theta_{i_{max}} = \sin^{-1} \left(\frac{n_1}{n_2} \sin \left(\tan^{-1} \left(\frac{0.5P}{\sqrt{R^2 - (0.5P)^2}} \right) - \sin^{-1} \left(\frac{1}{n_1} \sin \left(\tan^{-1} \frac{0.5P}{\sqrt{R^2 - (0.5P)^2}} \right) \right) \right) \right) \quad (4.7)$$

For the example in consideration $P=0.371\text{mm}$, calculated iteratively, using the above equation. The derivation of this equation, relating the angle of incidence, and the feature pitch is given in Appendix A2.

- (vi) With the radius and pitch of the concentrator lens features known, the thickness of the bottom layer of the waveguide, t_2 , can be calculated more precisely by:

$$t_2 = f - t_1 \quad (4.8)$$

For the example waveguide being considered the thickness is calculated at $t_2=0.382\text{ mm}$. The optimal thickness is derived from the precise focal length of the micro-lens f . Refer to Appendix A3 for the precise equation, and derivation of the layer thickness equation.

- (vii) Ideally the rays would focus at a single point, however due to the use of layers with different refractive indices, and spheric lenses which result in some focal shift, thus the focal width depends on the feature geometry. The focal width will dictate the minimum feature size for the coupling prisms, however for micro-scale features, the relationship between feature size and wavelength must be considered. For this waveguide it is determined that the minimum feature dimension should not be less than ten times the wavelength of visible light, or approximately 0.01 mm.

For the example waveguide, the theoretical minimum feature size, based on the equations derived in Appendix A1, is $b_{min}=0.005\text{ mm}$. Since this value is smaller than the minimum allowable feature size – according to the geometric optics limit – the base width $b=0.01\text{ mm}$, should be used. Another important consideration in regards to the size of the coupling features, is the relationship between their size and pitch. The efficiency of the concentrator is highly dependent on the proportion of its

surface area occupied by coupling features, as this corresponds with the likelihood of a ray decoupling. In order to maintain sufficiently high concentrator efficiency, the coupling feature width b , should not exceed one-tenth of the features' pitch;

$$b_{max} = \frac{P}{10} \quad (4.9)$$

- (viii) The diffuser wedge angle can be calculated based on the geometry of the coupling features, as these features dictate the propagation angle of rays in both the concentrator and diffuser. The maximum angle of propagation, θ_{Pmax} , and the minimum propagation angle, θ_{Pmin} , (Figure 4.6) are calculated according to equation 4.10, below.

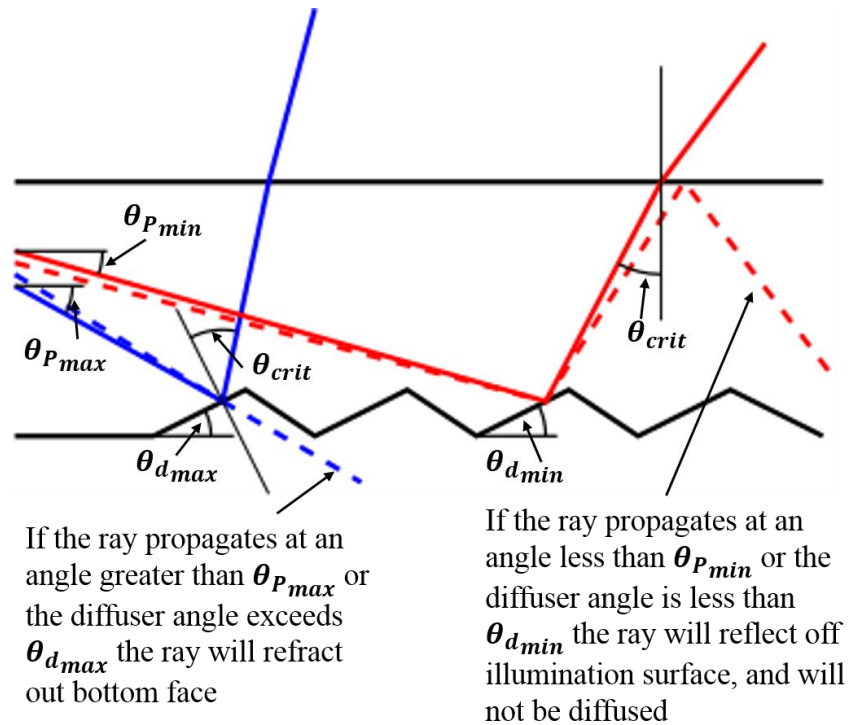


Figure 4.6 Ray diagram which illustrates the minimum and maximum angles of propagation required to ensure the rays are properly diffused out the face of the illuminating region.

$$\theta_{Pmin} = 2\alpha - 90 - \theta_{i_{max}} = 2*52.5 - 90 - 5 = 10^\circ \quad (4.10)$$

$$\theta_{Pmax} = 2\alpha - 90 = 2*52.5 - 90 = 15^\circ \quad (4.11)$$

Subsequently the minimum and maximum diffuser angles can be calculated based on the angles of propagation as well as materials' refractive indices:

$$\theta_{d_{min}} = \frac{90 - \sin^{-1}\left(\frac{1}{n_1}\right) - \theta_{P_{min}}}{2} = \frac{90 - \sin^{-1}\left(\frac{1}{1.55}\right) - 10}{2} = 20^\circ \quad (4.12)$$

$$\theta_{d_{max}} = 90 - \sin^{-1}\left(\frac{1}{n_2}\right) - \theta_{P_{max}} = 90 - \sin^{-1}\left(\frac{1}{1.55}\right) - 15 = 35^\circ \quad (4.13)$$

A larger angle will ensure that rays are diffused closer to the normal to the diffuser's illuminating face, however an angle closer to the mid-range will improve efficiency by diffusing rays which propagate at angles slightly higher or lower than the predicted values. For a flexible waveguide, a mid-range value is ideal as it will help ensure reflection off the wedge features and refraction out the illuminating face for variations in waveguide curvature. An upper mid-range, diffuser wedge angle of $\theta_d=30^\circ$ is used for the example waveguide.

- (ix) The minimum diffuser length is calculated based on the minimum length required for all rays to strike a diffusing feature once. This equation is dependent on the wedge angle θ_d , and the diffuser thickness t_2 , which is equivalent to the lower layer thickness from the concentrator.

$$l_{min} = 2 * \left(\frac{t_2}{\tan(\theta_{P_{min}})} \right) = \frac{2 * 0.415}{\tan(10)} = 4.7 \text{ mm} \quad (4.14)$$

- (x) Finally, the diffuser wedge size, w , must be calculated. The feature size may vary according to the application, as a larger feature size may be more appropriate for a flexible waveguide. For a rigid, planar waveguide a smaller feature size is conducive to higher uniformity of the illuminator, so the feature height is limited to one-tenth the diffuser region thickness:

$$w = \frac{t_2}{5 * \tan(\theta_d)} = \frac{0.415}{5 * \tan(30)} = 0.144 \text{ mm} \quad (4.15)$$

The above equations may be applied to any waveguide design for controlled light guidance. The final waveguide is fully scalable, down to the geometric optics limit, if variations in thickness or area are desired. As noted in the above descriptions, there is some discretion in the selection of the geometric parameters calculated in this section; the impact of these variations is examined more thoroughly in Chapter 5.

4.6 Performance of Functionally Designed Flat Waveguide

Based on equations outlined in Section 4.5, a theoretically optimal waveguide is designed and simulated in Zemax OpticStudio. As outlined above, the geometry for the theoretically ideal waveguide is defined as: $t_1=0.382$ mm, $t_2=1.6$ mm, $R=0.57$ mm, $P=0.371$ mm, $\alpha=52.5^\circ$, $b=0.01$ mm, $\theta_d=30^\circ$, $l=4.7$ mm, and $w=0.144$ mm. The concentrator and diffuser are modelled separately to examine the performance of each of the individual features, and finally the hybrid waveguide is simulated and performance is evaluated.

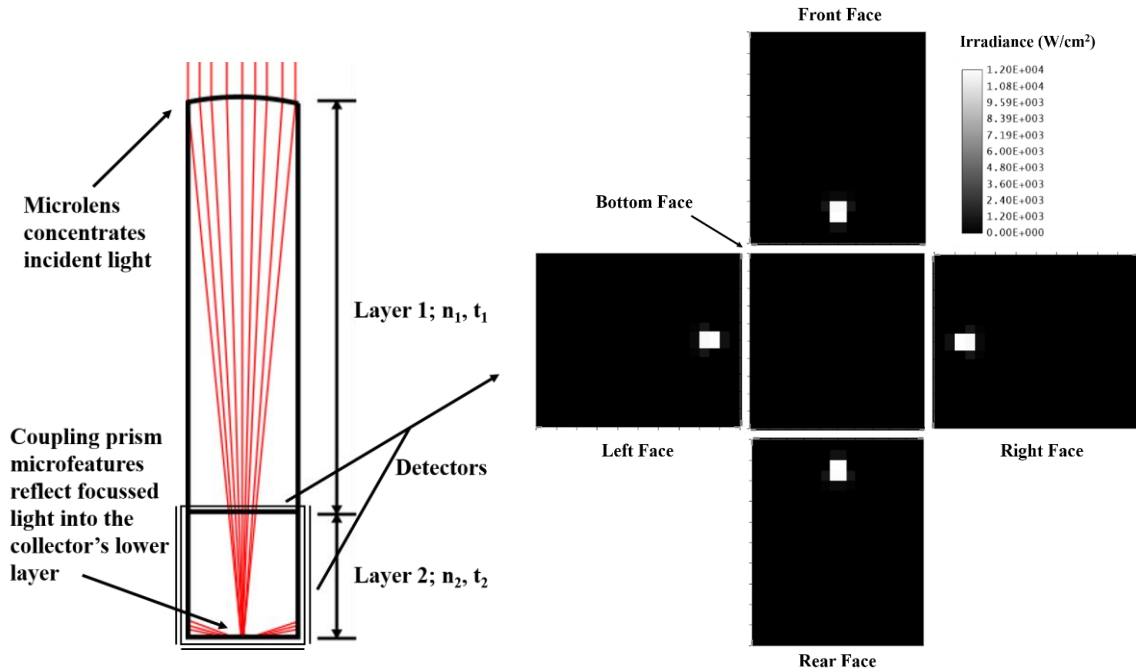
4.6.1 Single Microstructure

First a single microstructure is modelled and simulated to examine the efficiency of the design, and validate the geometry choices.

4.6.1.1 Concentrator

For the concentrator feature, a single lens over a single coupling pyramid is modelled according to the geometry identified above. In order to confirm its concentrating and coupling ability, the percent of incident rays collected by the feature, and directed to the four concentrator faces, is used to estimate its efficiency.

The ray trace for a single concentrator feature, as well as the detector data from each of the faces of the lower layer of the concentrator feature, are shown in Figure 4.7. This configuration demonstrated an efficiency of 99.64% with the concentrated rays evenly distributed among the four concentrator faces. The losses exhibited were determined to be a result of the focal shift causing the distribution of rays to be wider than the coupling features' base. This could be rectified by increasing the feature size, however this is not advisable as larger coupling features will correspond to greater decoupling losses, as discussed above, and a 99.64% efficiency is sufficient for nearly all applications.



(a) Ray diagram of single concentrator feature.

(b) Detector data for each of the concentrator edges, and the bottom face.

Figure 4.7 A single concentrating feature successfully collects over 99% of incident illumination based on the Zemax analysis and results.

4.6.1.2 Diffuser

The efficiency of the diffuser feature is examined by modelling a single wedge, and using the illumination pattern from the concentrator as the light source. The ray trace for a single diffuser feature is illustrated below in Figure 4.8.

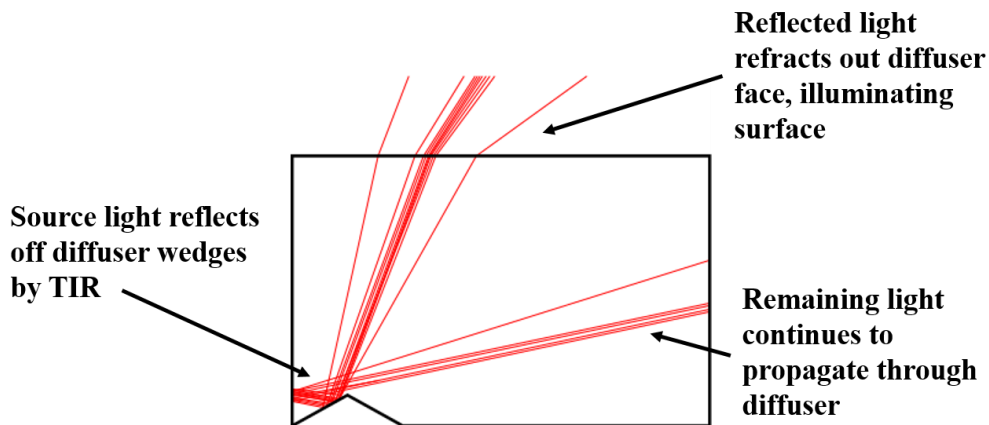


Figure 4.8 Ray trace of a single diffusing wedge; over 98% of the illumination which strikes the wedge is successfully diffused, while the remaining incident light continues to propagate through the diffuser.

In this configuration only 4.04% of the total incident illumination is diffused by a single wedge feature. This efficiency appears quite low, but each feature is only expected to diffuse a fraction of the total propagating light, therefore the ability of the wedge to diffuse light that strikes the feature is also evaluated. In this case the feature has a 98.62% efficiency, indicating that nearly all the light rays which strike the feature are successfully diffused. It appears that the majority of the losses occur due to rays which strike the wedge being lost out the sides of the waveguide, rather than the top as desired. The proportion of rays lost out the sides of the waveguide is minimized with a larger area waveguide, and are not a significant concern.

4.6.2 Linear Array of Microstructures

While the model of the single micro-features validates its functionality, the features must be patterned in an array to confirm their lightguiding performance for large-area applications. Therefore, the next step is to consider a linear array of microstructures.

4.6.2.1 Concentrator

For the concentrator it is important to consider a linear array of micro-structures in order to investigate the confinement of the rays to the guiding layer, as well as examining the decoupling losses of the rays as they propagate through the concentrator.

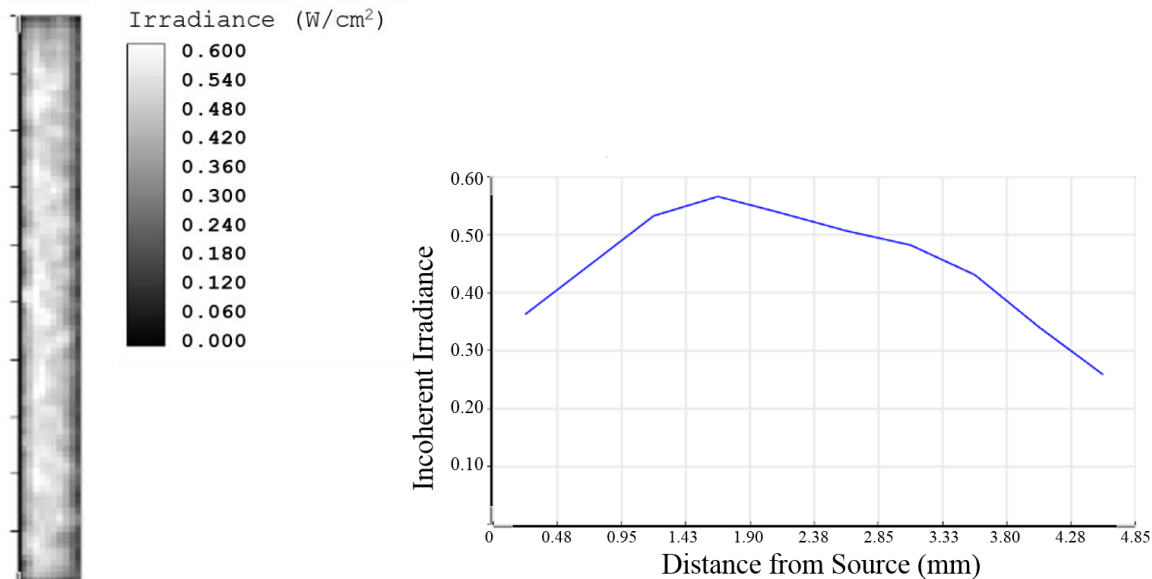


Figure 4.9 Detector data from the Zemax simulation of the row of concentrating features, showing light intensity patterns around the edges, and some illumination escaping the bottom face of the concentrator.

A linear array of the concentrating lenses and coupling pyramids is modelled and simulated, exhibiting an efficiency of 99.50%, based on the Zemax results seen in Figure 4.9. The waveguide demonstrated an excellent ability to confine propagating rays to the lower layer of the waveguide, however there were some resulting decoupling losses as propagating rays struck subsequent pyramids. These losses are represented in the small drop in efficiency seen between the single feature, and the linear array of features.

4.6.2.2 Diffuser

For the diffuser a linear array of wedge features represents the final design of the illuminator. Again the illumination pattern from the concentrator face is used as the light source for the diffuser, and a linear array of wedge features is used to diffuse the incident illumination.



(a) Detector data demonstrating diffuser illumination pattern.

(b) Graph illustrating the change in illumination intensity with distance from source.

Figure 4.10 The Zemax simulation of the linear array of diffuser wedges demonstrates high efficiency, high intensity illumination of the waveguide's face.

By this evaluation the diffuser demonstrated an efficiency of 94.45% efficiency, notably lower than the efficiency of a single diffuser feature. The majority of these losses occur as a result of some rays propagating at angles lower than the predicted minimum angle of propagation. For this reason, a portion of the illumination does not strike a diffusing wedge and remains in the waveguide. This could be rectified by elongating the diffusing region, or tapering the waveguide thickness towards the end of the diffuser to enhance both efficiency and uniformity of the illumination. It should be noted that while these losses only appear in the analysis of the diffusing region, they result primarily from the concentrator failing to collect light at the predicted angle of propagation.

Uniformity must also be considered when evaluating the performance of the diffusing waveguide (Figure 4.10). It is calculated by dividing the average irradiance over the entire diffusing face, by the peak irradiance. By this measure the linear array of diffusing

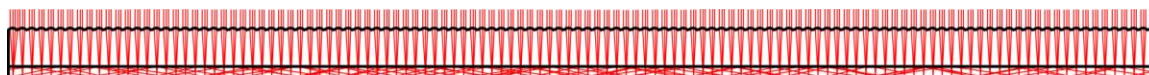
wedges achieves a uniformity of approximately 56%. While this is a reasonably high degree of uniformity for the diffuser waveguide, it is apparent when examining the detector data that the leading half of the diffuser has a much higher level of illumination than the trailing half. This is evidenced in the average illumination in the first half of the diffuser being 5.48 W/cm^2 while the average illumination in the second half is 2.10 W/cm^2 . Although the net uniformity of the diffuser is acceptable, it can be massively improved by using a reflective coating on the end face of the diffuser. Not only does this improve the uniformity up to 84%, by reducing the required length and increasing the likelihood of a ray being diffused towards the end of the diffuser, but it increases the efficiency by reflecting rays which may otherwise be lost out the end of the diffuser. While the diffuser certainly displays sufficient efficiency and uniformity without a reflective coating, this could greatly enhance the performance if such results are desired.

4.6.3 Area Array of Microstructures

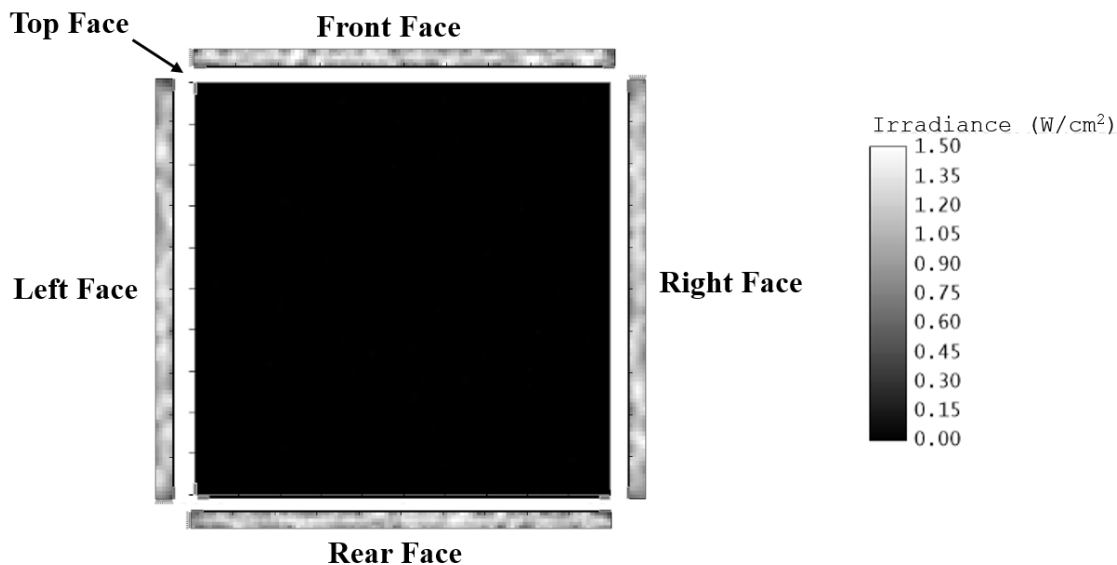
Finally, an area array of microstructures is optically simulated, representing the final waveguide configuration for a planar, rigid lightguide. The efficiency and uniformity must be considered to evaluate the waveguide's performance.

4.6.3.1 Concentrator

The area array of concentrator features is quite similar to the linear array, but provides a more accurate representation of the final waveguide model. Again there are expected to be decoupling losses due to undesired interactions between the propagating rays and the coupling pyramids. The Zemax ray trace and detector data are included in Figure 2.11.



(a) Ray trace of area array of concentrator micro-features.



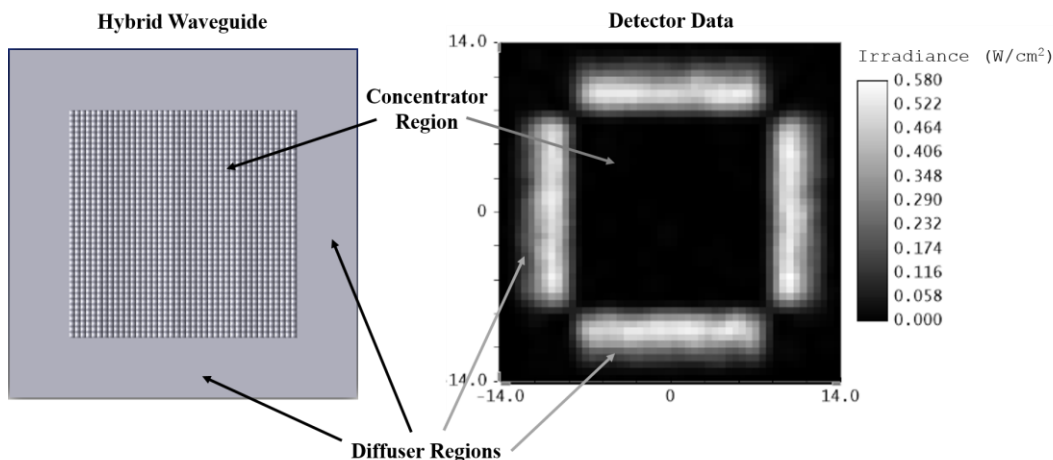
(b) Detector data illustrating illumination pattern for area array of concentrator features.

Figure 4.11 Zemax results from the area array of concentrator micro-features demonstrated high efficiency collection of incident illumination with greater uniformity over the collection region than previous results.

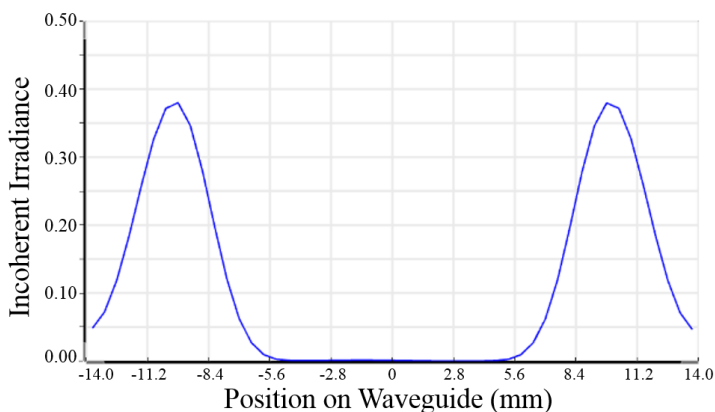
The efficiency of the concentrator in this case is 99.14%, as expected there is another small drop in efficiency caused by the decoupling losses. The total loss in efficiency exhibited by the area array of concentrator features is less than 1%, and is therefore not a great concern for the concentrator's performance, however the impact of decoupling losses will increase if the area is increased or if the waveguide thickness is decreased. Therefore, any increase to the concentrator's geometric factor of concentration will result in some decrease to the waveguide's efficiency. This is an inherent limitation of micropatterned concentrators and the waveguide must therefore be optimized according to the required efficiency and concentration ability of a particular application [29].

4.6.3.2 Concentrator-Diffuser Waveguide

The hybrid concentrator diffuser waveguide was modelled as the area array of concentrator features with the linear array of diffusing wedges bordering each of the four faces. This waveguide illustrates this design's ability to guide light in a controlled manner with a high efficiency. The hybrid waveguide had an efficiency of 94.33% when comparing the proportion of the light incident on the concentrator, to the proportion which was successfully diffused by the illuminator (Figure 4.12a). This was somewhat higher than the multiplied efficiencies of the concentrator and diffuser, likely due to rays which may otherwise have been lost being contained by the adjacent waveguide regions.



(a) Hybrid concentrator-diffuser waveguide geometry and Zemax detector data.



(b) Zemax detector data illumination profile across the centre of the hybrid waveguide.

Figure 4.12 Zemax simulation results displaying the illumination pattern and cross-sectional profile of the combined concentrator-diffuser waveguide.

The proposed waveguide model functions with a remarkably high efficiency which could be increased with small adaptations to the design (coupling feature size, reflective coatings etc.). The waveguide considered in this case however, is relatively small in area, only 750 mm², and if larger area waveguides are desired there will be some subsequent losses due to decoupling as the rays propagate through the guiding layer. The proposed waveguide as well as the above method for determining the ideal waveguide geometry provide an excellent basis on which to design a rigid planar waveguide for controlled guidance of light, however various modifications may be made to adapt the design for limitations derived from the material, geometry or application.

4.7 Discussion – Light Transmission Efficiency of Optimized Planar Waveguide

As evidenced by the results of the Zemax simulations the theoretically optimal waveguide, as calculated in Section 4.5, proves to have very high efficiency. In order to analyse the effectiveness of the concentrator features, the diffuser features, the concentrating region, the diffusing region, and the waveguide as a whole, each of these items was modelled and simulated separately. Based on the analyses of the individual features it is demonstrated that the concentrating features have an efficiency of over 99% and the diffusing features have an efficiency over 98%. Since both feature types were designed based on the theoretically ideal geometric optics model, it is not surprising that the ray tracing analysis in Zemax would demonstrate high efficiency, however this serves to validate the equations presented in Section 4.5.

Upon analysing the performance of the individual micro-features, the concentrating and diffusing region were analysed individually. For the diffusing region only the linear array of features was considered, as the long features may be patterned linearly to cover the entire desired illumination region. This linear array of features demonstrated an efficiency of approximately 95% and a uniformity of up to 84%. The augmented uniformity of 84% is achieved by applying a reflective coating to the far edge of the diffusing region, however without any modification the uniformity is 55%. For many applications 55% would prove to be a sufficient degree of uniformity, however if high uniformity is required, it is easily achieved with only a small modification to the

waveguide. Although the efficiency of the waveguide remains quite high at 95%, the lost 3% as compared to a single feature can largely be attributed to rays which fail to strike a diffusing feature and pass straight through the waveguide. Some of these losses too, can be recovered by adding a reflective coating to the diffuser edges if a higher efficiency is necessary.

When considering the performance of the concentrating region of the waveguide, an area array of features must be used to cover the entire collecting region. This simulation corresponded with an efficiency of over 99%, barely any lower than the single feature analysis. It must be noted however, that the larger the concentrator area the more decoupling losses there will be as the rays propagate through the transmission layer. As well, some of the lost illumination in the diffuser, as mentioned above, results from a propagating ray striking a subsequent coupling prism, but staying in the waveguide. Such rays are thus travelling at an undesirable angle and are ultimately lost in the diffusing region. Although there are some small losses, especially as the concentrator area increases, in general the optimized concentrator proves to function with a remarkably high efficiency.

Finally, the combined concentrator-diffuser waveguide is modelled and analysed demonstrating an efficiency of about 94%. While this is somewhat lower than the efficiency of the corresponding micro-features, it is rather high and suitable for nearly all proposed waveguiding applications. Additionally, the distribution as illustrated in Figure 4.12b, it illuminates the diffusion regions very effectively and efficiently. Overall the proposed optimal combined concentrator-diffuser waveguide effectively collects, directs and diffuses light with excellent efficiency.

4.8 Concluding Remarks

Chapter 4 demonstrates the successful optimization of a planar waveguide for light collection, and illumination. The optimized model demonstrates an efficiency of nearly 95%, and optimal distribution of light to the targeted areas. The chapter outlines the process of optimization for the idealized waveguide described, as well as a process for optimization of similar planar waveguides with different parameters or applications.

Upon examining the performance of the optimized concentrating and diffusing features, it is evident that they operate highly effectively with the individual concentrator feature demonstrating an efficiency over 99% and the diffuser feature with an efficiency over 98%. When these features are patterned in a large area array the efficiency is still well over 90% verifying the theoretical optimization described in Section 4.5.

Although this chapter thoroughly describes the ideal waveguide for a planar application, the same parameters will not be optimal if flexibility of the waveguide is required. It is thus necessary to examine how deviations from the optimal geometry will impact the performance of the waveguide, and determine how best to adapt the features' geometry under these circumstances. These variations will be addressed in Chapter 5, as well as presenting design guidelines for non-optimal waveguide conditions.

Chapter 5 Performance of Non-Rigid Waveguide Sheets

In order to understand how bending of the waveguide will impact its performance, the relationships between key parameters and waveguide efficiency are examined. Based on this analysis, it is possible to predict how the bending and deformation of the non-rigid waveguide sheet, will impact the performance, and potential solutions are proposed in the sections below. The proposed waveguides are simulated and their results are compared in order to characterize how best to modify the waveguide design for non-rigid performance. Finally, a summary of these results is included in order to dictate how the design should be modified according to various potential applications and requirements.

5.1 Key Parameters and Waveguide Performance

Although the optimal waveguide geometry may be identified for some of the relevant parameters, for others a range of acceptable values is identified. It is important to understand what impact variations of these parameters will have on the performance of the waveguide. Using the optimal geometry as defined in Section 4.5, the impact of varying the waveguide area; the refractive indices, n_1 and n_2 ; the concentrating lens pitch, P ; the coupling feature base angle, α , and size, b ; the diffusing wedge angle, θ_d , and width, w ; and the diffuser length, l , is investigated. The initial values for the waveguide parameters are: $n_1=1.4$, $n_2=1.55$, $t_1=0.382$ mm, $t_2=1.6$ mm, $R=0.57$ mm, $P=0.37$ mm, $\alpha=52.5^\circ$, $b=0.01$ mm, $\theta_d=30^\circ$, $l=4.75$ mm, and $w=0.144$ mm, as were previously defined as the optimal geometry for the given conditions.

5.1.1 Waveguide Parameters

Firstly, variations in waveguide area are considered, while maintaining optimal geometry for all other variables. The concentrating region of the waveguide is modelled with a surface area ranging from 225 mm² to 250,000 mm² in order to investigate what impact the increased surface area will have on the efficiency of the concentrator. The increase in surface area of the concentrator has the desired effect of creating a larger area waveguide, with a higher geometric factor of concentration, but conversely it increases the distance which a ray must propagate in order to reach the concentrator face. This increased

distance corresponds with an increased likelihood of a propagating ray striking a prism feature and decoupling from the concentrator, so it is expected that a larger area concentrator will exhibit a lower efficiency than a small area concentrator. The idealized waveguide was modelled and simulated in Zemax OpticStudio in order to examine the impact of variations in area on efficiency, with respect to W_C , the concentrator width – or the square root of the surface area – and these results are summarized in Figure 5.1.

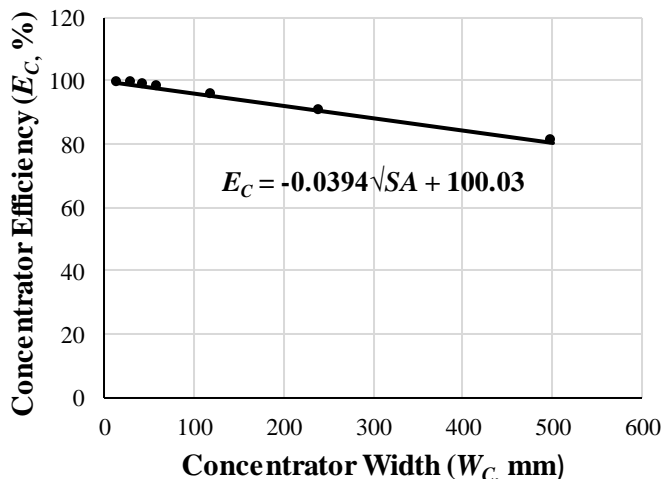


Figure 5.1 Relationship between the efficiency of the concentrating region (E_C) and the width of the concentrating region (W_C) based on the results of Zemax simulations.

As expected the simulations showed that the efficiency dropped with an increase in surface area. The results showed an approximately linear relationship between the width of the concentrator and its efficiency with a slope of -0.0394, thus indicating a strong negative correlation. Although the slope of the line of best fit is rather low, for large increases in area there is a relatively large drop in efficiency, with the 500 mm x 500 mm concentrator exhibiting an efficiency of only 80%, compared to the maximum efficiency of over 99%. So although the concentrator maintains functionality for any size, it is important to acknowledge that there will be a corresponding drop in efficiency if the area is increased without any other variations to the waveguide geometry.

The relationship between the refractive indices of the waveguide layers and the performance of the waveguide is also considered. To compare the performance for

variations in refractive indices, the ratio of the refractive index of the upper layer over the refractive index of the lower layer is used. The larger the difference in refractive indices, the larger the ratio n_2/n_1 . Since the concentrator is optimized for an n_1 of 1.4 and an n_2 of 1.55, the ratio of refractive indices for the optimal configuration is approximately 1.1. It is thus expected that the efficiency will be maximized for any value of n_2/n_1 greater than 1.1 and that the efficiency will drop off for values less than 1.1 as the difference in refractive indices will be insufficient to contain the propagating rays by total internal reflection; the results are summarized below (Figure 5.2).

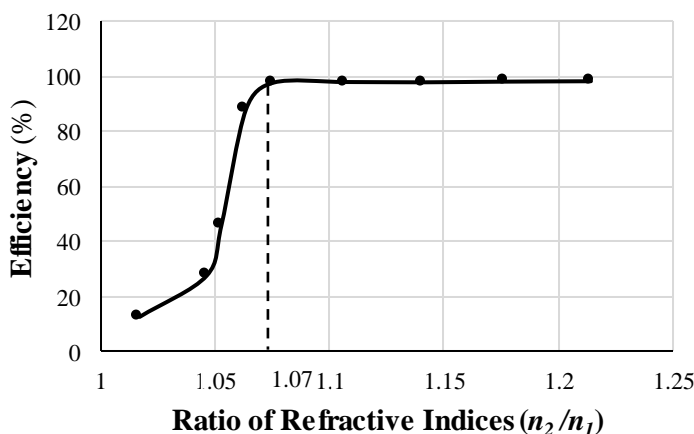


Figure 5.2 Relationship between the ratio of the refractive indices of the waveguide layers and the efficiency of the waveguide, demonstrating a large drop in efficiency for insufficient differences in refractive index.

As predicted, a very high efficiency is exhibited for ratios greater than or equal to 1.1, followed by a subsequent drop off in efficiency. However, the drop in efficiency in fact occurs for smaller ratios, and a high efficiency is maintained for n_2/n_1 greater than 1.07. This occurs because the optimized waveguide does not require the maximum difference in refractive indices in order to confine the rays to the bottom layer by total internal reflection, thus a smaller difference can still confine the rays with a high efficiency. Beyond the 1.07 threshold a steep drop of efficiency is observed, and the waveguide would have to be modified to further limit the angles of propagation if a smaller difference of refractive indices were to be used.

5.1.2 Concentrator Parameters

5.1.2.1 Concentrator Feature Pitch

As well as looking at the geometry of the waveguide as a whole, the individual parameters of each the concentrator and diffuser must be examined. First the relationship between the pitch, P , of the lens features and the concentrator's efficiency was investigated. Based on the optimization of the waveguide geometry the pitch $P=0.371$ mm, however this is one of the variables for which there is a range of acceptable values. The optimal feature pitch is based on the desired angle of incidence of the rays on the coupling prisms. The optimal angle is estimated as 5° , but there is a broader range of acceptable angles. The waveguide is thus modelled for values $P=0.010$ mm to $P=0.808$ mm, corresponding to angles of incidence from approximately 0° to 7° . A smaller pitch will lessen the effect of focal shift, and allow the concentrated rays to be reflected more efficiently off the coupling pyramids, but a smaller pitch also results in a higher density of pyramids, and therefore a greater likelihood of the propagating rays decoupling. It is therefore, important to investigate the relationship between the lens pitch and concentrator efficiency, in order understand the impact of these variations (Figure 5.3).

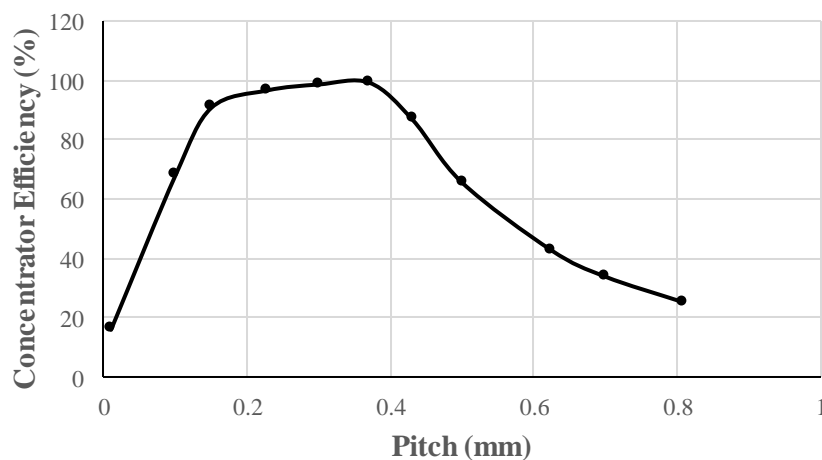


Figure 5.3 Relationship between the concentrator region's efficiency and the Pitch (P) of the concentrator micro-features based on the Zemax results.

The highest efficiency was exhibited for the 0.371 mm pitch, as this is the pitch for which the coupling prisms were optimized, and all concentrated rays could successfully be coupled into the lower layer of the waveguide. For lower pitches the efficiencies were relatively high, as the coupling prisms are still able to reflect all incident rays by total internal reflection, however when the pitch becomes excessively small, the increased density of coupling features causes a drop in efficiency. For larger pitches the efficiency drops substantially. Since the coupling prisms are optimized for an angle of incidence of 5° , or a pitch $P=0.371\text{mm}$, a larger pitch or angle of incidence will result in rays striking the coupling prisms at an angle less than the critical angle and being refracted out of the concentrator rather than coupled into the propagation layer. Although there is a range of acceptable values for the lens pitch, it is essential that the coupling prisms are designed in accordance with the value selected for the pitch; the angle of acceptance of the prisms must be greater than or equal to the angle of incidence corresponding with the lenses' pitch.

5.1.2.2 Concentrating Lens Radius

Next, variations to the radii of the concentrating lens features are considered. Since the radius of the lens features corresponds directly to the thickness of the concentrating region of the waveguide, any variations to the radius will result in a significant change to the lens' focal length. Since the coupling features are minimized in size any variation in the focal point of the lens will cause a significant drop in efficiency, as the concentrated rays will fail to strike the prism features and will not be successfully coupled into the propagation layer of the waveguide. This is evidenced by the results of the simulations in Figure 5.4.

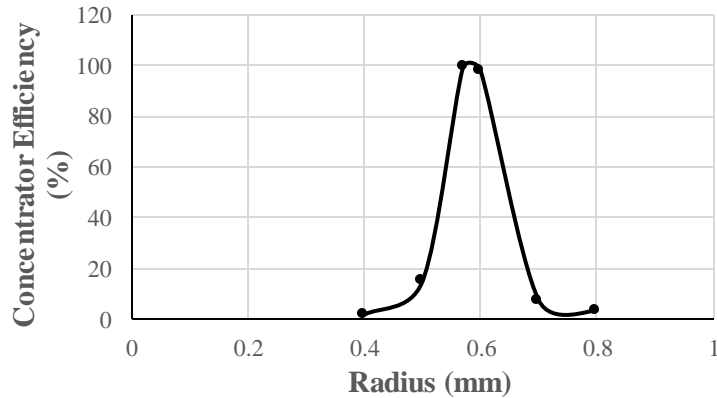


Figure 5.4 Relationship between the concentrating region's efficiency and the Radius (R) of the micro-lens features demonstrates a peak efficiency for the Radius as determined by the parametric modelling of the lens dimensions.

The optimized concentrator has a lens radius of 0.57 mm and it may be noted that the efficiency of the waveguide peaks at the 0.57 mm point. For very small variations in lens radius a high efficiency is maintained, but the drop in efficiency seen, even for moderate variations in radius, the efficiency drops to below 10%. Based on these results it can be determined that any variation to concentrator lens radius should be in conjunction with either a variation in concentrator thickness, or an increase in the size of the coupling features.

5.1.2.3 Concentrator Coupling Features

Similarly, the geometry of the coupling features is investigated in relation to the concentrator's efficiency. The base angle, α , of the coupling prisms is optimized as $\alpha=52.5^\circ$, however there are in fact a range of acceptable angles for this parameter defined by $\alpha_{min}=45.2^\circ$ and $\alpha_{max}=57.7^\circ$. The concentrator is modelled and simulated with angles ranging from 35° to 65° , to see the impact in variations in angle both inside and outside the range of acceptable angles. For values inside the acceptable range, it is expected that the efficiency will be consistently high, perhaps dropping slightly towards the limits of the range, but dropping significantly for angles outside the acceptable range. These substantial losses occur for angles below the acceptable range since this will result in the

concentrated rays striking the coupling prisms at angles less than the critical angle, and refracting out of the concentrator. For angles larger than the upper limit of acceptable values, the rays will be successfully reflected off the coupling features, however once they are coupled into the concentrator they will propagate at too great an angle to be confined to the lower layer by total internal reflection. The results from these simulations are summarized in Figure 5.5.

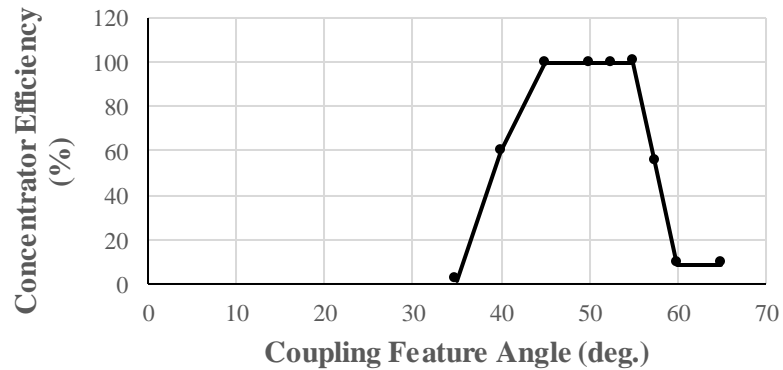
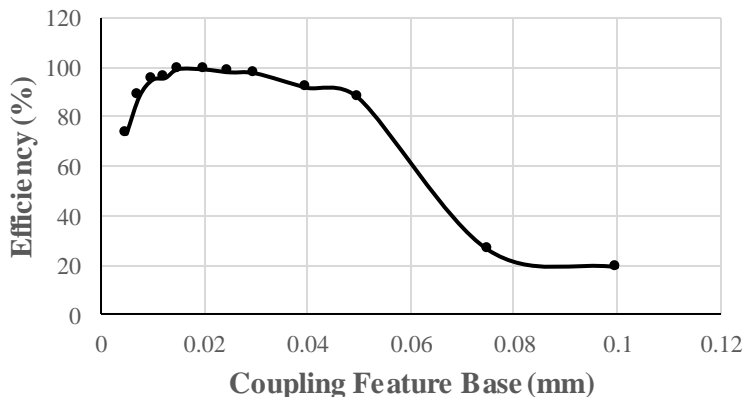


Figure 5.5 Relationship between the efficiency of the concentrating region, and the base angle (α) of the coupling features, denoting a high efficiency region of acceptable angles.

As predicted the efficiency is approximately constant, and remains very high, for all angles within the acceptable range. For angles outside the range, both above and below, there is an approximately linear decrease in efficiency, dropping sharply, to near-zero for the lower angles, and dropping to about 9° for angle above the range. The reason some efficiency is maintained for angles above the acceptable range, is that some rays are able to reflect off the lens feature in the upper layer, and propagate through the waveguide, but this efficiency is still far too low to be significant. Although any angle in the acceptable range could be selected for the coupling pyramid angle, it is still beneficial to select an angle in the middle of the range as this will ensure the concentrator is best able to accept small variations in ray angles, feature geometries, or material refractive indices.

Variations in the size of coupling features are also considered, this is modelled by varying the base size of the coupling features. The minimum allowable value was defined as 0.01 mm, according to the limits of geometric optics, however base widths are

considered from $b=0.005$ mm to $b=0.1$ mm, to investigate the theoretical impact of these variations in coupling prism size. For coupling features smaller than the minimum size defined in Section 4.5, the feature will be smaller than the focal width of the rays, resulting in rays refracting out the bottom of the concentrator without ever striking a coupling feature. Conversely, the larger the features, the greater the likelihood that propagating rays will strike a subsequent feature and decouple.



5.1.3 Diffuser Parameters

5.1.3.1 Diffuser Wedge Angle

Similar to the concentrator geometry, variations to the diffuser geometry are also considered, however in order to evaluate the performance of the diffusing region of the waveguide, it is important to investigate the impact on both efficiency and uniformity of illumination. First, the diffuser wedge geometry is considered. The optimal wedge angle is defined as $\theta_d=30^\circ$, as this is in the upper mid-range of acceptable values, which range from $\theta_d=19.9^\circ$ to $\theta_d=34.8^\circ$. Again, the diffuser efficiency and uniformity should be consistently high for values inside the acceptable range, however for angles outside the range, the efficiency will drop. For angles below the desired range, the angle of the ray striking the active face is greater than the critical angle, and thus the ray is reflected back into the waveguide, and is not diffused. For angles larger than the target range, the rays will refract out the bottom face upon striking a diffusing wedge, rather than being reflected off the wedge and refracted out the active face:

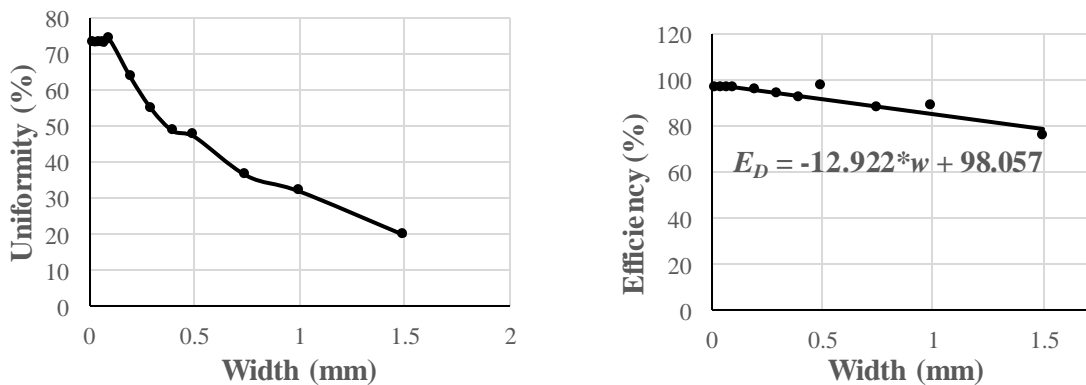
Table 5.1 Data from Zemax simulations representing the uniformity and efficiency of the diffusing region with respect to the diffusing wedge angle (θ_d).

Angle (deg.)	Uniformity (%)	Efficiency (%)
15	17.39	19.241
20	73.12	94.526
25	73.73	95.950
28.5	72.65	96.169
30	71.25	94.622
34.8	62.59	88.891
35	62.58	89.466
40	40.19	19.776
45	44.58	41.056
50	50.34	31.188

While the results were, for the most part, predictable, there were some anomalies in the data, relating in particular to the diffuser angles greater than the recommended maximum. While there was a definite decline in both efficiency and uniformity for angles above the range, the efficiency actually increases again, before dropping back down, as the diffuser angle increased. Although the cause of this increase is not entirely clear, it appears to be caused by rays which are refracted out of the diffusing features, striking the opposite side of the wedge features, and being refracted back into the waveguide, and ultimately being successfully diffused. Beside this anomaly, the efficiency and uniformity were consistently high in the acceptable range, and dropped off for angles below the minimum acceptable angle.

5.1.3.2 Diffuser Wedge Size

The size of the diffusing wedges, and its impact on the diffuser region's efficiency and uniformity is also considered. Wedge sizes ranging from 0.025 mm to 1.5 mm are modelled and simulated in Zemax. Smaller wedge sizes are expected to exhibit a higher degree of uniformity, as they distribute the light across the illuminating face more evenly. The efficiency should remain relatively constant with wedge size, as the length of the diffuser is designed to ensure all rays strike a diffusing wedge, regardless of wedge size, as seen in Figure 5.7 below.



(a) Uniformity (U_D) of diffusing region. (b) Efficiency (E_D) of diffusing region.

Figure 5.7 Results of Zemax simulations representing the relationship between the performance of the diffuser and the width (w) of the diffuser micro-features.

As expected, there is a negative correlation between uniformity of the diffuser illumination, and the size of the diffuser features, as the smaller features distribute illumination more effectively. There was also a strong negative correlation between the feature size and the diffuser efficiency, exhibiting an approximately linear relationship, with a slope of -13. This appeared to be due to illumination reflecting off the bottom face of the concentrating region, and striking the first diffuser feature at such an angle that the illumination is lost. The proportion of total illumination which is affected by this phenomenon is directly proportional to the size of the first diffuser feature, hence the linear relationship between feature size and efficiency. While there are some simulations which did not adhere to this trend, this does explain the general relationship between wedge size and waveguide efficiency, and allows for the approximate prediction of diffuser performance for a given feature size.

5.1.3.3 Diffuser Region Length

Additionally, the length of the diffusing region of the waveguide must be considered. The minimum length calculated according to the waveguide optimization is 4.75mm; for the simulation diffuser lengths from 3mm to 5.5mm are considered. It is expected that the efficiency will increase with diffuser length, while the uniformity will decrease with diffuser length. This is because a longer diffuser will increase the likelihood of a ray striking a diffusing wedge, and refracting out the illuminating face, therefore increasing the efficiency. However, this will cause a corresponding decrease in uniformity, as the number of rays remaining in the waveguide will decrease with distance from the concentrating region, and therefore the intensity of illumination will decrease as well, reducing the overall waveguide uniformity. The results of this analysis are summarized below in Figure 5.8.

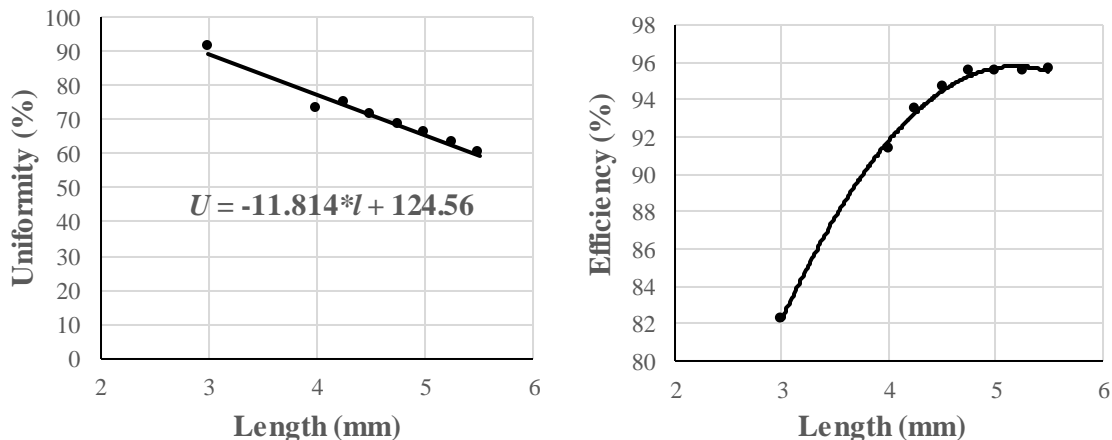
(a) Uniformity (U_D) of diffusing region.(b) Efficiency (E_D) of diffusing region.

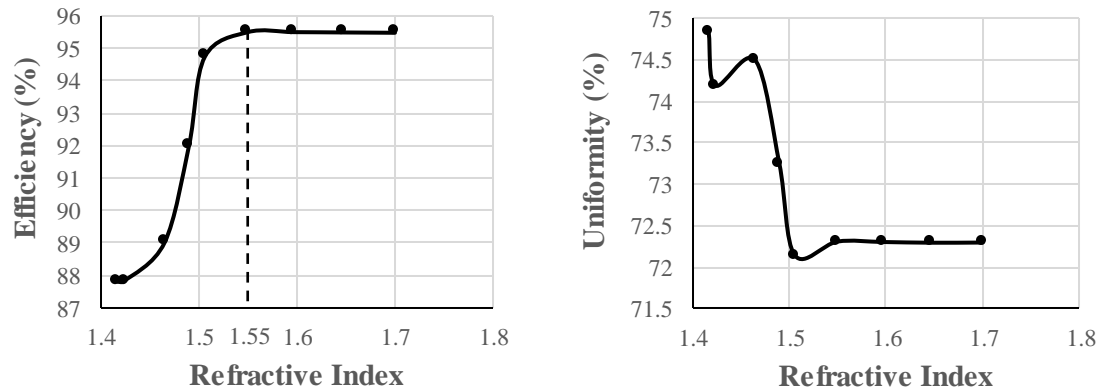
Figure 5.8 Results of Zemax simulations representing the relationship between the performance of the diffuser and the total length (l) of the diffusing region.

The variations in length affected the diffuser performance according to the predictions, however some notable trends emerged. The decrease in uniformity is linear with increase in diffuser length with a slope of approximately -12, whereas the relationship between length and efficiency is non-linear. The efficiency increases dramatically with diffuser length, up to the minimum length $l=4.75$ mm, but for increases in length beyond 4.75 mm, the incremental increase in efficiency is negligible. Therefore, the optimized length proves to be the ideal diffuser length if a balance between uniformity and efficiency is desired, however if a higher degree of either uniformity or efficiency is desirable, the length may be adjusted accordingly.

5.1.3.4 Diffuser Refractive Index

Finally, the impact of the variations in refractive index of the waveguide layers on the diffuser performance is considered. Since the diffuser is composed of only one layer, only the refractive index of the bottom layer, n_2 , must be considered. Since the diffuser is parametrically optimized for a refractive index of 1.55, a refractive index greater than 1.55 should reflect the rays with a high efficiency, but still diffuse them as necessary. For refractive indices less than 1.55 the efficiency will drop off as some rays will strike the

diffusing features without being reflected, and be diffused out the bottom of the waveguide without illuminating the diffuser's active face. The uniformity of the diffuser will also be impacted by its refractive index. The optimized waveguide allows the diffused rays to exit the waveguide at an angle approaching the normal to the active surface, however by increasing the refractive index, the diffusion angle will decrease, presumably decreasing its uniformity as well (Figure 5.9).



(a) Efficiency (E_D) of diffusing region.

(b) Uniformity (U_D) of diffusing region.

Figure 5.9 Relationship between the refractive index of the diffuser region and its efficiency and uniformity of illumination.

The results demonstrate the predicted drop in efficiency for refractive indices which are too small to contain the reflected rays, and a high efficiency for all refractive indices above the optimization threshold. Although the uniformity appears to be optimized for a low refractive index, with a relatively steep drop-off proceeding the optimized refractive index, the actual variation between the minimum and maximum uniformity is only 2%, while the range in efficiency is 10%, so in most cases it would be preferable to sacrifice some uniformity to achieve a significantly higher efficiency.

5.2 Impact on Performance of Waveguide Bending

Similar to the above investigation of the impact of varying the geometric parameters of the waveguide, the impact of bending on the waveguide's performance is analyzed too.

Flexibility of the waveguide results in deformation of the optical micro-features, reorientation of the features with respect to the light source, and variation in the angle of propagation due to bending. These variations will impact the collection, transmission and diffusion ability of the waveguide, and thus they must be understood in order to design a high efficiency, non-rigid waveguide sheet.

5.2.1 Waveguide Bending

In order to understand the impact which bending of the waveguide has on its performance, and to isolate the impact of bending, the efficiency of an unpatterned transmission region of the waveguide was considered. Using the detector data from the concentrator face, the angles of propagation seen in the concentrator were mimicked in the transmission region, and the waveguide was modelled for varying radii of curvature. When the radius of curvature becomes too small for the waveguide to confine the propagating rays with the given difference in indices of refraction, the rays escape the waveguide and are lost. The results are summarized in Figure 5.10.

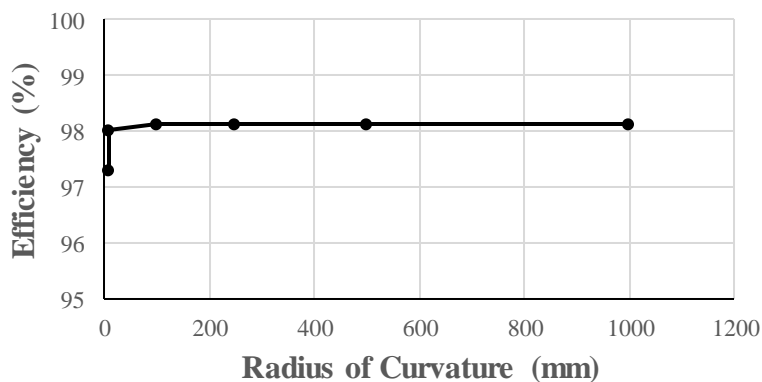


Figure 5.10 Relationship between radius of curvature (C) of the waveguide and the efficiency, demonstrating a steep drop in efficiency for small radii of curvature.

Although the efficiency of the waveguide drops-off quickly for very small radii of curvature, the transmission region was modelled with a radius of curvature down to 7.5mm, and still maintained a reasonably high efficiency. This is due to the significant difference between the refractive indices of the waveguide layers, and as well, even when rays enter the upper layer, the surrounding air acts as a cladding, and the rays are

confined to the waveguide. This indicates that traditional bending losses, which occur when the waveguide is bent at a radius less than the critical radius, will not be a factor of primary concern, as substantial losses occur for much larger radii in both the concentrating and diffusing regions of the waveguide.

5.2.2 Concentrator Bending

Bending of the concentrating region of the waveguide results in two major forms of losses. Firstly, bending of the concentrator results in deformation of the concentrating features, lessening the efficiency due to misalignment of the focal point, or variation in micro-feature angles. The second, and most significant, source of loss is the misalignment between the source and the features. For the planar waveguide a planar source is considered with the incident illumination perpendicular to the concentrator face, reminiscent of how overhead lighting, or sunlight, would strike the waveguide. If the same direct illumination is considered for a flexible waveguide, the orientation at which the light strikes the features is skewed, causing the lens' focus to be offset from the coupling features, resulting in major losses. In order to investigate both the realistic and ideal configurations, the concentrator is modelled under planar, overhead, illumination, and curved illumination which conforms to the geometry of the concentrator.

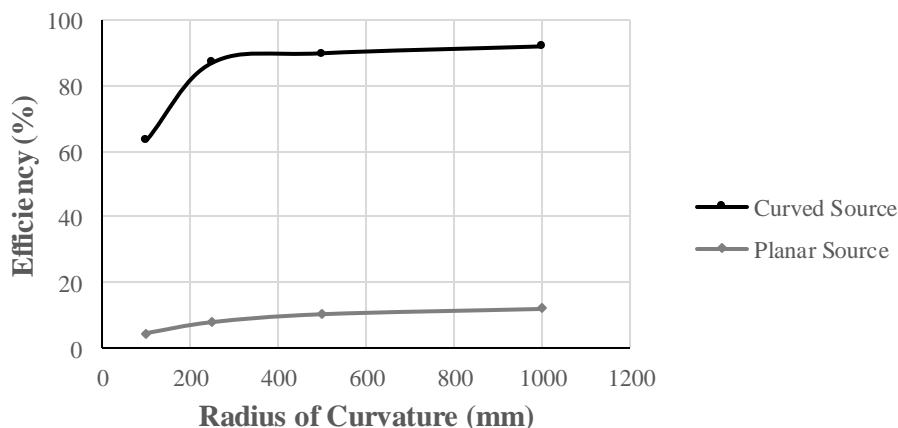
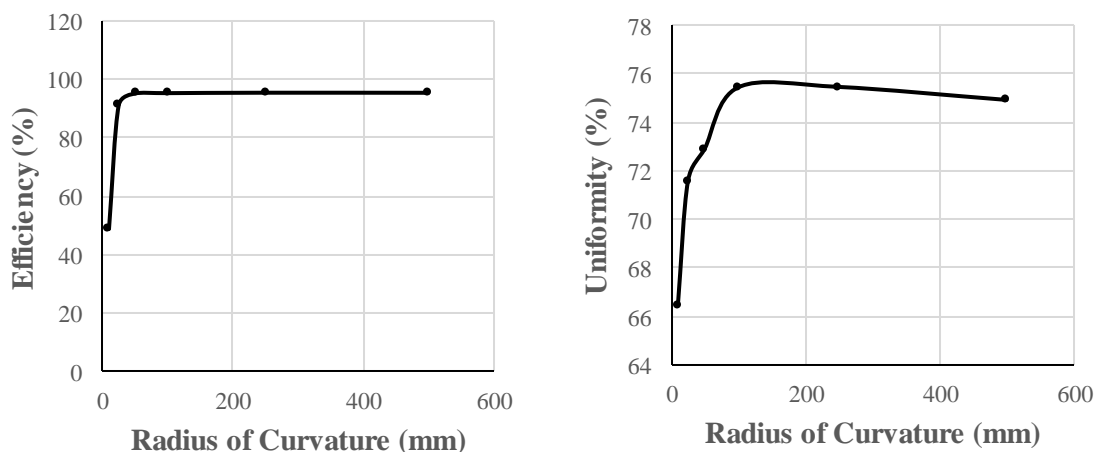


Figure 5.11 Relationship between the efficiency of the concentrator and its radius of curvature (C) comparing the use of a planar light source and a source which conforms to the curvature of the waveguide.

As evidenced by the data (Figure 5.11), the waveguide modelled with the light source conforming to the geometry of the concentrator has a relatively high efficiency, while the planar source results in efficiencies less than 10%. Both simulations however, exhibited similar trends, with the efficiency being approximately constant for radii of curvature greater than 300mm, and the efficiency dropping significantly for smaller radii. This data indicates that if the lighting conditions are to remain constant, some variation to the concentrator geometry is necessary to improve its efficiency.

5.2.3 Diffuser Bending

Similarly, the bending of the diffuser is considered, since the concentrator acts as the light source for the diffusing region, the orientation of the waveguide with respect to the waveguide need not be considered. The primary source of loss for the flexible diffuser waveguide is the resulting deformation of the diffuser features. The change in orientation of the diffuser wedges can cause the propagating rays to be refracted out the bottom face and lost. Additionally, the uniformity of illumination is impacted by the variations in diffuser feature orientation.



(a) Efficiency (E_D) of the diffuser region. (b) Uniformity (U_D) of the diffuser region.

Figure 5.12 Relationship between the radius of curvature (C) and the performance of the waveguide, illustrating a large drop in both efficiency and uniformity of the diffuser for small radii.

As expected both the efficiency and uniformity of the waveguide display significant losses for small radii of curvature, as seen in Figure 5.12, however the threshold for these losses is much lower than that of the concentrator. For the concentrating region, the efficiency dropped at close to 300 mm, while for the diffusing region the radius can be reduced to 50mm without significant impact on its efficiency or uniformity. Thus in optimizing the waveguide design for non-rigid configurations, emphasis should be on the modification of the concentrating region, as this region limits the waveguides flexibility, however consideration must also be given to the design of the diffusing region.

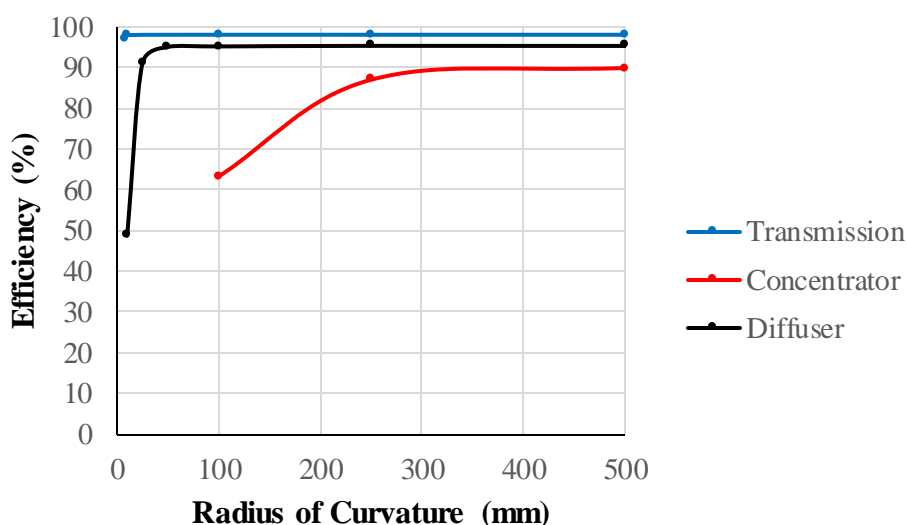


Figure 5.13 Relationship between the radius of curvature (C) and the performance of the waveguide, illustrating the largest drop in efficiency for bending in the concentrator area.

While a substantial drop in efficiency has been identified for each the transmitting, concentrating and diffusing areas of the waveguide, it is necessary to compare these losses. Figure 5.13 illustrates the relationship between the efficiencies for the different regions, and it is evident that the loss in efficiency is greatest in the concentrating area of the waveguide. Because the efficiency drops substantially for larger radii of curvature in the concentrating area, particular attention must be given to the redesign of the collector micro-features in order to ensure high efficiency for a flexible waveguide.

5.3 Microstructure Geometry for Non-Rigid Waveguide

In order to optimize the performance of the non-rigid waveguide sheet, various feature shapes, sizes and configuration must be considered for both the concentrator and diffuser features. In order to mitigate the losses in the concentrating region, variations on the geometry of the coupling prisms are considered, to improve the coupling ability of the waveguide, for suboptimal illumination conditions. For the diffuser waveguide variations in the shape and distribution of the diffusing wedges are considered in an effort to optimize efficiency and uniformity.

5.3.1 Concentrator Geometry

There are a number of limitations associated with the design of a membrane-like flexible waveguide. The optimization of the concentrator is based on the precise placement of the reflecting micro-features, and any relocation of the focal point will inhibit the rays from being reflected into the concentrating layer of the waveguide. Both the deformation of the waveguide, due to bending, and the variations in angle of incidence will result in some relocation of the focal point and therefore, some associated losses.

The deformation of the lens features causes a stretching along the direction of the bend, essentially increasing the radius in this direction [40]. The larger radius of the features will equate to a longer focal length, meaning the light won't be focused at the location of the reflecting features. This results in large losses in regions of significant stretching, as seen in Figure 5.14. In order to design a flexible waveguide with high efficiency, the original concentrator design must be modified to account for these losses. The stretching of the concentrating lenses is proportional to the size of the features and thus, can be controlled by scaling down the features. Having smaller lens features will allow the stretching to be distributed over more features and the resulting displacement of the focal point can be significantly reduced, as proven in Appendix A4.2. Additionally, relatively larger reflecting pyramid features can be used to increase the acceptance of the prisms, to account for any small variations in focal length caused by stretching.

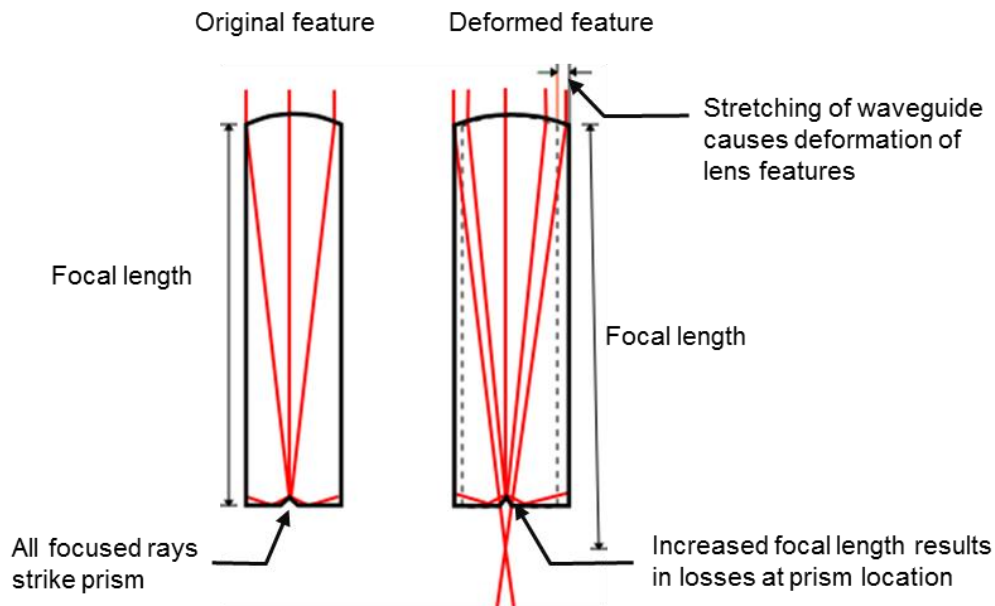


Figure 5.14 Deformation of features due to bending of the waveguide results in misalignment between the focal point of the micro-lenses and location of the coupling features.

Additionally, the bending of the concentrator results in an increased angle of incidence of the light hitting the waveguide surface. The larger the curvature of the waveguide, the larger the angle of incidence. The change in angle of incidence results in a shift of the focal point of the rays. The shifted focal point does not align with the reflecting prisms, as they have been optimized for direct illumination. Small changes in angle of incidence, therefore correspond to large losses of efficiency [40].

The focal shift due to increased angle of incidence is much harder to control than the stretching of the lens features. It is important that the size of the prism features is minimized to control the decoupling losses of propagating rays, but this limits the flexibility of the concentrator. Small variations in angle of incidence correspond to complete displacement of the focal point, as shown in Appendix A4.1. If the size of the reflecting features was increased to accommodate this focal shift, the efficiency of the waveguide would drop to near-zero, due to the subsequent decoupling losses. There are a few possible design modifications which can be made in an effort to maintain concentrator efficiency and enhance waveguide flexibility. The potential concentrator

configurations include; increasing the size of the reflecting pyramids, increasing the density of the pyramids, and the use of long wedge-type features, as illustrated in Figure 5.15.

Increases in the size or density of the reflecting features come at some expense to transmission efficiency of the concentrator. If a larger proportion of the concentrator surface is patterned, there is a greater likelihood of a ray striking a feature and decoupling. Conversely, this will produce the desired effect of increasing the likelihood that the focused rays strike the prism, increasing the flexibility of the waveguide. By increasing the size of the features, the acceptance angle of the waveguide can be increased to about 5° . However, the reflecting features become quite large and subsequently, the concentrator efficiency drops. Variations in feature size allow for deformations in any orientation over a very limited range. If only small variations in angle are required, the feature size can be increased to accept the maximum desired angle.

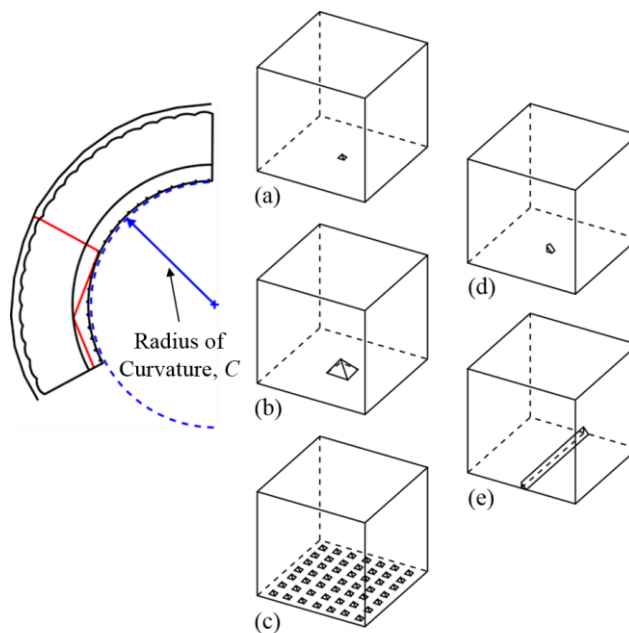


Figure 5.15 Various coupling features shapes, sizes and orientations are considered to evaluate their impact on efficiency of a flexible waveguide. (a) Minimized pyramid features, (b) Larger pyramid features, (c) Densely patterned pyramid features, (d) Minimized wedge features, and (e) Long wedge features are considered and compared.

Increases in feature density can similarly improve the acceptance angle of the waveguide. Unlike increasing the size, increasing the density of the features permits a large range of acceptance angles. The greater the proportion of the bottom face patterned with pyramids, the greater the likelihood that the focused rays will strike a reflecting feature. Thus, a greater feature density will correspond with more decoupling losses. By increasing the feature density, the flexibility of the waveguide can be greatly increased, and a high level of efficiency is maintained for the planar waveguide. However, a high efficiency for the bent waveguide cannot be attained without sacrificing the efficiency of the planar model [28].

Another possible modification to the design is using wedge-shaped features running the length of the concentrator, rather than individual pyramids. This would ensure that for any focal position along the concentrating axis, all the light would be successfully collected in the concentrator. This configuration still permits the minimization of the wedge features, and optimization of the transmission efficiency, however it has some significant limitations. The wedge-shape of the reflecting features means that the concentrator can only be used for directing light to one, or two faces, not all four like the pyramid features. Additionally, this concentrator can only be bent along the axis of the wedge feature, as bending in any other orientation would result in a misalignment between the focal point and the wedge. If bending is only desired in one direction, this option would be ideal as it produces the highest efficiencies for both the planar and bent configurations.

For the alternate concentrator geometries, proposed above, the ideal design will vary according to waveguide conditions. When considering small variations in angle of incidence in all directions, the increased prism feature size is suitable. If larger variations in angle of incidence are desired in all directions, an increased feature density is preferable. And, if flexing of the waveguide only occurs along a given axis, the wedge-shaped prisms, running the length of the concentrator are optimal. However, depending on the desired application of the concentrator, design modifications may not be necessary at all. The waveguide optimized for performance under direct illumination could, in fact, be beneficial for some sensing applications, or if the waveguide is moving in relation to

the light source, ensuring that regardless of the orientation, some of the incident light is being concentrated.

In order to verify and evaluate the performance of the concentrator, a number of different configurations were modelled and simulated in Zemax. In order to facilitate analysis, only a segment of the concentrating waveguide was considered. The optimal, rigid waveguide under direct illumination was modelled, as well as a flexed waveguide with varying angles of incident illumination.

Additionally, five different waveguide configurations are considered. First the optimized concentrator design with pyramid reflecting features, minimized in size (Figure 5.15a). Second, the same pyramid features, with a larger size are considered (Figure 5.15b), these features have a greater angle of acceptance than the optimized features, and are ideal for situations with minimal flexing. Third, small reflecting wedges are used, rather than pyramids, these features can only direct light to one face of the collector, but the wedge features are more easily manufactured than the pyramids (Figure 5.15d). Fourth, the pyramid shape is used again, but a higher density of features is used to increase the acceptance for greater changes in angle of incidence (Figure 5.15c). Finally, the wedge features running the length of the concentrator are considered, these are optimal for bending along the feature axis; bending in the opposite direction is considered as well (Figure 5.15e). These results from the simulations are summarized below, in Table 5.2.

As expected, in all configurations the planar waveguide exhibited much higher efficiency than the curved waveguide, however this loss of efficiency was much smaller for the long wedge features. The wedge features maintained a high efficiency (about 80%) for bends along the feature direction, however this dropped to less than 2% for bends in the opposite direction. As expected, this configuration is ideal if, and only if, the flexing is one directional. Additionally, these wedge features displayed the highest average efficiency as a result of the high efficiency for one-directional bending. Another notable result was the concentrator with the high pyramid density. While this model had the lowest average efficiency, it was the only configuration which had an efficiency greater than 5% for three-dimensional waveguide flexing.

Table 5.2 Summary of concentrator performance for variations in coupling features geometry for both planar, and flexible waveguide orientations.

Type of Micro-feature	Concentrator Efficiency (%)		
	Planar	Flexible	Mean
Minimized pyramid	98	0.8	49.4
Larger pyramid	94	3	48.5
Wedge feature	86	2	44
Increased density	65	15	40
Long wedge (along bend)	89	78	83.5
Long wedge (against bend)	-	1.7	-

In summary, the parameters which have to be modified to adapt the concentrator for performance in non-planar conditions are the reflecting feature shape and size and the waveguide feature scale. For a flexible waveguide a smaller feature scale distributes the deformation and corresponds to minimized stretching losses. The reflecting feature geometry must be selected based on the desired application as described above. The variability in performance of the concentrator based on the geometry, lighting, and flexibility of the waveguide is evidenced by these results. It is therefore essential that for a given application the associated constraints and goals are well identified, and the appropriate concentrator configuration can be selected.

5.3.2 Diffuser Geometry

Similar to the modification of the concentrator design for improved performance of a non-rigid waveguide, the diffusing features may also be modified to enhance their performance. Since the primary source of losses in the diffuser is the deformation of the features, scaling down the features should limit losses by distributing the deformation

over a larger number of features, and thereby lessening its effect. Four other diffuser configurations were considered to understand their impact on waveguide performance as well.

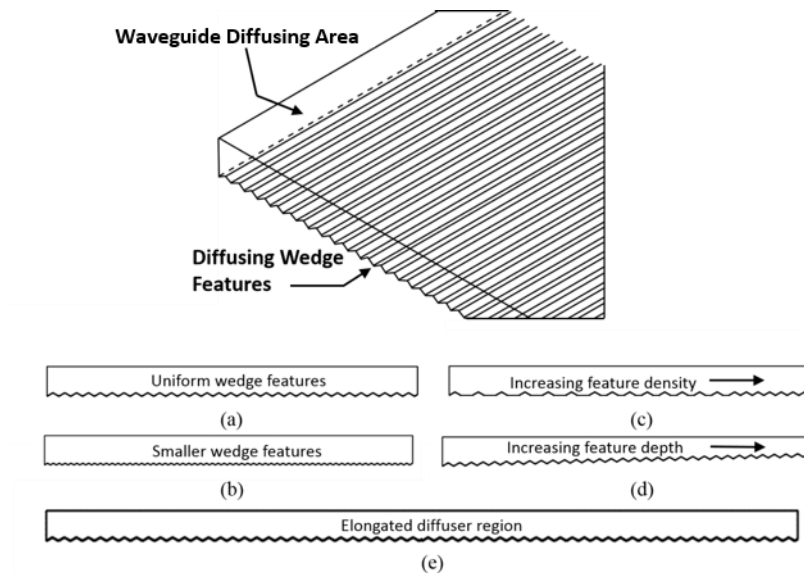


Figure 5.16 Numerous variations to the geometry of the diffuser micro-features and the diffusing region as a whole are considered in order to optimize the waveguides performance for each flexible and rigid configurations.

The diffuser models were considered and efficiencies were compared for a planar waveguide versus a flexible waveguide. Five different diffuser geometries were evaluated. First the diffuser wedges are modelled with uniform shape and size with maximum feature density and minimum waveguide length; optimized for a planar waveguide (Figure 5.16a). Second, the same diffusing wedges are used, with varying feature density along the length of the diffuser (Figure 5.16c). Third, the diffusing features with uniform shape, size and density are modelled, with the waveguide itself changing in thickness, tapering towards the end (Figure 5.16d). Fourth, the original waveguide is modelled with a longer length to ensure diffusion of all rays (Figure 5.16e). And fifth, the diffuser is modelled with maximum feature density and uniform thickness, but with smaller, higher density, diffusing wedges (Figure 5.16b). The results from these simulations are summarized in Table 5.3.

Table 5.3 Summary of diffuser performance of the diffuser, with respect to its efficiency, in consideration of the various feature configurations.

Type of Micro-feature	Diffuser Efficiency (%)		
	Planar	Flexible	Mean
Uniform	83.2	57	70.1
Varying density	81.4	44.5	62.95
Varying height	72.7	60	66.35
Long waveguide	98.8	78	88.4
Small wedges	80.5	44	62.25

The results for all configurations are quite similar, with the most notable difference being the performance of the elongated waveguide being somewhat higher than the other waveguides. This occurs because the longer length ensures that all rays interact with the wedge features and are diffused, however this comes with some reduction to the uniformity of the illumination, as discussed below. The next highest performing waveguide was that with the variations in waveguide thickness. Similar to the elongated waveguide, the tapering of the waveguide increases the likelihood of an interaction between the rays and the diffusing features. A similar effect can be had by adding a reflective coating to the end of the diffuser, to increase its efficiency without compromising size or uniformity. The uniformity of the diffuser must be considered as well. Each variation in the diffuser geometry will correspond to changes in the uniformity of the waveguide's illumination.

Table 5.4 Summary of the performance of the diffuser, with respect to its uniformity, in consideration of the various feature configurations.

Type of Micro-feature	Diffuser Uniformity (%)		
	Planar	Flexible	Mean
Uniform	82	41	61.5
Varying density	73	35.5	54.25
Varying height	65	42	53.5
Long waveguide	47	45	46
Small wedges	69	36	52.5

Notably, the uniformity of the lengthened waveguide was significantly lower than all other configurations for the planar waveguide, and the uniformity dropped for all configurations when considering the bent diffuser. The diminished uniformity of the long waveguide was expected, since the length of the diffuser is much greater than the associated minimum waveguide length, so the illumination decreases with distance from the source; while this model ensures maximum efficiency it is associated with lower uniformity. This could be rectified by using a reflective coating on the end of the diffuser to improve the efficiency without increasing length at the expense of its uniformity. The drop in uniformity for the flexible diffuser results, in part, from the curvature of the waveguide causing the rays to strike the diffusing wedges at an angle too small to cause diffusion. The rays therefore must strike two wedge features before being diffused, causing reduced illumination closer to the source, resulting in the reduction to uniformity. Additionally, the use of discretized detectors to measure the efficiency and uniformity of the diffuser impacts the results, and uniformity may in fact be greater than it is measured in this simulation, the results would be more accurate with improved discretization of the detectors.

For the diffuser, the parameters which had most impact on its performance for waveguide bending is the geometry of the waveguide itself. A longer diffuser and thinner

waveguide will have a higher efficiency; however, this corresponds to a reduced uniformity of illumination as evidenced by the simulations. This uniformity can be recovered by varying the feature geometry, size or density in association with the increased length, or decreased thickness of the waveguide.

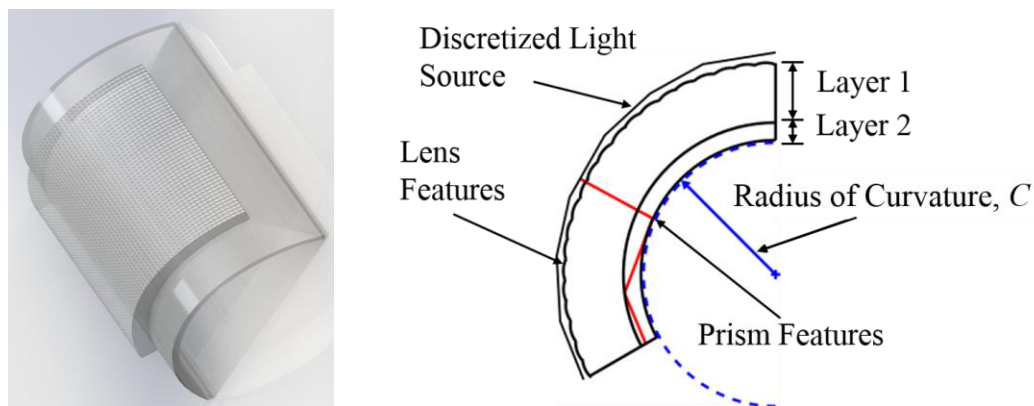
The variations in feature design, for both the concentrator and diffuser, can be used to optimize the waveguide performance for numerous applications. The appropriate concentrator and diffuser feature types, sizes and spacing may be selected according to the desired size, geometry, material and flexibility of the given application.

5.4 Evaluating Performance of a Non-Rigid Waveguide

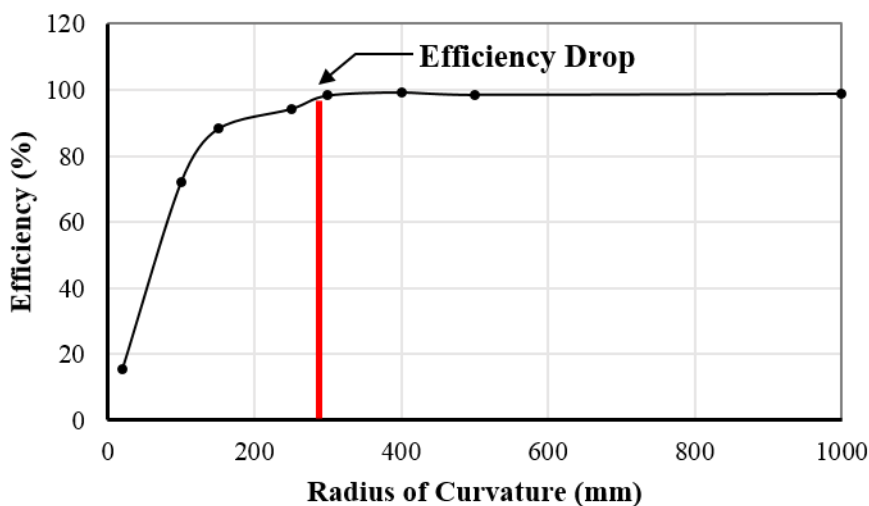
5.4.1 Performance of the Concentrator as a Non-Rigid Waveguide

In order to investigate the performance of the concentrator as flexible waveguide variations in both the angle of incidence of illumination, and the waveguide geometry must be considered. In these concentrator was modelled with radii of curvature of 20, 100, 150, 250, 300, 400, 500 and 1000 mm. As expected, the smaller the radius, the lower the efficiency. For radii of curvature of 300 mm and greater the effect of the curvature on the concentrator efficiency is minimal, but there is a sharp drop off in efficiency for smaller radii (Figure 5.17). This could be observed visually from the Zemax simulations as well, and may be attributed to a number of factors.

The loss of efficiency arises, in large part, because the propagating rays traveling through the curved concentrator strike the surface at an angle greater than that observed with a planar concentrator. Consequently, the angle of propagation may be large enough that they can no longer be contained by total internal reflection. In addition, any misalignment between the concentrated rays and prism features will cause some of the light to miss the prism features and refract out of the concentrator. This occurs because the radii of the micro-lenses on the top layer are stretched when the concentrator flexes. The increased radius corresponds to a longer focal length which leads to some of the rays to missing the prism features, decreasing the overall concentrator efficiency. These losses can be reduced by varying the feature geometry, the waveguide geometry, and the material properties, as discussed above.



(a) Curved waveguide and cross-sectional view of ray traces through the concentrator.

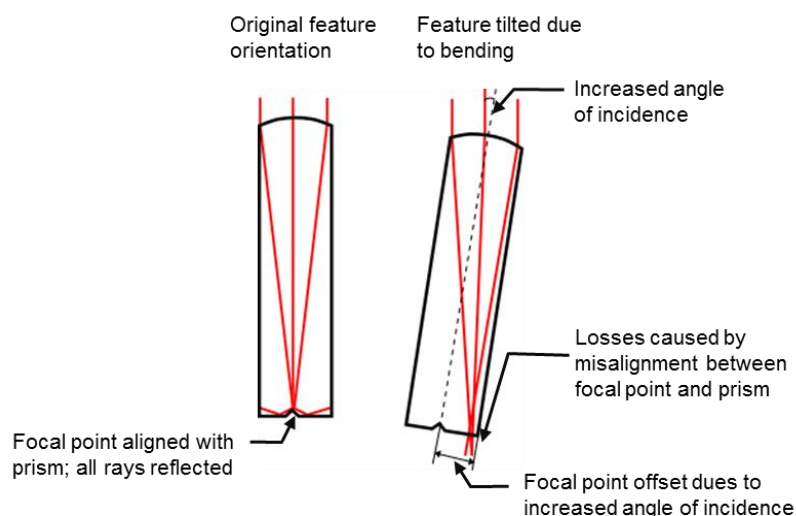


(b) Efficiency (E_c) of the concentrator with respect to radius of curvature (C).

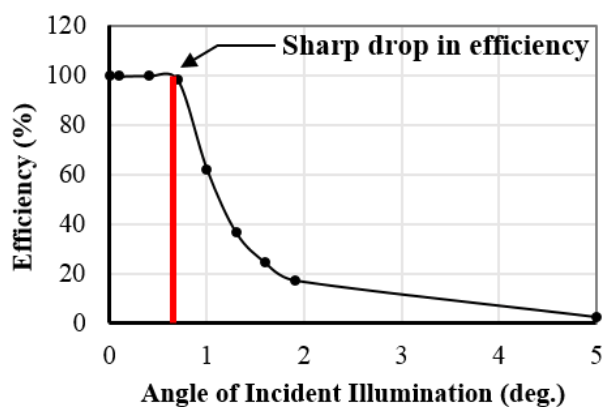
Figure 5.17 The concentrator efficiency (E_c) of the simulated waveguide for various bending radii (R) as determined by the Zemax OpticStudio ray-tracing software. Note that as the radius becomes smaller (i.e. a tight bend) the efficiency drops rapidly.

The same concentrator was also modelled with variations in the source angle of incidence (θ_i), of the illumination from 0 to 5°. For this study a planar concentrator was simulated in an effort to isolate the variations in angle of incidence and understand their impact on concentrator performance. As expected, the efficiency drops significantly with

the increase in the angle of incidence, dropping to a near-zero efficiency with an angle of incidence of only five degrees (Figure 5.18). This is primarily due to the misalignment between the concentrated rays and the prism features on the bottom face of the waveguide [41].



(a) Bending of concentrator increases the angle of incidence (θ_i) resulting in an offset between location of focal point and micro-prism position.



(b) Efficiency of the concentrator at various angles of incidence (θ_i).

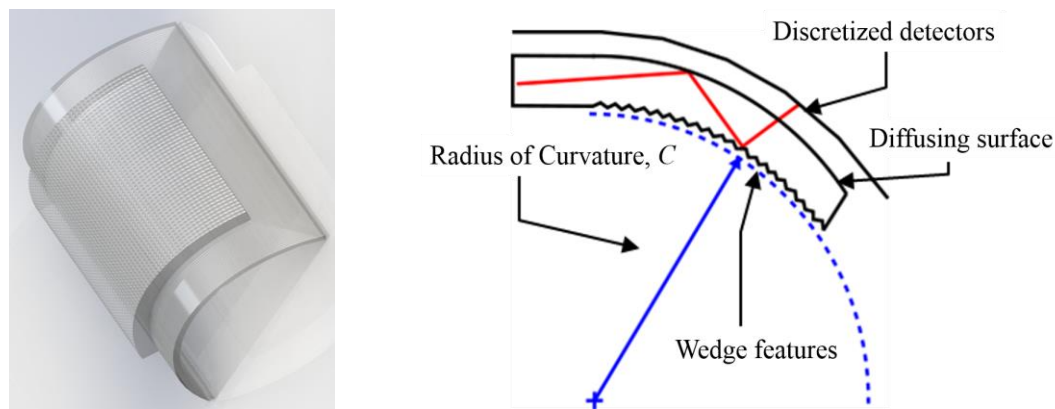
Figure 5.18 Impact of waveguide bending changing the angle of incidence (θ_i) of light rays entering the waveguide on concentrator efficiency. Note the rapid reduction in efficiency as the angle of incidence is greater than 1° .

While the proposed concentrator design performed satisfactorily for small changes in radius of curvature and angle of incidence of illumination, the parameters are optimized based on a rigid, planar waveguide with direct illumination and therefore the corresponding micro-feature geometries must be adjusted for enhanced performance. A number of potential modifications, to improve the performance of a flexible concentrator region, are described and evaluated in the following section.

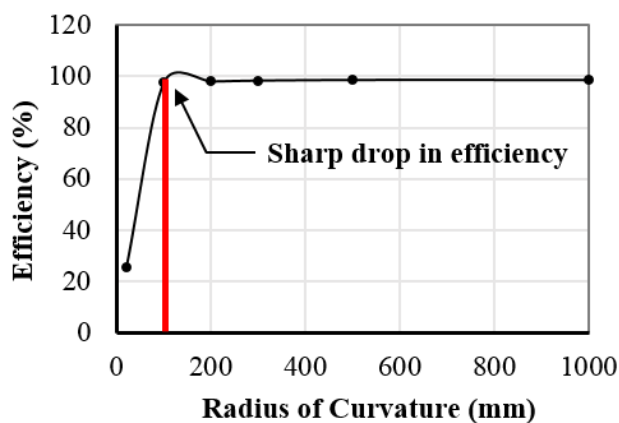
5.4.2 Performance of the Diffuser as a Non-Rigid Waveguide

The diffusing region of the waveguide was simulated with varying radii of curvature and the efficiency was estimated. However, unlike the concentrator, the variations in the position of the light source were not a factor because the diffuser acts as an illuminating surface. The curved model of the diffuser region performed as predicted, demonstrating a drop in efficiency with the increased curvature of the waveguide (Figure 5.19) below $R = 200$ mm. The drop in efficiency occurs due to the changes in angle of reflection for the propagating rays. This can be mitigated by redesigning the diffusing micro-features so that their angle of inclination is sufficient to produce refraction, or by patterning both faces to ensure diffusion of the rays for varying waveguide geometry. Overall, the performance of the diffuser is sufficient for small variations in waveguide geometry. However, the design would have to be adapted for a more flexible waveguide.

Another factor important for diffuser design is the uniformity of illumination emitted by the active region. It was observed that the leading edge of the waveguide had a significantly lower level of emitted illumination than the end of the diffuser. This appears to be the result of the angle of propagation as the light rays travel through the curved diffuser, where the angle is insufficient for exiting the waveguide at the leading edge. This characteristic may be controlled by varying the thickness of the waveguide, or introducing micro-features with varying density. Again, losses caused by changes in the optical feature geometry, due to stretching, may be mitigated by minimizing the feature size. The losses observed in the diffusing region are therefore, managed more easily than those in the concentrating region.



(a) Curved waveguide and cross-sectional view of ray traces due to diffuser curvature.



(b) Efficiency (E_D) of the diffuser with respect to radius of curvature (C).

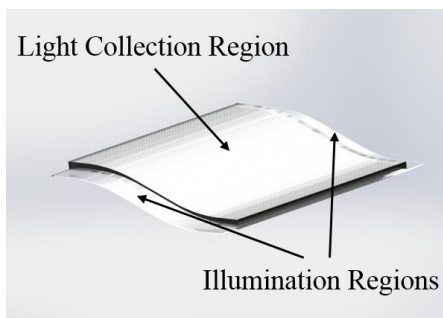
Figure 5.19 The diffuser efficiency (E_d) of the simulated waveguide for various bending radii (C) as determined by the Zemax OpticStudio ray-tracing software.

5.4.3 Combined Controlled Light Guidance and Distribution through Flexible Optical Waveguide Sheet

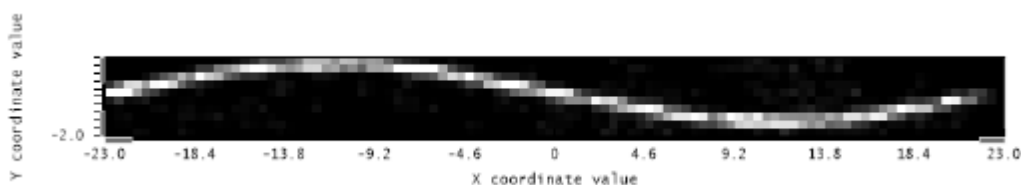
Although there are substantial losses observed for both the flexible concentrator and the flexible diffuser, Section 5.3 proposes methods of mitigating these losses. In order to evaluate the optimal performance of a flexible waveguide, the best performing micro-features for both the concentrator and diffuser are modelled in the combined controlled light guidance and distribution example. For this analysis the deformation is assumed to be one-directional in order to demonstrate the maximum efficiency of the flexible waveguide. Thus, in this case the wedge coupling features, running the length of the

concentrator in the direction of the bend are used. For the diffusing wedges, a constant size and distribution is used, but with increasing depth in order to enhance extraction efficiency in spite of the bend. Due to the nature of the wedge coupling features, the illumination is directed to only two of the concentrator edges, thus only two diffusing regions are required.

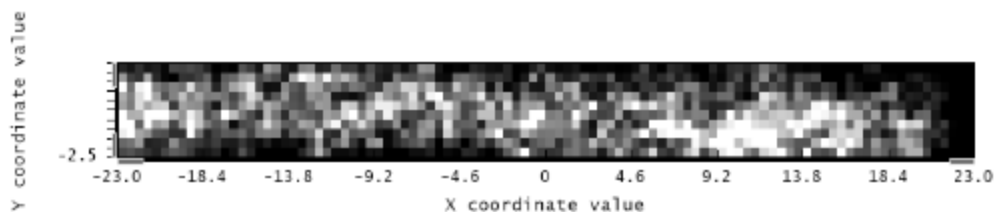
This waveguide was modelled in SolidWorks (Figure 5.20a) and the simulation was conducted in Zemax (Figures 5.20b and 5.20c), using a planar overhead light source, to replicate the analyses done in Chapter 4. In this case the efficiency of the waveguide is determined by comparing the total light diffused by in the illumination regions to the total incident light. By this measure the combined concentrator diffuser, flexible waveguide demonstrated a maximum efficiency of nearly 60%.



(a) SolidWorks model of the flexible waveguide.



(b) Zemax detector data resulting from the illuminated concentrator edge.



(c) Zemax detector data resulting from the illuminated diffuser face.

Figure 5.20 The optimized geometry for the flexible concentrator-diffuser waveguide is modelled in SolidWorks and analyzed in Zemax in order to validate design.

Although the flexible waveguide has significantly lower efficiency than the idealized planar waveguide (95% efficiency vs. 60% efficiency), this simulation demonstrates the ability of the waveguide to perform with reasonably high efficiency for complex underlying geometries. According to the requirements of a particular application, the appropriate waveguide and micro-feature geometry may be selected, and optimal efficiency can be achieved in spite of the associated limitations.

5.5 Guidelines for the Design of a Non-Rigid Waveguide Sheet

While Chapter 4 provides guidelines for the optimization of the waveguide geometry for theoretically ideal conditions, Chapter 5 examines how variations from ideal conditions impact the optimal geometry. For each deviation from the ideal waveguide geometry or conditions, there is an appropriate method for adapting the waveguide design for optimal performance with the given constraints. In all cases, if one variable deviates from the optimal value, the subsequent geometric and material parameters may be recalculated according to the equations outlined in Section 4.5 for maximum efficiency, however if the optimal geometry for a given application cannot be attained, the parameters may be varied to compensate for the losses. A summary of these adaptations is given below, based on the results of the simulations discussed in Chapter 5.

First variations in the overall waveguide material and geometric properties are considered, including refractive indices, material transmission efficiency (E_T), and total surface area. For changes in refractive index, the ratio of the indices (n_1/n_2), must be large enough to confine the rays to the transmission layer by total internal reflection, thus if the ratio is too small, the waveguide must be adapted accordingly. This can be achieved by either redesigning the coupling features to reduce the angle of propagation to a suitable degree, or by adding a dopant, or using an entirely different material to increase the relative refractive index of the transmission layer. If the transmission efficiency of the selected material is excessively low, there will be increased attenuation as the light propagates to the waveguide edges. This can be limited by selecting a material with a higher transmission efficiency for the whole waveguide, or a section thereof, including a high efficiency transmission region, or reducing the size of the waveguide to limit the

losses. Similarly, if the overall surface area of the waveguide is very large, the impact of attenuation and decoupling losses will be amplified. If a large surface area is desired for a particular application, high efficiency can be maintained by scaling up waveguide geometry, to reduce feature density, or including an unpatterned transmission region to reduce decoupling losses.

For the concentrating region of the waveguide, variations from the optimal micro-feature geometry must be considered for both the micro-lens features, and the coupling prisms. For the lenses their pitch, P , and their radius, R , must be considered, and for the prisms their angle, α , and their base width, b , must be considered. The equations given in Section 4.5, define the pitch in terms of the angle of incidence of focused rays on the coupling prisms, so there is a range of acceptable values for pitch, however for values either too large or too small, there will be a subsequent drop in efficiency. If the pitch is too large, the focused rays will strike the prisms at such an angle that they are not reflected by TIR, but rather refracted out the bottom of the waveguide. To limit such losses, the prism angle may be increased to increase its acceptance angle for the focused rays, or the entire waveguide may be scaled up to suit the desired increase in pitch. Conversely, if the feature pitch is too small the density of coupling features is increased, and thus there are more decoupling losses due to the increased proximity of coupling features. These losses may be mitigated by reducing the size of the coupling prisms in correspondence with the reduced pitch, or scaling the entire waveguide to the desired pitch. For any variation in the radius, R , of the micro-lenses, the losses are rather substantial, since the coupling features are located at the focal point, as defined by the lens' radius. For a high efficiency waveguide, it is therefore essential, that the micro-features' geometry is optimized according to the desired radius.

Considering the geometry of the coupling features; both their angle, α , and their size, b , are defined by a range of acceptable values, as described in Section 4.5. If the base angle is below the acceptable range of values, this will result in the rays being refracted out the bottom face, and not being coupled into the transmission layer. This deviation could be corrected by increasing the refractive index of the lower layer to encourage TIR, or by reducing the lens' pitch to reduce the maximum angle of incidence of the focused

rays on the couplers. If the angle, α , exceeds the maximum allowable value the rays will be reflected at off the prisms at such an angle that they cannot be confined to the transmission layer by TIR. Similar to the previous case, the refractive index of the lower layer could be increased to promote total internal reflection, and reduce losses. For variations in the coupler size, if the features are excessively small the effects of interference and diffraction are not considered by geometric optics analysis, thus b cannot exceed the geometric optics limit. When the size of the coupling prisms becomes too large however, the likelihood of a propagating ray striking a prism and decoupling increases. These losses should be mitigated by increasing the pitch of the concentrator micro-features, or scaling up all waveguide geometry.

Variations in the geometry of the diffusing features must be considered as well, with respect to their impact on both efficiency and uniformity of the waveguide's illumination. Based on the design equations for the diffuser, a range of acceptable values for the wedge angle, θ_d , is established. If the angle is too large, the rays will not be reflected off the wedge faces, but rather refract out of the waveguide. This would be corrected by either reducing the angle of propagation of the light from the concentrator, or increasing the refractive index of the diffuser region to promote TIR. Conversely, if the wedge angle is too small, the reflected rays will not be refracted out the waveguide's illuminating face, but will be reflected, and continue to propagate through the diffuser. The corrections in this case would be the opposite of the previous case; increasing the angle of propagation or decreasing the refractive index.

The size of the diffusing features, and the length of the entire diffusing region will also impact its performance. Both the efficiency and uniformity of the diffuser will be reduced if the wedge features are too large. The efficiency decreased since the losses on the first diffuser feature are proportional to its size, and the uniformity is lost due to the reduced feature density. This can be mitigated by increasing wedge size gradually, or scaling the diffuser region to match the desired wedge size. The length of the diffusing region has opposite impacts on efficiency and uniformity; if the waveguide is too short it will not successfully diffuse all rays, reducing the efficiency, but if the waveguide is too long the uniformity will be compromised as intensity decreases with distance from the

source. In both cases the efficiency and uniformity can be optimized by implementing a reflective coating on the end face as this will allow rays to pass through the diffusing region twice. This increases the efficiency by increasing the likelihood of an interaction between the rays and the diffusing wedges, and increases uniformity by having more rays interact with the far edge as they reflect off the end face. Also, if a shorter diffuser length is desired a higher density of features may be used, whereas for a longer diffuser region, the feature density should start rather low, and increase with distance from the source.

Finally, the effect of bending on the waveguide's performance is to be considered, and design modifications are proposed to control the subsequent losses. Bending of the waveguide has three primary impacts on its performance; the deformation and stretching of the micro-features, the reorientation of the features with respect to the light source, and with respect to each other, and the macro-bend losses. The bend losses are best mitigated by increasing the ratio of refractive indices and/or decreasing the angle of propagation in the transmission layer, as this decreases the critical bend radius, and increases TIR. The losses caused by deformation of the individual micro-features are mitigated by scaling down the waveguide geometry as described in Section 5.3, as this distributes the bending and reduces stretching. The angle of the light source with respect to the deformed features is a significant source of loss, as this causing in a relocation of the focal point resulting in the micro-prisms failing to couple the light into the waveguide. It is therefore necessary to vary the coupling features' geometry according to the bending which occurs. If the bending is minimal, the coupling feature base may be scaled up to increase its acceptance angle. For larger degrees of bending, if the direction of bending unknown, it is best to increase the density of coupling features, thereby increasing the likelihood that the focused rays strike a prism, but this configuration will have a low transmission efficiency due to the increased decoupling losses. If the bending occurs primarily in one direction, however, a long wedge feature running along the direction of the bend, can be used for a high efficiency flexible waveguide. With respect to the diffusing region of the waveguide, the angle of propagation will not be predictable since the curvature of the waveguide will define this angle. For a flexible diffuser it is best therefore, to have a high density of diffusing features with their depth increasing with distance from the source, increasing both light extraction efficiency and uniformity. Table 5.5, below provides a

summary of how the waveguide optimization may be varied for geometry, material and illumination conditions which deviate from the ideal conditions.

Table 5.5 Design guidelines for varying waveguide geometry according to the requirements and limitations of a particular waveguide application.

	Parameter	Deviation	Correction
Waveguide Geometry	n_1/n_2	Too small	Decrease α Increase n_1
	E_T	Too small	Change material Transmission region Decrease SA
	SA	Too large	Scale up waveguide Transmission region
Concentrator Geometry	P	Too Small	Decrease b Scale down waveguide
		Too Large	Increase α Scale up waveguide
	R	Non-ideal	Increase α Scale waveguide to R
	α	Too Small	Increase n_2 Decrease P
		Too Large	Increase n_2
	b	Too Small	Increase b Cannot exceed minimum
Too Large		Increase P Scale up waveguide	
Diffuser	θ_d	Too Small	Decrease n_2 Increase θ_P
		Too Large	Increase n_2

			Decrease θ_P
	w	Too Large	Increase gradually Scale up waveguide
	l	Too Short	Increase density Reflective coating
		Too Long	Vary density Reflective coating
Waveguide Bending	Micro-feature Deformation	Stretching	Scale down all geometry
	Concentrator Region	Small Bends	Increase coupler size, b
		Unidirectional Bends	Use long wedge-shaped coupling features
		Multidirectional Bends	Increase coupling feature density
Diffuser Region	Bending	Increase diffuser feature density Increasing depth of diffuser features	

5.6 Discussion – Limitations of Controlled Light Guidance

As described in Section 5.5, for any deviation from the optimal waveguide material, geometry, or orientation there is a corresponding modification to the waveguide design which can be made to recover the losses. While these design guidelines serve to maximize the efficiency according to the desired application, there are some distinct limitations to the controlled guidance of light in a flexible waveguide. The main such limitation relates to the collection of light in the concentrating region of the waveguide. If the orientation of the deformed waveguide with respect to the light source is unknown, the concentrator cannot effectively focus light onto the coupling features. As the orientation of the micro-lenses varies in relation to the source, so too does the location of their focal point. Since the efficiency of the concentrator depends on the precise positioning of the coupling features at the focal point of the lens, the coupling features cannot be accurately positioned. This Chapter proposes numerous designs which mitigate the subsequent losses, however a flexible waveguide cannot achieve the same efficiencies

as the rigid waveguide. Thus if the desired geometry of the waveguide is known, the waveguide should be designed with the coupling prisms located at the lens focal point, for maximum efficiency.

Other limitations associated with the design of the flexible waveguide include the stretching, and deformation of the MOSs and the losses in the diffusing region of the waveguide. These losses are more easily managed and have a less significant impact on the waveguide performance. The impact of stretching can be minimized by scaling down the features, to distribute the deformation. This can be done either over the entire waveguide surface, or locally in areas of most deformation, to limit such losses. For the diffusing region of the waveguide, the relative position of the features with respect to the light source is not a concern, as the concentrating region illuminates the diffuser, rather than using an external source. The diffuser efficiency is therefore, optimized by minimizing the feature size to limit the impact of feature stretching, and by increasing either feature depth, or diffuser region length to ensure diffusion of all rays. Although there are methods of limiting the losses associated with bending in the waveguide, designing a fully flexible waveguide comes at significant expense to its efficiency. A flexible waveguide increases its adaptability, as well as the potential applications, however it introduces additional design challenges and sources of loss. Depending on the desired waveguide application, the flexibility may be essential, and thus this chapter outlines the optimal feature configuration to offset the inherent losses in a flexible concentrator-diffuser waveguide.

5.7 Concluding Remarks

Where Chapter 4 presented the optimal waveguide geometry for an idealized flat, rigid waveguide, Chapter 5 presents a summary of how this waveguide may be modified for circumstances which deviate from the ideal. By analyzing the impact of variations in each of the important parameters, the associated losses are better understood, and thus several design modifications are proposed in order to offset these losses. Subsequently these potential modifications are simulated and analysed to compare their performance as a flexible concentrator waveguide, and it is determined that by varying the feature

geometry the efficiency of the flexible waveguide can be increased from 1% up to nearly 60%. While the optimal feature design varies depending on the requirements and constraints of the particular application, Chapter 5 provides a summary of the potential modifications to optimize performance and how they should be applied under different circumstances. Whether designing a rigid waveguide for ideal conditions, or a flexible waveguide for sub-optimal conditions, Chapters 4 and 5 present the equations and guidelines required for selecting the suitable waveguide and micro-feature geometries.

Chapter 6 Conclusions

6.1 Thesis Summary

In its entirety this thesis offers the background information, and theoretical equations and analysis, required for the design of a multi-functional concentrating and diffusing optical device, for controlled guidance of light. The waveguide proposed in this work is able to collect, transmit and diffuse light towards an illumination target with an efficiency of up to 95% for an ideal, planar waveguide, and up to 60% for a flexible, membrane-like waveguide.

Chapter 1 of the thesis describes how this work fits into the landscape of the existing research on the topic of micro-patterned, and flexible, optical waveguides. Chapter 1 also presents a summary of potential applications for these devices, in order to illustrate why this work is important. Specifically, existing research does not address the design of flexible micro-pattern concentrator waveguides, nor is there much research on combined light collection and distribution, making the waveguide discussed here novel. Chapter 2 provides a review of the existing literature in the field, helping to put the research into context, identify which existing work is built upon in this research, and develop the background required for understanding this research.

Chapters 3, 4, and 5 detail the specifics of the research done in the course of this project. Chapter 3 focuses on the design methodology, describing the parameters used to evaluate the waveguide performance, as well as a description of how the analyses were executed. The primary parameters used to evaluate the waveguide performance are the efficiency and uniformity of the illumination, and this data was acquired using the detector data feature in the Zemax OpticStudio software. By this method, the ideal waveguide was designed and evaluated in Chapter 4, while Chapter 5 served to evaluate the performance of the waveguide in non-optimal conditions. These simulations corresponded with a high efficiency waveguide for both the optimal and suboptimal conditions.

Chapter 4 demonstrated the highly successful parametric optimization of the idealized waveguide achieving an overall efficiency of 95%. Chapter 5 demonstrated that for non-optimal waveguide parameters the efficiency demonstrates a wide range of efficiency from under 1%, up to nearly 60%. These results illustrate the necessity for understanding the requirements and limitations of the particular waveguide application, and selecting the appropriate geometric parameters, in order to achieve optimal performance under any conditions.

6.2 Concluding Comments

This thesis presents the theory, evidence and methodology for designing an optimal concentrator-diffuser waveguide for targeted illumination. In addition, the recommended deviations from the optimal geometry for variations in waveguide materials, geometry, flexibility or application, are summarized. These guidelines are supported by corresponding Zemax OpticStudio simulations which illustrate and confirm the predicted results. The Zemax simulations demonstrated an efficiency of over 94% for the optimized planar concentrator-diffuser waveguide, and efficiencies between 1% and 85% for non-optimal conditions.

The large variability in efficiency for non-optimal waveguide conditions for controlled guidance of light, emphasizes the necessity of the design guidelines presented in Chapter 5 of this thesis. If the ways in which the waveguiding conditions are suboptimal are well defined the appropriate modifications can be made, and the efficiency of the waveguide will fall in the upper range of possible values, maintaining maximum performance. Regardless of the waveguide's flexibility, material composition, or geometric parameters, the suitable geometry for each configuration may be identified by the guidelines presented in this thesis, for a high efficiency waveguide sheet.

The optical devices presented in this thesis differ from existing work in several ways; particularly in that they combine both concentrating and diffusing regions, and the waveguide is mechanically flexible. The combined light collection and diffusion permits concentration of light in low light regions, transmission to, and distribution over the illuminating face for: sensing, interior lighting, light therapy and other applications. This

eliminates the need for an externally powered source, by the collection of ambient or solar light. The flexibility of the waveguide is achieved by designing the waveguide out of a mechanically flexible polymer, with a variable refractive index. This permits the use of the same polymer for adjacent waveguide layers, ensuring feature alignment as the waveguide flexes, as well as material compatibility and optical quality interface.

The waveguide's unique properties make it widely applicable as a thin, large area, flexible waveguide sheet which can conform non-invasively to the geometry of any underlying surface, and act as both a concentrating and diffusing waveguide. According to the requirements and constraints of the desired application, the optimal material and geometry may be identified by the equations and guidelines presented in Chapters 4 and 5 of this thesis, in order to design a high efficiency, flexible waveguide for a wide variety of applications. In conclusion this thesis describes the successful design and analysis of a flexible waveguide capable of both light collection and illumination.

6.3 Recommendations and Future Work

While this thesis provides a thorough description and analysis of the parametrically optimized geometry for variations of rigid and flexible concentrator-diffuser waveguides, it does not investigate the fabrication and performance of the proposed waveguide. Though there has been some limited investigation into the fabrication and evaluation of the PDMS diffusers [31], there has been little research done on concentrator waveguides [17]. In order to compare, validate, and ameliorate the results of the Zemax simulations, it is necessary to compare them to empirical results as well. It is therefore recommended that future work on this topic focuses on the empirical validation of the theoretical results. Specifically, it would be recommended to repeat the waveguide analysis as it was done in Chapters 4 and 5; beginning with the analysis of a single feature, followed by an array of features, and the entire waveguide geometry. The results of such experiments could be compared to the simulation results in order to develop a baseline as to how the theoretical model predicts the empirical results.

Subsequently the simulations done in Chapter 5 for the non-optimal waveguide conditions could be repeated to compare the performance of the proposed flexible

waveguide geometries to their actual performance. Such experiments would be an excellent means of validating the theoretical results, and understanding their limitations. It is advised that the waveguide be fabricated by the means proposed by Green et al. [17], and thus the experiment would serve as a method of understanding the limitations of both the theoretical model, and the method of fabrication itself.

Additional future work could address some of the limitations of the analysis done in this work, specifically the limitations of the geometric optics approach, and the limitations of the Zemax OpticStudio software. As discussed in Chapter 3, the Zemax software limits the use of non-planar sources and detectors. As a result, the detector data for a curved waveguide may either be interpreted visually, or the detectors may be discretized. In order to extract as much information as possible from the simulations described in this thesis, the detectors for the curved waveguide were discretized, resulting in some irregularities in the results, particularly as they relate to the measurements of the diffuser's uniformity. In future analyses this effect could be minimized by using alternate software, using a different approach to the Zemax software, or further discretizing the detector and source elements to closer imitate the waveguide curvature.

The geometric optics approach to the analysis of the waveguide also limits the minimum thickness of the waveguide. Thus, if the impact of interference and diffraction surrounding the smallest features – the coupling prisms – were considered with respect to the associated wave optics, the thickness could be further reduced. Although the waveguide presented in this work could be scaled to achieve a thickness of under 1mm, a thinner waveguide film may be attained through future development, for specialized applications, if the geometric optics limit were lifted by consideration of the wave-properties of light surrounding the optical micro-features. The waveguide discussed in this work represents the beginning of the development of highly complex, efficient and adaptable waveguide designs for targeted light collection and illumination. While there remain numerous areas for this work to develop and progress to more efficient, diverse designs, this thesis presents the fundamentals required for the design of an efficient, effective waveguide for controlled guidance of light through a large area, flexible optical waveguide sheet.

References

- [1] S. Bouchard and S. Thibault, "Planar waveguide concentrator used with a seasonal tracker," *Appl. Opt.*, vol. 51, no. 28, p. 6848, 2012.
- [2] J. H. Karp, E. J. Tremblay, and J. E. Ford, "Micro-Optic Solar Concentration and Next-Generation Prototypes," *Proc. Photovoltaic Specialists Conference*, Honolulu, HI, p493, 2010.
- [3] J. H. Karp, E. J. Tremblay, J.M. Hallas, and J. E. Ford, "Orthogonal and Secondary Concentration in Planar Micro-Optic Solar Collectors," *Optics Express*, vol. 19, pA673, 2011.
- [4] J. H. Karp and J. E. Ford, "Planar micro-optic solar concentration using multiple imaging lenses into a common slab waveguide," *SPIE Sol. Energy+ Technol.*, vol. 7407, p. 74070D–74070D–11, 2009.
- [5] J. H. Karp, E. J. Tremblay, and J. E. Ford, "Planar micro-optic solar concentrator," *Optics Express*, vol. 18, no. 2, January, p.1122, 2010.
- [6] A. Gombert, B. Bläsi, C. Bühler, P. Nitz, J. Mick, W. Hoßfeld, and M. Niggemann, "Some application cases and related manufacturing techniques for optically functional microstructures on large areas," *Opt. Eng.*, vol. 43, no. 11, p. 2525, 2004.
- [7] R. A. Ronny, G. K. Knopf, E. Bordatchev, and S. Nikumb, "Micromilled optical elements for edge-lit illumination panels," *J. Micro/Nanolithography, MEMS, MOEMS*, vol. 12, no. 2, p. 23002, 2013.
- [8] Y. Okuda and I. Fujieda, "Polymer waveguide technology for flexible display applications," *Proc. SPIE, Adv. Disp. Technol.*, vol. 8280, pp. 122–131, 2012.
- [9] S. R. Park, O. J. Kwon, D. Shin, S.-H. Song, H.-S. Lee, and H. Y. Choi, "Grating micro-dot patterned light guide plates for LED backlights," *Opt. Express*, vol. 15, no. 6, pp. 2888–99, 2007.

- [10] J. Yeon, J. Lee, H. Lee, H. Song, Y. Mun, Y. Choi, and J. Yoon, "An effective light-extracting microstructure for a single-sheet backlight unit for liquid crystal display". *J. Micromech. Microeng.*, vol. 22, no. 9, 2012. doi:10.1088/0960-1317/22/9/095006
- [11] L. C. Maxley, "Flexible Sunlight – The History and Progress of Hybrid Solar Lighting", *Emerging Environmental Technologies*, Oak Ridge, TN, Springer Science and Business Media, 2008.
- [12] J. Shen, C. Chui, and X. Tao, "Luminous fabric devices for wearable low-level light therapy," *Biomedical Optics Express*, vol. 4, no. 12, p.2925, 2013.
- [13] M. Rothmaier, B. Selm, S. Spichtig, D. Haensse, and M. Wolf, "Photonic textiles for pulse oximetry," *Optics Express*, vol. 16, no. 17, p.12973, 2008.
- [14] V. Koncar, "Optical fiber fabric displays," *Optics and Photonics News*, vol. 16, no. 4, p.40, 2005.
- [15] J.-C. Yu, J.-H. Chen, and S.-C. Liu, "Design of LED edge-lit light bar for automotive taillight applications," *Proc. of SPIE*, vol. 8835, p. 88350G, 2013.
- [16] C. Nicholson-Smith, G. K. Knopf, and E. Bordatchev, "Controlled guidance of light through a flexible optical waveguide sheet". *Proc. SPIE 9759*, 97590C-97590C, 2016.
- [17] R. Green, G. K. Knopf, and E. Bordatchev, "Fabrication of large area flexible PDMS waveguide sheets," *Proc. of SPIE*, vol. 9759, p. 97590U, 2016.
- [18] W. J. Cassarly, "Backlight pattern optimization," *Optical Design and Testing*, vol. 6834, pp. 683407, 2007.
- [19] K. Shanks, S. Senithilarasu, and T. K. Mallick, "Optics for concentrating photovoltaics: Trends, limits and opportunities for materials and design", *Renew Sust Energ Rev*, vol. 60, p.394-407, 2016.
- [20] N. Sellami, T. Mallick, and D. McNeil, "Optical Characterisation of 3-D Static Solar Concentrator," *Energy Conversion and Management*, vol. 64, p.579-586, 2012.

- [21] R. E. Cohen, D. R. Lide, and G. L. Trigg, *AIP physics desk reference* (3rd ed.). Chapter 11 Electricity and Magnetism, New York: Springer/AIP Press, p.387, 2003.
- [22] S. A. Rashkovskiy “A rational explanation of wave-particle duality of light,” Paper presented 8832, 2013. doi:10.1117/12.2022585
- [23] R. E. Cohen, D. R. Lide, and G. L. Trigg, *AIP physics desk reference* (3rd ed.). Chapter 19 Optics New York: Springer/AIP Press, p.568-596, 2003.)
- [24] C. A. Dimarzio, *Optics for Engineers*. Chapter 2 Basic Geometric Optics, Boca Raton, FL: CRC Press, p.35-59, 2012.
- [25] C. A. Dimarzio, *Optics for Engineers*. Chapter 7 Interference, Boca Raton, FL: CRC Press, p.181, 2012.
- [26] C. A. Dimarzio, *Optics for Engineers*. Chapter 8 Diffraction, Boca Raton, FL: CRC Press, p.233, 2012.
- [27] B. P. Pal, *Guided wave optical components and devices: Basics, technology, and applications*. Amsterdam; Boston: Elsevier Academic Press, p.2-21, 2006.
- [28] D. Marcuse, “Curvature loss formula for optical fibers”, *J Opt Soc Am*, vol. 66 no. 3, p.216-220, 1976.
- [29] J. H. Karp, “Planar Micro-Optic Solar Concentration,” *UC San Diego*, b6975177, 2010.
- [30] W. Y. Lee, “Fast ray-tracing methods for LCD backlight simulation using the characteristics of the pattern,” *Opt. Eng.*, vol. 44, no. 1, p. 014004, 2005.
- [31] L. H. Sperling, *Introduction to physical polymer science* (4th ed.). Hoboken, N.J: Wiley-Interscience, p.350, 2004.
- [32] D. Chang-Yen, R. Eich, and B. Gale, “A monolithic PDMS waveguide system fabricated using soft-lithography techniques”, *Journal of Lightwave Technology*, vol.23, no. 6, pp. 2088–2093, 2005. doi: 10.1109/JLT.2005.849932.

- [33] Y. Xia and G. M. Whitesides, "Soft lithography", *Angewandte Chemie International Edition*, vol.37, no.5, p.550–575, 1998. doi: 10.1002/(SICI)1521-3773(19980316)37:5<550::AID-ANIE550>3.0.CO;2-G.
- [34] Y. Xia, E. Kim, X.-M. Zhao, J. A. Rogers, M. Prentiss, and G. M. Whitesides, "Complex optical surfaces formed by replica molding against elastomeric masters", *Science*, vol. 273, p.347–349, Jul. 1996. doi: 10.1126/science.273.5273.347.
- [35] J. A. Rogers and R. G. Nuzzo, "Recent progress in soft lithography", *Materials Today*, vol. 8, no. 2, p.50–56, 2005. doi: 10.1016/S1369-7021(05)00702-9
- [36] Zemax Opticstudio LLC. (2016). Opticstudio, [Online]. Available: http://www.zemax.com/os/opticstudio_2016.
- [37] K. Chang, *Encyclopedia of RF and microwave engineering*, John Wiley, Hoboken N.J., Geometric Optics, 2005.
- [38] P. Xie, H. Lin, Y. Liu, and B. Li, "Total internal reflection based planar waveguide solar concentrator with symmetric air prisms as couplers," *Optics Express*, vol. 22, no.21, p.A1389-A1398, 2014.
- [39] "Optical design tools for backlight displays," *Optical Research Associates*, <https://optics.synopsys.com/lighttools/pdfs/ToolsforBacklights.pdf> 2010.
- [40] M. Hecke, and W. K. Schomburg, "Review on Micro Molding of Thermoplastic Polymers," *J. Micromech. Microeng.*, vol.14, 2004. doi: 10.1088/0960-1317/14/3/R01
- [41] J. Hallas, K. Baker, J. Karp, E. Tremblay, and J. Ford, "Two-axis Solar Tracking Accomplished through Small Lateral Translations," *Appl. Opt.*, vol.51, p.6117-6124, 2012.

Appendices

Appendix A: Derivations and Calculations

A.1: Derivation of Efficiency Equation

The concentrator design relies on two features; a lens to concentrate the incident light, and a prism which directs the light into the transmission layer of the waveguide. A two-layer waveguide design is used to confine the rays, in order to prevent the propagating rays from interacting with the lens features. This two-layer design results in the rays being able to strike only the prism-features as they propagate through the waveguide, when this occurs, the rays decouple, decreasing the waveguide's efficiency. The overall efficiency of the concentrator waveguide depends on four factors: the height of the waveguide, the propagation angle of the rays, the surface area of the waveguide, and the size of the prism-features. The efficiency of the concentrator (E_c) is calculated as:

$$E_c = (1 - D_p)^N, \quad (\text{A.1})$$

where D_p is the density of the coupling prisms, calculated as the ratio of the concentrator area to the feature pitch (A.6), and N is the number of time a ray strikes the bottom face of the diffuser, and is given by Equation A.2.

$$N = \frac{\frac{1}{6} \sqrt{SA} * (\tan \theta_{p_{max}} * \tan \theta_{p_{min}})}{t_2 * (\tan \theta_{p_{max}} + \tan \theta_{p_{min}})} \quad (\text{A.2})$$

Equation A.2 is based on the geometric parameters of the waveguide; SA its surface areas, and t_2 , the thickness of the transmission layer as defined in by Equation A.5. With the relevant waveguide geometry known, the average distance a ray travels through the concentrator waveguide can be calculated. Thus, in order to determine the number of times a propagating ray strikes the bottom face of the diffuser only its propagation angle, θ_p , must be known. Since the rays propagate between a minimum and maximum angle, the range is defined by these angles as shown below, where n_2 is the refractive index of the transmission layer, and θ_{3p} is the angle of the focused ray in the bottom layer (Equation A.19).

$$\theta_{p_{min}} = 2\pi - 2 * \sin^{-1} \left(\frac{1}{n_2} \right) - \theta_{3p} \quad (\text{A.3})$$

$$\theta_{p_{max}} = 2\pi - 2 * \sin^{-1} \left(\frac{1}{n_2} \right) \quad (\text{A.4})$$

Finally, the thickness of the bottom layer of the waveguide, t_2 , must be calculated (A.5) in order to fully define N . This equation is reliant on the micro-lens geometry; radius (R) and pitch (P), and the ray angles. These angles θ_{1p} , θ_{2p} , and θ_{3p} , represent the angle of the outermost ray as it strikes the lens surface, as it travels through the upper layer, and as it travels through the lower layer, respectively. The angles of the outermost ray are used, as this ray represents both the lens' focal point and the ray which strikes the coupling prisms with the largest angle of incidence.

$$t_2 = \frac{\tan(\theta_{1p} - \theta_{2p})}{\tan(\theta_{3p})} * \left(-t_1 + \frac{0.5P}{\tan(\theta_{1p} - \theta_{2p})} - R + \sqrt{R^2 - (0.5P)^2} \right) \quad (\text{A.5})$$

As discussed above, D_p is the density of the prism features and is determined by computing the proportion of the bottom face which is occupied by the coupling prisms, as this will correspond to the likelihood of a ray striking the prism features. It is thus calculated by dividing the coupling features area, by the area of a single feature.

$$D_p = \frac{b^2}{P^2}, \quad (\text{A.6})$$

where b is the width of a single coupling prism, and P is the width, or pitch, of a single lens micro-feature. In order to optimize the efficiency of the waveguide, the pitch of the lens, and prism features should be maximized and the width of the prisms should be minimized. Because the focused rays must all strike the prism in order to be directed into the concentrator waveguide, the prism must be located at the focal point of the rays. Although all rays would ideally focus at a single point, the spheric nature of the lenses cause a focal shift which must be accounted for in the prism design. In order to determine the minimum acceptable prism size, the equation of each ray should be determined, the focal point found, and the dispersion of rays at this point calculated which will correspond to the minimum prism width.

The equation of each ray may be calculated based on the lens geometry where the slope of the line corresponds to the angle at which the ray travels upon being focused and the y-intercept of the line is determined based on the point on the lens at which a given ray is incident and the slope of the line. Based on these parameters the equation of any ray is:

$$y = \frac{-x}{\tan(\theta_1 - \theta_2)} + \frac{x_0}{\tan(\theta_1 - \theta_2)} - R + \sqrt{R^2 - x_0^2} \quad (\text{A.7})$$

Based on the geometry of the micro-features and the path of the focused ray through the waveguide. The essential geometric parameters are the radius of the lens, R , and the position of incidence of the ray on the micro-lens, along the x -axis, x_0 . The important angles to consider are:

$$\theta_1 = \tan^{-1} \left(-\frac{x}{\sqrt{R^2 - x^2}} \right) \quad (\text{A.8})$$

$$\theta_2 = \sin^{-1} \left(\frac{\sin \theta_1}{n_1} \right), \quad (\text{A.9})$$

where θ_1 , is the angle of incidence of the ray on the lens based on the curvature of the lens at the point x_0 , and θ_{2p} , is the angle of the refracted ray inside the waveguide. These equations are based on the lens geometry, the materials refractive index, n_1 , and the x - and y - coordinates of the ray along its path, where the origin is the centre point on the surface of the lens.

Equation A.7, however only accounts for the upper layer of the waveguide, the difference in refractive indices will cause the ray to bend towards the normal as it refracts into the bottom layer, changing the equation of the line. The new slope of the line is calculated based on Snell's law:

$$m = \frac{1}{\tan \theta_3}, \quad (\text{A.10})$$

where m is the slope of the ray in the second layer of the waveguide and, θ_3 , is the angle of the focused ray as it passes through the bottom layer. This angle is calculated by:

$$\theta_3 = \sin^{-1} \left(\frac{n_1}{n_2} * \sin(\theta_1 - \theta_2) \right) \quad (\text{A.11})$$

Based on the angles of the ray θ_1 , and θ_2 , as defined above, and the refractive indices of the upper and lower layers, n_1 and n_2 , respectively. Additionally, the y -intercept, for the equation of the ray in the lower layer of the concentrator is calculated as:

$$y = -t_1 - \frac{x_t}{\tan \theta_3} \quad , \quad (\text{A.12})$$

where t_1 is the thickness of the upper layer of the waveguide, and x_t is the x -value of the ray at the interface between the waveguide layers. This is calculated by determining the x -position of a ray according to A.7, at the position t_1 .

$$x_t = \tan(\theta_1 - \theta_2) * \left(-t_1 + \frac{x_o}{\tan(\theta_1 - \theta_2)} - R + \sqrt{R^2 - x_o^2} \right) \quad (\text{A.13})$$

Since the ray travels at a different angle in each of the waveguide mediums, the equation of each ray must be broken up into two segments: $0 < y < t_1$ for the upper layer (A.14) and $y > t_1$ for the lower layer (A.15) of the waveguide:

$$y = -\frac{x}{\tan(\theta_1 - \theta_2)} + \frac{x_o}{\tan(\theta_1 - \theta_2)} - R + \sqrt{R^2 - x_o^2} \quad , \quad 0 \leq y \leq t_1 \quad (\text{A.14})$$

$$y = \frac{-x}{\tan \theta_3} - t_1 - \frac{\tan(\theta_1 - \theta_2) * \left(-t_1 + \frac{x_o}{\tan(\theta_1 - \theta_2)} - R + \sqrt{R^2 - x_o^2} \right)}{\tan \theta_3} \quad , \quad y > t_1 \quad (\text{A.15})$$

Based on the above equations, the minimum focal length of the rays for any concentrator geometry can be found by computing the y -intercept of the outermost ray, for which $x_o = P/2$, as the outside rays will cross with the shortest focal length.

$$f = t_1 + \frac{\tan(\theta_{1p} - \theta_{2p}) * \left(-t_1 - R + \sqrt{R^2 - (0.5P)^2} \right) + 0.5P}{\tan(\theta_{3p})} \quad , \quad (\text{A.16})$$

where the angles and waveguide geometry are as defined above, and θ_{1p} , θ_{2p} , and θ_{3p} , are calculated by computing the ray angles at $x_0 = 0.5P$:

$$\theta_{1p} = \theta_1(0.5P) = \tan^{-1} \left(-\frac{0.5P}{\sqrt{R^2 - 0.5P^2}} \right) \quad (\text{A.17})$$

$$\theta_{2p} = \theta_2(0.5P) = \sin^{-1} \left(\frac{\sin(\theta_{1p})}{n_1} \right) \quad (\text{A.18})$$

$$\theta_{3p} = \theta_3(0.5P) = \sin^{-1} \left(\frac{n_1}{n_2} * \sin(\theta_{1p} - \theta_{2p}) \right) \quad (\text{A.19})$$

With the focal length, f , known the x -value of all rays can be found at this location, in order to determine the focal shift at this point. The dispersion of rays at this point will correspond to the minimum prism radius required for the given concentrator geometry. The x -position of each ray is determined by:

$$x = \tan(\theta_1 - \theta_2) * \left(t_1 + R - \sqrt{R^2 - x_0^2} \right) - x_0 - \tan(\theta_3) * (t_1 - f) \quad , \quad (\text{A.20})$$

where x_0 is the coordinate at which the incident ray strikes the surface of the lens features. The maximum x -value can be found based on Equation A.20, and thus the optimal prism width is defined by:

$$\begin{aligned}
E_C = & \left(\left(\left(\tan \left(\tan^{-1} \left(\frac{-x_0}{\sqrt{R^2 - x_0^2}} \right) - \sin^{-1} \left(\frac{\sin \left(\tan^{-1} \left(\frac{-x_0}{\sqrt{R^2 - x_0^2}} \right) \right)}{n_1} \right) \right) \right) * \left(t_1 + R - \sqrt{R^2 - x_0^2} \right) - x_0 - \right. \\
& \left. \tan \left(\sin^{-1} \left(\frac{n_1}{n_2} * \sin \left(\tan^{-1} \left(\frac{-x_0}{\sqrt{R^2 - x_0^2}} \right) - \sin^{-1} \left(\frac{\sin \left(\tan^{-1} \left(\frac{-x_0}{\sqrt{R^2 - x_0^2}} \right) \right)}{n_1} \right) \right) \right) \right) \right) * \right. \\
& \left. \left(\left(\left(\tan \left(\tan^{-1} \left(\frac{-0.5P}{\sqrt{R^2 - (0.5P)^2}} \right) - \sin^{-1} \left(\frac{\sin \left(\tan^{-1} \left(\frac{-0.5P}{\sqrt{R^2 - (0.5P)^2}} \right) \right)}{n_1} \right) \right) \right) * \left(-t_1 - R + \sqrt{R^2 - (0.5P)^2} \right) + 0.5P \right) \right)^2 \right)^N \\
& \left. \left(\left(\left(\tan \left(\tan^{-1} \left(\frac{-0.5P}{\sqrt{R^2 - (0.5P)^2}} \right) - \sin^{-1} \left(\frac{\sin \left(\tan^{-1} \left(\frac{-0.5P}{\sqrt{R^2 - (0.5P)^2}} \right) \right)}{n_1} \right) \right) \right) * \left(-t_1 - R + \sqrt{R^2 - (0.5P)^2} \right) + 0.5P \right) \right)^2 \right)^N \right)_{max} \div P^2 \quad (A.22)
\end{aligned}$$

where

$$\begin{aligned}
N = & \frac{1}{6} \sqrt{SA} * \left(\sin \left(2\pi - 2 * \sin^{-1} \left(\frac{1}{n_2} \right) \right) * \sin \left(2\pi - 2 * \sin^{-1} \left(\frac{1}{n_2} \right) - \sin^{-1} \left(\frac{n_1}{n_2} * \sin \left(\tan^{-1} \left(\frac{-0.5P}{\sqrt{R^2 - 0.5P^2}} \right) \right) \right. \right. \right. \\
& \left. \left. \left. \sin^{-1} \left(\frac{\sin \left(\tan^{-1} \left(\frac{-0.5P}{\sqrt{R^2 - 0.5P^2}} \right) \right) \right)}{n_1} \right) \right) \right) * \csc \left(4\pi - 4 * \sin^{-1} \left(\frac{1}{n_2} \right) - \sin^{-1} \left(\frac{n_1}{n_2} * \sin \left(\tan^{-1} \left(\frac{-0.5P}{\sqrt{R^2 - 0.5P^2}} \right) \right) \right) \right. \\
& \left. \left. \left. \sin^{-1} \left(\frac{\sin \left(\tan^{-1} \left(\frac{-0.5P}{\sqrt{R^2 - 0.5P^2}} \right) \right) \right)}{n_1} \right) \right) \right) \div \left(\frac{\tan \left(\tan^{-1} \left(\frac{-0.5P}{\sqrt{R^2 - 0.5P^2}} \right) \right) \sin^{-1} \left(\frac{\sin \left(\tan^{-1} \left(\frac{-0.5P}{\sqrt{R^2 - 0.5P^2}} \right) \right)}{n_1} \right)}{\tan \left(\sin^{-1} \left(\frac{n_1}{n_2} * \sin \left(\tan^{-1} \left(\frac{-0.5P}{\sqrt{R^2 - 0.5P^2}} \right) \right) \right) \right) \sin^{-1} \left(\frac{\sin \left(\tan^{-1} \left(\frac{-0.5P}{\sqrt{R^2 - 0.5P^2}} \right) \right)}{n_1} \right)} \right) * \\
& \left(\left(-t_1 + \frac{0.5P}{\tan \left(\tan^{-1} \left(\frac{-0.5P}{\sqrt{R^2 - 0.5P^2}} \right) \right) \sin^{-1} \left(\frac{\sin \left(\tan^{-1} \left(\frac{-0.5P}{\sqrt{R^2 - 0.5P^2}} \right) \right)}{n_1} \right)} \right) - R + \sqrt{R^2 - 0.5P^2} \right) \right) \quad (A.23)
\end{aligned}$$

A.2: Relationship Between Angle and Pitch

In order to determine the relationship between the pitch of the micro-lens features, and the angle of incidence of the focused ray on the coupling prisms, the ray path of the lens' outermost ray should be considered. The pitch of the lens features is directly related to the maximum angle of incidence of the focused light on the coupling prisms, as the outermost rays will have the largest angle (Figure A.1).

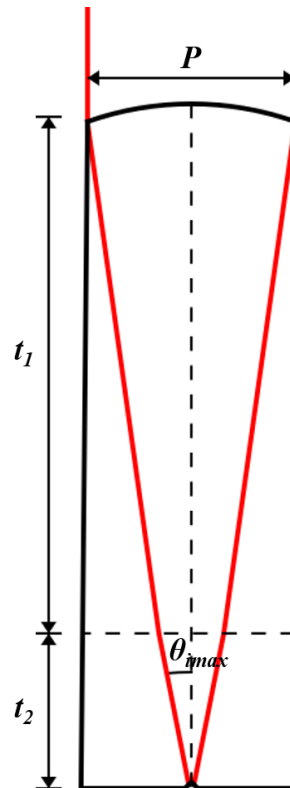


Figure A.1 Relationship between the lens feature pitch and the ray angle of incidence.

Based on the equations of the focused ray derived in Appendix A.1, the angle of the focused ray in the lower layer of the waveguide is defined by Equation A.11. The maximum angle of incidence is therefore defined based on the outermost rays, which strike the lens at $x_0=0.5P$.

$$\theta_{i_{max}} = \sin^{-1} \left(\frac{n_1}{n_2} \sin \left(\theta_{1p} - \theta_{2p} \right) \right) \quad (\text{A.24})$$

In order to examine the relationship between the angle of incidence and the feature pitch, P , this equation may be expressed as:

$$\theta_{i_{max}} = \sin^{-1} \left(\frac{n_1}{n_2} \sin \left(\tan^{-1} \left(\frac{-0.5P}{\sqrt{R^2 - (0.5P)^2}} \right) - \tan^{-1} \left(\frac{n_1}{n_2} \sin \left(\tan^{-1} \left(\frac{-0.5P}{\sqrt{R^2 - (0.5P)^2}} \right) \right) \right) \right) \right), \quad (\text{A.25})$$

where n_1 and n_2 are the refractive indices of the upper and lower layers respectively, P is the pitch of the lens features, and R is the radius of the lenses. Equation A.25 is solved iteratively, based on the known parameters, and the desired maximum angle of incidence, $\theta_{i_{max}}$, in order to determine the optimal value for pitch, P .

A.3: Calculation of Layer Thickness

The thickness of the bottom layer t_2 is estimated initially based on the desired surface area, and geometric factor of concentration of the particular waveguide. This estimate must be refined, however, to ensure that the coupling prisms are located at the precise focal point of the concentrator micro-lenses. Based on the equation for the focal length of the concentrator lenses (Appendix A.1; Equation A.16), the optimal thickness for the transmission layer of the waveguide may be calculated. Since the focal length corresponds to the total thickness of the concentrator region, and thickness of the upper layer, t_1 , is known, the focal length equation may be rearranged to calculate the thickness of the bottom layer t_2 as below.

The precise focal length is calculated by:

$$f = t_1 + \frac{\tan(\theta_{1p} - \theta_{2p}) * \left(-t_1 + \frac{x_0}{\tan(\theta_{1p} - \theta_{2p})} - R + \sqrt{R^2 - x_0^2} \right)}{\tan(\theta_{3p})} \quad (\text{A.26})$$

Since the focal length is the sum of the two layer thicknesses, the difference between the focal length, f , and the upper layer thickness, t_1 , constitutes the thickness of the lower layer. Thus the bottom layer thickness, t_2 , is accurately defined as:

$$t_2 = \frac{\tan(\theta_{1p} - \theta_{2p}) * \left(-t_1 + \frac{0.5P}{\tan(\theta_{1p} - \theta_{2p})} - R + \sqrt{R^2 - (0.5P)^2} \right)}{\tan(\theta_{3p})}, \quad (\text{A.27})$$

where P is the pitch, and R is the radius of the lens micro-features, and θ_{1p} , θ_{2p} , and θ_{3p} , are the ray angles on the lens surface, in layer 1, and in layer 2, respectively, as defined in Appendix A.1.

A.4: Feature Stretching and Deformation

A.4.1 Feature Orientation

As the feature orientation changes with respect to the light source, as a result of the waveguide bending, the position of the focal point changes too. The location of the focal point can be calculated with respect to the angle of incidence of the light rays on the concentrator surface, based on the ray optics of the lens micro-feature.

Figure A.2 illustrates the path of the outermost rays on the lens surface, with the incident light striking the waveguide at a non-zero angle.

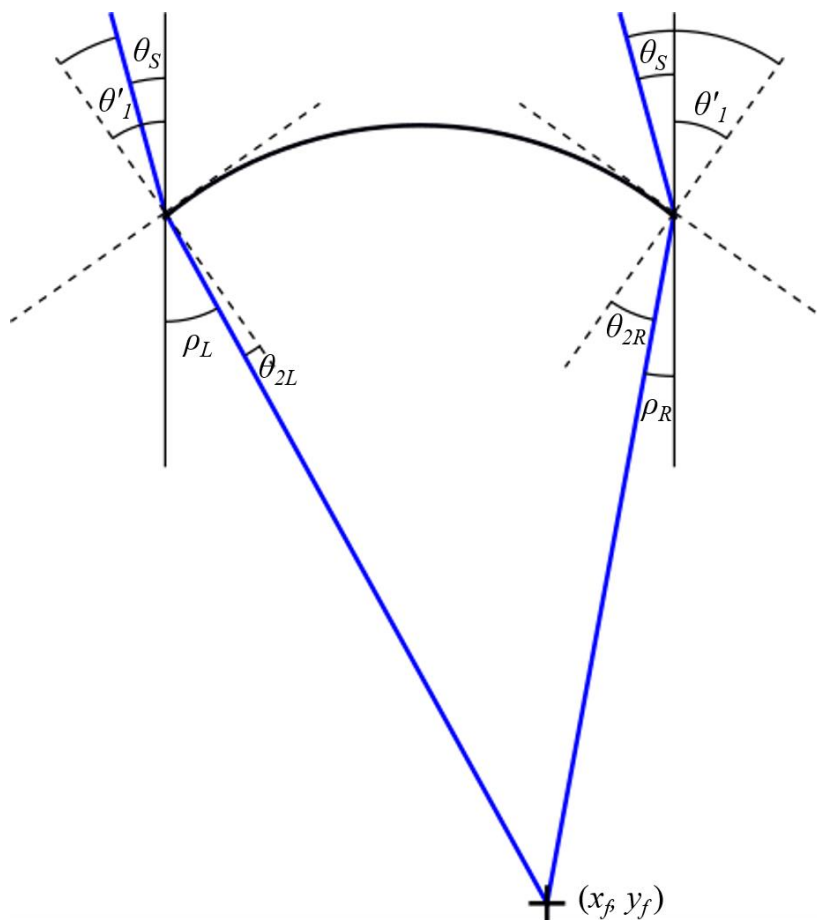


Figure A.2 Relocation of focal point due to reorientation of lens micro-features with respect to the light source.

In order to calculate the position of the focal point with respect to the angle of incidence of the light on the lens surface, the point of intersection of the outermost rays is calculated. Thus, the equation of the rays must be calculated, based on the angles of the ray on the waveguide surface and as they travel through the waveguide layers. The deviation from the normal to the lens surface is calculated by, for a direct ray:

$$\theta'_I = \tan^{-1} \left(\frac{-x_0}{\sqrt{R^2 - x_0^2}} \right), \quad (\text{A.28})$$

where x_0 is the x-position of the ray across the surface of the lens, where the centre of the lens is zero, and R is the radius of the lens micro-features. Since the focal point has shifted from the centre of the lens, the ray diagram for the micro-feature is no longer symmetrical and thus the ray angles are calculated for the left and right sides of the lens, separately.

For the left most side; the focused-ray angle ρ_L is calculated based on the angle between the surface normal and the incident ray, θ_{IL} , and the refracted ray as it enters the waveguide medium, θ_{2L} . These angles are calculated according to the geometry of the ray diagram, illustrated in figure A.2.

$$\theta_{IL} = \theta'_I - \theta_S \quad (\text{A.29})$$

$$\theta_{2L} = \sin^{-1} \left(\frac{1}{n_1} * \sin(\theta'_I - \theta_S) \right) \quad (\text{A.30})$$

Based on Equations A.29 and A.30, the required angles are known to calculate the angle of the focused ray in the waveguide, for the leftmost ray, ρ_L . This angle dictates the equation of the ray, required to determine the relocated focal point.

$$\rho_L = \theta'_I - \sin^{-1} \left(\frac{1}{n_1} \sin(\theta'_I - \theta_S) \right) \quad (\text{A.31})$$

Similarly, for the rightmost side, the ray angle ρ_R , and the corresponding angles, θ_{2L} , and θ_{2R} , are calculated by:

$$\theta_{1R} = \theta'_I + \theta_S \quad (\text{A.32})$$

$$\theta_{2R} = \sin^{-1} \left(\frac{1}{n_I} * \sin(\theta'_I + \theta_S) \right) \quad (\text{A.33})$$

$$\rho_R = \theta'_I + \theta_S - \sin^{-1} \left(\frac{1}{n_I} \sin(\theta'_I + \theta_S) \right) \quad (\text{A.34})$$

According to the derivations in Appendix A.1, the equation of the ray is calculated by Equation A.35, and the ray angles as defined in Equations A.29 through A.34, can be substituted in to calculate the ray angles in this instance.

$$y = \frac{-x}{\tan(\theta'_I - \theta_2)} + \sqrt{R^2 - x^2} - R + \frac{x_0}{\tan(\theta'_I - \theta_2)} \quad (\text{A.35})$$

Therefore, the equations of the outermost rays are for the left-hand side:

$$y_L = \frac{-x}{\tan(\theta'_{1L} - \theta_{2L})} + \sqrt{R^2 - (0.5P)^2} - R - \frac{0.5P}{\tan(\theta'_{1L} - \theta_{2L})} \quad (\text{A.36})$$

And for the right-hand side:

$$y_R = \frac{-x}{\tan(\theta'_{1R} - \theta_{2R})} + \sqrt{R^2 - (0.5P)^2} - R + \frac{0.5P}{\tan(\theta'_{1R} - \theta_{2R})} \quad (\text{A.37})$$

In order to calculate the location of the focal point, the point of intersection of the outermost rays is calculated by equating the equations of the rays:

$$\frac{-x}{\tan(\theta'_{1L} - \theta_{2L})} + \frac{x}{\tan(\theta'_{1R} - \theta_{2R})} = \frac{0.5P}{\tan(\theta'_{1L} - \theta_{2L})} + \frac{0.5P}{\tan(\theta'_{1R} - \theta_{2R})} \quad (\text{A.38})$$

Therefore, the x and y positions at the focal point are:

$$x_f = \frac{0.5P * \tan(\theta'_{1R} - \theta_{2R}) + 0.5P * \tan(\theta'_{1L} - \theta_{2L})}{\tan(\theta'_{1L} - \theta_{2L}) - \tan(\theta'_{1R} - \theta_{2R})} \quad (\text{A.39})$$

$$y_f = \frac{-x_f}{\tan(\theta_{1R} - \theta_{2R})} + \sqrt{R^2 - (0.5P)^2} - R + \frac{0.5P}{\tan(\theta_{1R} - \theta_{2R})} \quad (\text{A.40})$$

According to this equation the path of the focal point caused by variations in angle of incidence takes an approximately parabolic shape. An equation which will predict the focal point position for any angle of incidence is derived.

$$y_i = ax^2 + y_0 \quad , \quad (\text{A.41})$$

where:

$$a = \frac{y_i - y_0}{x_i^2} \quad (\text{A.42})$$

$$y_0 = \sqrt{R^2 - (0.5P)^2} - R + \frac{0.5P}{\tan\left(-\theta_I - \sin^{-1}\left(\frac{1}{n_I}\sin(-\theta_I - \theta_S)\right)\right)} \quad (\text{A.43})$$

$$y_I = \frac{-x_I}{\tan\left(-\theta_I - \sin^{-1}\left(\frac{1}{n_I}\sin(-\theta_I - \theta_S)\right)\right)} + \sqrt{R^2 - (0.5P)^2} - R + \frac{0.5P}{\tan\left(-\theta_I - \sin^{-1}\left(\frac{1}{n_I}\sin(-\theta_I - \theta_S)\right)\right)} \quad (\text{A.44})$$

$$x_I = \frac{0.5P * \tan\left(\theta_I - \sin^{-1}\left(\frac{1}{n_I}\sin(-\theta_I - \theta_S)\right)\right) + \tan\left(-\theta_I - \sin\left(\frac{1}{n_I}\sin(-\theta_I - \theta_S)\right)\right)}{\tan\left(\theta_I - \sin^{-1}\left(\frac{1}{n_I}\sin(-\theta_I - \theta_S)\right)\right) - \tan\left(-\theta_I - \sin\left(\frac{1}{n_I}\sin(-\theta_I - \theta_S)\right)\right)} \quad (\text{A.45})$$

$$\theta_I = \tan^{-1}\left(\frac{0.5P}{\sqrt{R^2 - (0.5P)^2}}\right) \quad (\text{A.46})$$

The equation of the parabola which predicts the focal location of the rays with respect to the source angle of incidence, θ_S , is therefore defined as:

$$\begin{aligned}
y_i = & \left(\left(\left(\frac{-x_I}{\tan \left(- \left(\tan^{-1} \left(\frac{0.5P}{\sqrt{R^2 - (0.5P)^2}} \right) \right) - \sin^{-1} \left(\frac{1}{n_I} \sin \left(- \left(\tan^{-1} \left(\frac{0.5P}{\sqrt{R^2 - (0.5P)^2}} \right) \right) - \theta_S \right) \right) \right) \right) + \sqrt{R^2 - (0.5P)^2} - R + \left(0.5P \div \tan \left(- \right. \right. \right. \\
& \left. \left. \left. \left(\tan^{-1} \left(\frac{0.5P}{\sqrt{R^2 - (0.5P)^2}} \right) \right) - \sin^{-1} \left(\frac{1}{n_I} \sin \left(- \left(\tan^{-1} \left(\frac{0.5P}{\sqrt{R^2 - (0.5P)^2}} \right) \right) - \theta_S \right) \right) \right) \right) \right) \right) - \\
& \left(\sqrt{R^2 - (0.5P)^2} - R + \left(0.5P \div \tan \left(- \left(\tan^{-1} \left(\frac{0.5P}{\sqrt{R^2 - (0.5P)^2}} \right) \right) - \sin^{-1} \left(\frac{1}{n_I} \sin \left(- \left(\tan^{-1} \left(\frac{0.5P}{\sqrt{R^2 - (0.5P)^2}} \right) \right) - \right. \right. \right. \right. \\
& \left. \left. \left. \left. \theta_S \right) \right) \right) \right) \right) \right) * x^2 * \left(\tan \left(\left(\tan^{-1} \left(\frac{0.5P}{\sqrt{R^2 - (0.5P)^2}} \right) \right) - \sin^{-1} \left(\frac{1}{n_I} \sin \left(- \left(\tan^{-1} \left(\frac{0.5P}{\sqrt{R^2 - (0.5P)^2}} \right) \right) - \theta_S \right) \right) \right) \right) - \tan \left(- \right. \\
& \left. \left(\tan^{-1} \left(\frac{0.5P}{\sqrt{R^2 - (0.5P)^2}} \right) \right) - \sin \left(\frac{1}{n_I} \sin \left(- \left(\tan^{-1} \left(\frac{0.5P}{\sqrt{R^2 - (0.5P)^2}} \right) \right) - \theta_S \right) \right) \right) \right) \right) \right) \div \\
& \left(0.5P * \tan \left(\left(\tan^{-1} \left(\frac{0.5P}{\sqrt{R^2 - (0.5P)^2}} \right) \right) - \sin^{-1} \left(\frac{1}{n_I} \sin \left(- \left(\tan^{-1} \left(\frac{0.5P}{\sqrt{R^2 - (0.5P)^2}} \right) \right) - \theta_S \right) \right) \right) \right) + \tan \left(- \right. \\
& \left. \left(\tan^{-1} \left(\frac{0.5P}{\sqrt{R^2 - (0.5P)^2}} \right) \right) - \sin \left(\frac{1}{n_I} \sin \left(- \left(\tan^{-1} \left(\frac{0.5P}{\sqrt{R^2 - (0.5P)^2}} \right) \right) - \theta_S \right) \right) \right) - \right. \\
& \left. \left. \left. \left. \theta_S \right) \right) \right) \right) \right) \right) + \sqrt{R^2 - (0.5P)^2} - R + \frac{0.5P}{\tan \left(- \left(\tan^{-1} \left(\frac{0.5P}{\sqrt{R^2 - (0.5P)^2}} \right) \right) - \sin^{-1} \left(\frac{1}{n_I} \sin \left(- \left(\tan^{-1} \left(\frac{0.5P}{\sqrt{R^2 - (0.5P)^2}} \right) \right) - \theta_S \right) \right) \right) \right) \right) \right) \right)
\end{aligned} \tag{A.47}$$

A.4.2 Feature Stretching

It may be demonstrated numerically that the scale of the micro-features will dictate their relative deformation due to stretching caused by the waveguide bending. The smaller the scale of the features, the less the impact of deformation will be. Considering the case where a 10 mm length of the waveguide is being bent through a curve with a radius of 10 mm. A comparison of the two waveguides with a features pitch of 0.8 mm and 0.4 mm, respectively (and all other geometry scaled accordingly), is shown in Figure A.3.

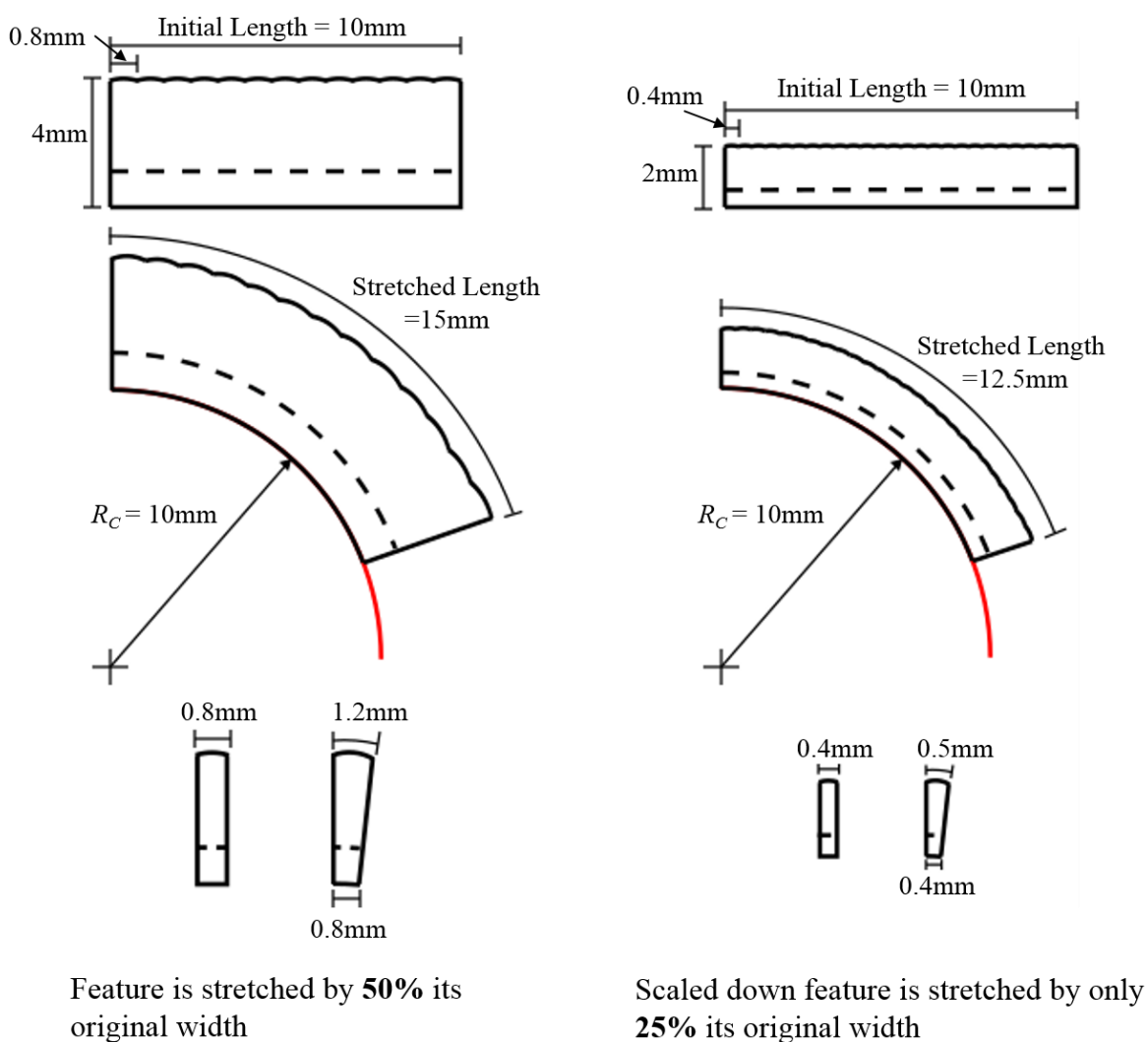


Figure A.3 Reduction of the scale of the waveguide over the same range of curvature reduces the proportional deformation of the individual micro-features.

Since the larger feature size corresponds to a greater waveguide thickness, the radius of curvature of the outer surface of the concentrator is larger. This results in more stretching of the upper surface, amplifying the deformation of features, resulting in the greater proportional deformation of larger features.

Appendix B: CAD Drawings of Waveguide Geometry

Appendix B includes CAD drawing of the important waveguide, and micro-feature geometries used in the simulation discussed in Chapter 4 of this thesis. Figure B.1 below illustrates the combined concentrator-diffuser layered waveguide, composed of a small array of concentrating features, surrounded on all four edges by the illuminating region of the waveguide.

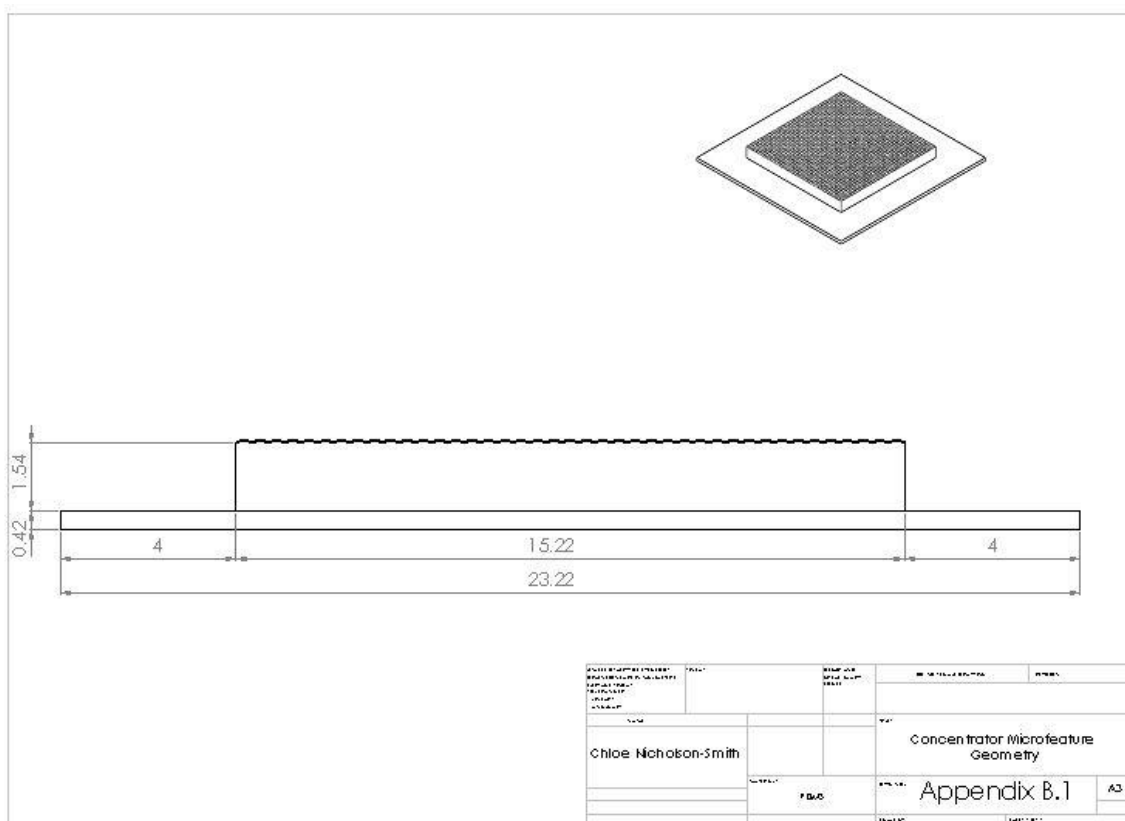


Figure B.1 SolidWorks drawing of layered concentrator-diffuser waveguide, illustrating geometry used in Chapter 4 simulations.

Figure B.2 shows the diffusing region of the waveguide, composed of a linear array of the diffusing wedges. The wedges are patterned along the bottom face of the diffuser, and are defined by their base angle, and their width as indicated in the image below. Additionally, Figure B.2 depicts the tree dimensional rendering of the diffuser region, in the upper right-hand corner.

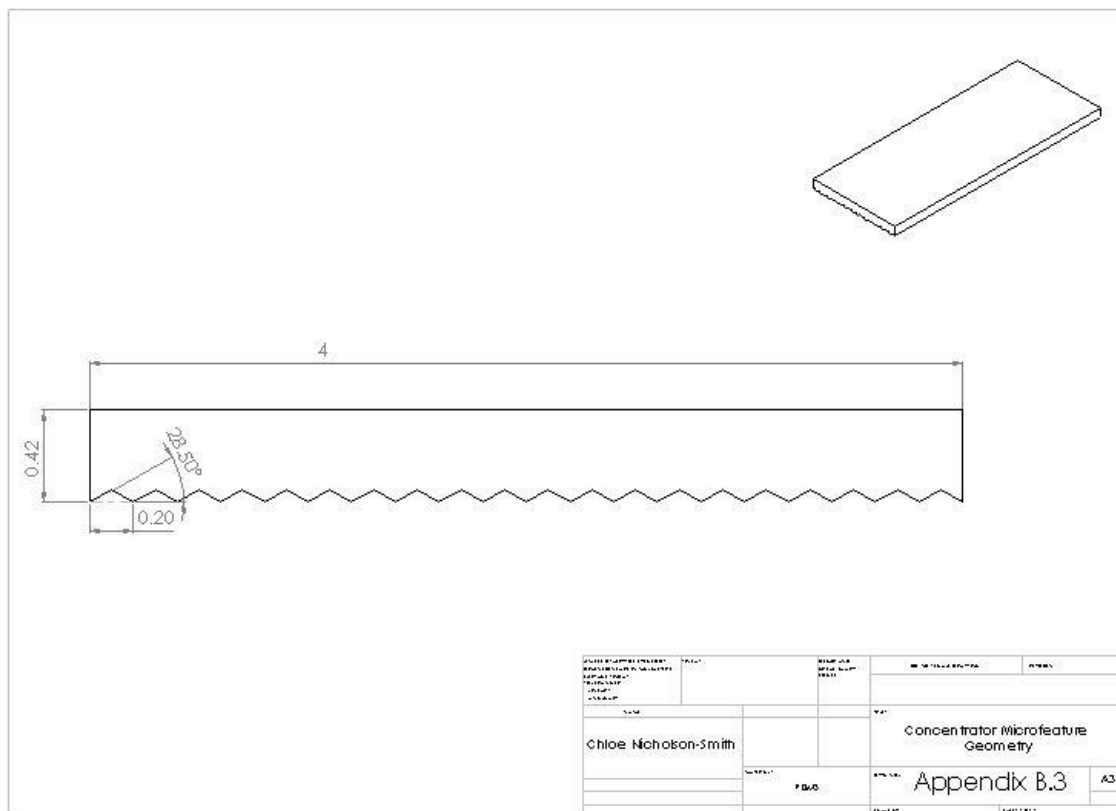


Figure B.2 SolidWorks drawing of concentrator micro-features illustrating radius, pitch, coupling feature and layer dimensions.

Finally, Figure B.3 illustrated a single concentrating feature, composed of the micro-lens on its upper surface with the coupling prism embedded on the bottom face. The key parameters which define the lens micro-feature are the radius, and pitch, and for the coupling features it is their angle and width, as indicated in the image below. Also important to the geometry of the concentrating micro-features are the thicknesses of each of the layers, and their combined thickness.

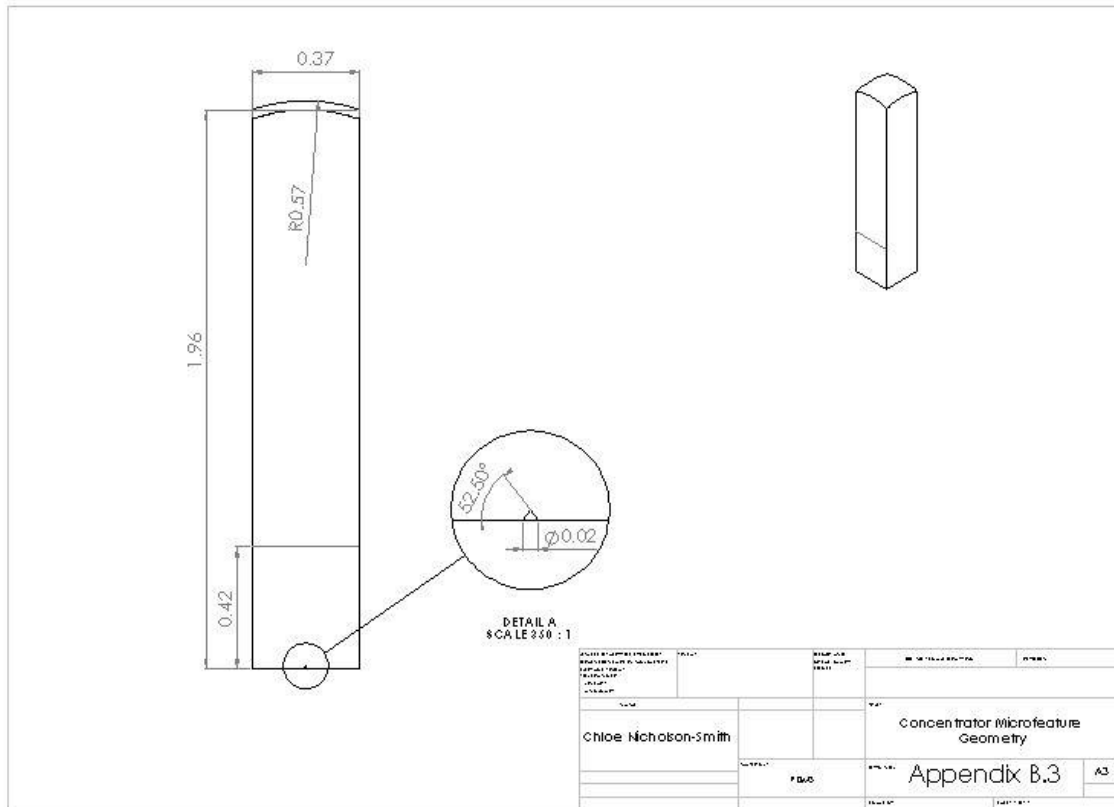



Figure B.3 SolidWorks drawing of diffuser micro-features illustrating size and angle of the diffusing wedges, and diffuser region thickness.

Appendix C: Sample Zemax Program

This appendix presents a sample Zemax NSC editor which illustrates the parameters assigned for the analysis of a dual functional concentrator – diffuser waveguide. This particular example incorporates two CAD objects, a rectangular source and five detector rectangles, as illustrated in Figure C.1.



The screenshot shows the Zemax Non-Sequential Component Editor interface. The main window displays a table of object properties for a simulation. The table has the following columns: Object Type, Comment, Ref Object, Inside Of, X Position, Y Position, Z Position, Tilt About X, Tilt About Y, Tilt About Z, Material, Scale, and Mode. The objects are numbered 1 through 9.

Object Type	Comment	Ref Object	Inside Of	X Position	Y Position	Z Position	Tilt About X	Tilt About Y	Tilt About Z	Material	Scale	Mode
1 CAD Part: STEP/IGES/SAT	0525 C Area.STEP.ZOF	0	0	0.000	0.000	0.000	0.000	0.000	0.000	N14.ZTG	1.000	1
2 CAD Part: STEP/IGES/SAT	0525 H Area.STEP.ZOF	0	0	0.000	5.000E-03	0.000	0.000	0.000	0.000	N155.ZTG	1.000	1
3 Source Rectangle		0	0	0.000	2.500	0.000	90.000	0.000	0.000	-	50	10000
4 Detector Rectangle		0	0	0.000	0.210	-7.605	0.000	0.000	0.000		7.650	0.220
5 Detector Rectangle		0	0	0.000	0.210	7.605	0.000	0.000	0.000		7.650	0.220
6 Detector Rectangle		0	0	-7.605	0.210	0.000	0.000	90.000	0.000		7.650	0.220
7 Detector Rectangle		0	0	7.605	0.210	0.000	0.000	90.000	0.000		7.650	0.220
8 Detector Rectangle		0	0	0.000	2.300	0.000	90.000	0.000	0.000	ABSORB	14.000	14.000
9 Null Object		0	0	0.000	0.000	0.000	0.000	0.000	0.000	-		

Figure C.1 Zemax NSC editor for a dual functioning concentrator-diffuser waveguide, including CAD geometry and Zemax defined source and detectors.

For more information on the Zemax simulations conducted in this research, or for a copy of the original Zemax files, please contact Dr. George K. Knopf (gkknopf@uwo.ca).

Curriculum Vitae

Name: Chloë Nicholson-Smith

Post-secondary The University of Western Ontario

Education and London, Ontario, Canada

Degrees: 2010-2014 BESC

The University of Western Ontario

London, Ontario, Canada

2014-2016 MESC

Honours and Western Graduate Research Scholarship

Awards: 2014-2016

Dean's Honour List

2010-2012, 2013-2014

Queen Elizabeth II Aiming for the Top Scholarship

2010-2012

Related Work Teaching Assistant

Experience The University of Western Ontario

2014-2016

Publications:

Nicholson-Smith, C., Knopf, G. K., & Bordatchev, E. "Controlled guidance of light through a flexible optical waveguide sheet". Proc. *SPIE* 9759, 97590C-97590C (2016).